AIR UNIVERSITY
UNITED STATES AIR FORCE

SCHOOL OF ENGINEERING

WRIGHT-PATTERSON AIR FORCE BASE, OHIO

DISCLAIMER NOTICE

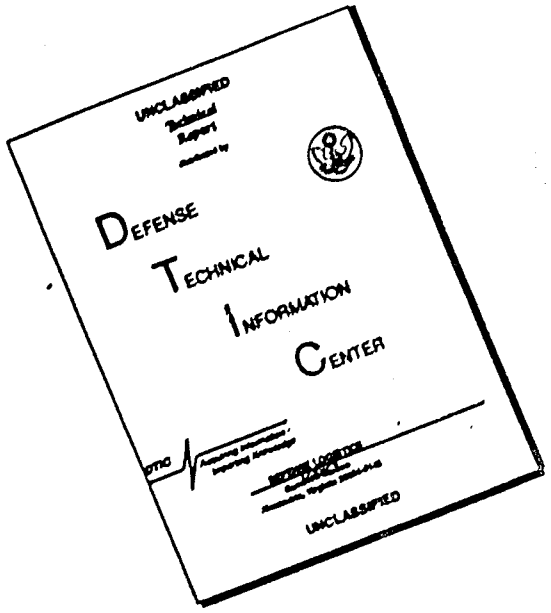

THIS DOCUMENT IS BEST QUALITY AVAILABLE. THE COPY FURNISHED TO DTIC CONTAINED A SIGNIFICANT NUMBER OF PAGES WHICH DO NOT REPRODUCE LEGIBLY.

GE/EE/76-33

HIGH ACCURACY AIRCRAFT TO SATELLITE TRACKING: AN EVALUATION OF TWO PROPOSED FILTER MODELS

THESIS

GE/EE/76-33 Robert E. Mann, Jr.
Capt USAF

Approved for public release; distribution unlimited.

GE/EE/76-33

HIGH ACCURACY AIRCRAFT TO SATELLITE TRACKING: AN EVALUATION OF TWO PROPOSED FILTER MODELS

THESIS

Presented to the Faculty of the School of Engineering

of the Air Force Institute of Technology

Air University

in Partial Fulfillment of the

Requirements for the Degree of

Master of Science

by

Robert E. Mann, Jr.

Capt USAF

Graduate Engineering

December 1976

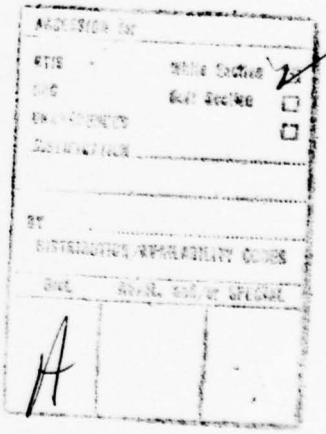

Approved for public release; distribution unlimited.

Acknowledgements

This work is partly a follow on to a study by a previous AFIT student, R. A. K. Mitchell. Though errors were found in his study which necessitated its reaccomplishment, I still hold his work in the highest regard for its scope and depth.

A great deal of thanks is due to Professor (Capt) Pete Maybeck, my Thesis Advisor, without whose help and insights this project could not have been accomplished. He is a good friend and an outstanding educator. I would also like to express my appreciation to Capt Gary Reid of the Avionics Laboratory for sponsoring the study and for sharing his insights into the problem with me. Thanks are also in order for my readers, Majors Parker Sproul and Dick Potter and to two of my classmates, Captains Bob Lutter and Keith Fitschen.

Most of all, I would like to thank my loving and understanding wife and daughter, Pat and Christina, for all of their help and encouragement over the last 18 months.

Capt Robert E. Mann, Jr.

December 1976

Contents

List of Figures

Abstract

This study treats the high accuracy tracking of a satellite from an aircraft. The purpose is to evaluate the feasibility of several reduced order system models for implementation in an extended Kalman filter formulation whose estimates would be used to aid the tracker. The first filter model is a twelve state model in which filter estimates of the satellite inertial position and velocity are obtained and used in the estimation of the tracker states. A second, six state-model deletes these six satellite states, and tracker state estimation is accomplished by exploiting the information already available in the tracking geometry, dominant modes of satellite dynamics, and the range measurement. Tracker state estimation is accomplished in the line of sight coordinate frame for both filter formulations. A covariance analysis was performed, evaluating each filter against a 42 state truth model. The tracking profile used in the study was specifically designed to evaluate each filter's state estimation capability when faced with a highly nonlinear tracker angular rate history. It was concluded that the six state filter is a viable alternative, and, with some proposed modifications, is preferable (because of its simplicity and lower computational burden) and warrants further study.

HIGH ACCURACY AIRCRAFT TO SATELLITE TRACKING: AN EVALUATION OF TWO PROPOSED FILTER MODELS

I. Introduction

Problem Statement and Study Objectives

The high resolution tracking of one accelerating vehicle from another (possibly) accelerating vehicle has many military applications - aircraft to aircraft tracking, aircraft to missile tracking, missile to aircraft tracking, etc. The use of linear or nonlinear system analysis techniques to obtain the state estimate of the target and/or tracker and subsequent use of this information to aid the tracking device is well documented in the literature (see, for instance Ref 1) and (Ref 2). In this work, the case of tracking a satellite from an aircraft will be studied.

The purpose of this study is to develop a reduced order system model to be used in an extended Kalman filter to aid a typical tracking system. The work is to be viewed as a *feasibility* study and not a complete performance analysis. To accomplish this end, two reduced order system models will be studied using a covariance analysis as an evaluation tool. The reduced order system model must be of low enough dimension to be readily implemented on currently available digital flight computers - on the order of 20 or fewer states (Ref:).

To develop and evaluate a reduced order system model using a covariance analysis computer program [supplied by the U. S. Air Force Avionics Laboratory (AFAL)], requires that the following general objectives be met:

1. Develop the truth model representation of the actual system dynamics.
2. Generate a tracking profile generation program to provide nominal data for an aircraft to satellite tracking scenario.

3. Develop a reduced order system model - usually, but not always, the truth model with certain states removed or combined.
4. Using the truth model and the nominal tracking profile, perform a covariance analysis on the filter based upon the proposed reduced order system model.
5. Adjust the filter system model until the desired performance is obtained.

The objectives of this study are somewhat different than the general guidelines listed above. Originally, the work of Mitchell (Ref 4) was to be used as a baseline for the evaluation of a new reduced order system model. However, close examination of his study revealed several serious errors in the formulation of the truth model and in the generation of the nominal tracking profile. With this in mind, the first objective of this study then became to reaccomplish Mitchell's work by

1. Correcting the errors in the truth model.
2. Correcting the errors found in the profile generation program.
3. Reaccomplishing the evaluation of the 12 state reduced order filter proposed by Mitchell.

The second objective of this study remained the same: to develop and evaluate (against the same corrected truth model) a second reduced order (6 state) system model proposed by Captain (Dr.) J. Gary Reid of the AFAL. The final objective is to compare the performance of the two proposed suboptimal filters and to make recommendations concerning possible implementation and follow-on work. Because of the time limitations in the accomplishment of this work, and the inherent limitations in applying a covariance analysis to an extended Kalman filter (discussed in Chapter IV), no attempt was made to "tune" either reduced order filter "perfectly" to obtain the best possible performance. This philosophy is consistent with

the objective of performing a feasibility study of the two proposed filters. Sufficient tuning will be accomplished to discern differences in performance (if any) between the two models.

Assumptions and Limitations

Because the system dynamics and measurements are nonlinear for the aircraft to satellite tracking problem, the basic linear Kalman filter formulation cannot be applied in this study. Several nonlinear estimation techniques are available to handle problems of this type. The extended Kalman filter formulation, which linearizes the state equations about the most recent state estimate, was chosen because of its simplicity and low computational burden. Inherent in the application of an extended Kalman filter, is the assumption that due to relinearizations, a linear perturbation model driven by white Gaussian noise in an additive fashion is adequate.

For a truly linear system, the results of a well tuned covariance analysis depict the true behavior of a proposed filter. For a linear Kalman filter, the covariance propagation is not dependent on the measurements or the state estimate. Such is not the case when this evaluation tool is used with an extended Kalman filter. Because of the nature of the covariance analysis, the state estimate is not propagated and is unavailable for the linearization process discussed above. Therefore, the linearized state and measurement equations are evaluated along an apriori nominal trajectory - the nominal tracking profile discussed in the objectives section of this chapter. Thus, an inherent limitation of applying a covariance analysis to an extended Kalman filter is that the apriori nominal must be close to the actual state estimate. Otherwise, what might occur is that a proposed suboptimal filter may perform quite well in a

covariance analysis and quite poorly when implemented. For the above reasons, the results of a covariance analysis for an extended Kalman filter must be viewed as tentative or as a small perturbation analysis. One method - usually more expensive in terms of computer time and manhours - for obtaining a better indication of expected filter performance is to perform a Monte Carlo analysis of the filter. This is most often performed after the feasibility of a filter design has been shown with a covariance analysis.

Due to time limitations, only one nominal tracking profile was employed in this study. The profile which was used represents one of the worst case conditions in that, at the beginning of the simulation, the tracker (aircraft) lies in the orbit plane of the satellite and as the simulation progresses, the aircraft moves orthogonal to the orbit plane. Thus, the tracking geometry in this study restricts the flow of "information" about some of the states in the filter and observability problems are created.

The assumptions made concerning the instrumentation of the aircraft/tracker system are as follows:

1. Essentially perfect measurements of the tracker acceleration with respect to inertial space, coordinatized in the tracker frame are available as the derived (specific force minus computed gravity) output from three accelerometers, one mounted along each tracker axis.
2. The tracking system will provide noise-corrupted measurements of the inertial angular rates of the tracker, small angle deviations between the boresight and line-of-sight frames (discussed in Chapter II), and range. It is also assumed that the system has

the capability of instantaneous correction driven by the state error estimates from the extended Kalman filter.

3. The tracker Y axis will be inertially stabilized such that it always lies parallel to the geocentric equatorial X-Y plane (see Figure 1, Chapter II).
4. The second proposed reduced order system model (Filter II) requires that an inertial navigation system be on board the aircraft to provide high precision (essentially perfect relative to other errors inherent in the problem) measurements of the inertial position and velocity of the tracker origin.
5. Essentially perfect measurements of the tracker elevation and azimuth angles will be available from resolvers.

II. System State Equations

Introduction

In this chapter, the satellite (target) and tracker state and measurement equations will be developed for the system (truth) model. Because the initial part of this study is a follow-on to the work of Mitchell (Ref 4), much of what follows in this chapter parallels his developments. One modification to his truth model is in the modeling of acceleration measurements. The system state equations model (as accurately as desired) the true system dynamics. On the other hand, the reduced order system model (filter) state equations are implemented using the best information available. Thus, while the true acceleration of the tracker with respect to the inertial frame, coordinatized in the tracker frame, is used in the truth model, the filter model obtains this information from accelerometers mounted on the tracker axes (sensed specific force minus computed gravitational acceleration). As mentioned in the Introduction, an assumption of this study is that the acceleration information received by the filter is essentially uncorrupted. This assumption negates the need to model accelerometer noises in the truth model.

Before continuing, a few words concerning the notation adopted in this study will be considered. The matrix which transforms a vector coordinatized in the "i" frame into a vector coordinatized in the "j" frame will be denoted by C_i^j. Unless otherwise indicated, letter superscripts on vectors will indicate coordinatization in the frame indicated by the superscript. Where it is necessary to address individual components of vectors coordinatized in specific frames, subscripts will be used to indicate individual components i.e.

$$(\underline{A})^I = \begin{bmatrix} A_X \\ A_Y \\ A_Z \end{bmatrix} \tag{2-1}$$

The superscript "I" indicates that the vector $\underline{A}$ is expressed in the inertial frame. The subscripts X, Y, and Z indicate the components of $\underline{A}$ along the X, Y, and Z axes of the "I" frame.

The remainder of this chapter will cover the physical description of the total system and major modeling assumptions made in this study, the development of the satellite and tracker state equations, and the system measurement equations. The satellite state equations will not be formally derived, as the approach taken is straightforward and the derivations of the models of individual perturbative effects may be found by the interested reader in any good astrodynamics book (see for instance Ref 5). On the other hand, a complete derivation of the tracker state equations will be given, as they reflect the modeling assumptions made in this study.

Configuration of System and Modeling Assumptions

Physically, the system consists of a satellite (target) and an aircraft equipped with a radar tracking device. The radar system is equipped with three rate gyros to measure the three components of the tracker inertial angular velocity. For the purposes of this study, it is assumed that the tracker base is inertially stabilized such that the tracker Y axis always lies parallel to the inertial X-Y equatorial plane (see Figure 1 and discussion in the next section). In addition, it is assumed that uncorrupted tracker inertial position and velocity information is available from an inertial navigation system (INS) on the aircraft. (This implies that the aircraft is assumed to be a rigid body, non-collocation

errors are negligible, and INS errors are small enough to be neglected.) It is assumed that the tracking system has a control loop capable of instantaneously correcting the tracker angular velocities according to the optimal estimates of the rate errors provided by the extended Kalman Filter. Imperfect measurements of the range to the target and the small angular deviations between the tracker boresight and the true line of sight will also be available from the radar system.

Satellite State Equations

The system model for the satellite will be presented in this section. The dynamics model used in Mitchell's earlier work was designed to account for all accelerations greater than 10^{-12} Km/sec^2 (Ref 4:7). Because of limitations in the standardized computer program used to perform this covariance analysis, the solar pressure perturbative acceleration was deleted from the system model. To account for this unmodeled effect, the strengths of the driving noises on the satellite state equations were increased by an appropriate amount.

The target state equations are expressed in the geocentric equatorial nonrotating coordinate system with the X-axis lying along the line of the mean vernal equinox (Figure 1). This coordinate system will be considered to be an inertial frame for this application.

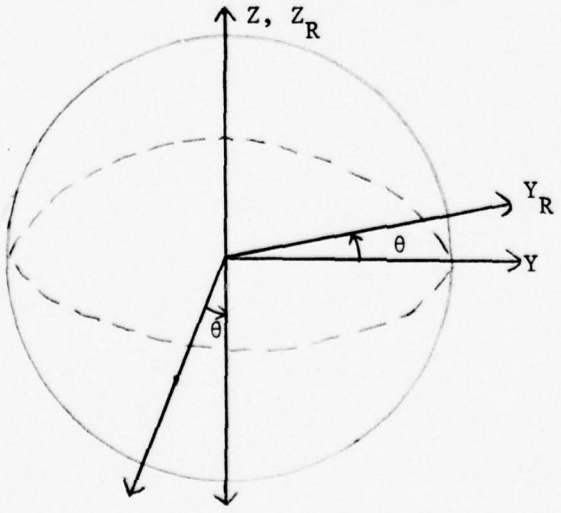

Figure 1. Inertial and Rotating (R) Coordinate Systems

The state equations describing the satellite's motion are

$$\dot{X}_1 = X_4$$
$$\dot{X}_2 = X_5$$
$$\dot{X}_3 = X_6$$
$$\dot{X}_4 = A_{g_1} + A_{m_1} + A_{s_1} + A_{d_1} + W_1$$
$$\dot{X}_5 = A_{g_2} + A_{m_2} + A_{s_2} + A_{d_2} + W_2$$
$$\dot{X}_6 = A_{g_3} + A_{m_3} + A_{s_2} + A_{d_2} + W_3 \qquad (2\text{-}2)$$

where

X_1, X_2, X_3 represent the target inertial position components along the X, Y, Z axes respectively

X_4, X_5, X_6 represent the target inertial velocity

$\underline{A}_g$ is the earth's gravitational acceleration vector

$\underline{A}_m$ is the lunar gravitational perturbation vector

$\underline{A}_s$ is the solar gravitational perturbation vector

$\underline{A}_d$ is the atmospheric drag acceleration vector

W_1, W_2, W_3 are zero-mean independent white Gaussian noises included to account for unmodeled effects such as solar pressure perturbations and higher order gravitational terms, and uncertainties in the models used in this study, such as deviations in the atmospheric density.

In order to determine the strengths of the white noises, consider the following. For a relatively small satellite - in a 200 Km circular, near polar orbit - with a solar pressure coefficient equal to that of a vehicle with a projected surface towards the sun of $10m^2$ and a ballistic coefficient of 1.5, the terms of $\dot{X}_4$ have deterministic values of:

$A_{g_1} = -7.55 \times 10^{-3}$ Km/sec^2 - acceleration due to full gravity

$A_{m_1} = +5.0 \times 10^{-10}$ Km/sec^2 - lunar perturbative acceleration

$A_{s_1} = +2.0 \times 10^{-12}$ Km/sec^2 - solar gravitational perturbative acceleration

$A_{d_1} = -9.0 \times 10^{-12}$ Km/sec^2 - drag acceleration.

These values have been determined using the models proposed later in this section with the satellite at 30° north latitude and the sun and moon positioned for worst case effects. The unmodeled solar pressure perturbation on the satellite under these assumptions would be -2.0×10^{-12} Km/sec^2. Because of the aforementioned criteria of modeling all perturbative accelerations of magnitude greater than 10^{-12} Km/sec^2, a reasonable value for the contribution to the distribution standard deviation of W_1 due to modeling uncertainty and higher order effects is 1×10^{-12} Km/sec^2. Taking into account the unmodeled effects due to the solar pressure perturbations, W_1, W_2, and W_3 are modeled a zero mean independent white Gaussian noises with distribution one σ values of 3×10^{-12} Km/sec^2.

Gravitational Field Modeling

Modeling of the earth's gravitational field is accomplished in a geocentric, equatorial, rotating coordinate frame. The relationship between this frame $R(X_R, Y_R, Z_R)$ and the inertial I(X, Y, Z) coordinate frame used in the previous section is shown in Figure 1. The transformation matrix from the rotating (R) to the inertial (I) frame C_R^I is defined as

$$C_R^I = \begin{bmatrix} \cos\theta & -\sin\theta & 0 \\ \sin\theta & \cos\theta & 0 \\ 0 & 0 & 1 \end{bmatrix} \qquad (2\text{-}3)$$

where

$$\theta = \theta g + \omega_e t$$

and

θ_g = local sidereal time at t = 0

ω_e = earth's angular rotation rate (7.292×10^{-5} rad/sec)

t = time.

The potential model that was chosen includes tesseral, zonal, and sectorial harmonics up to and including (6,6) (Ref 5:173-180). The gravitational potential $U(X_R, Y_R, Z_R)$ in the R frame is (Ref 5,175)

$$U = \frac{k_e^2 m}{r}\left[1 + \sum_{k=2}^{6}\left(\sum_{m=0}^{6} P_k^{(m)} \frac{\sin\phi}{r^k}\left\{C_{k,m}\cos(m\lambda_E) + S_{k,m}\sin(m\lambda_E)\right\}\right)\right] \tag{2-4}$$

where the terms in Equation (2-4) are defined as follows:

$P_k^{(m)}(\sin\phi)$ are Legendre functions:

$$P_k^{(m)}(\sin\phi) = (1 - \sin\phi)^{m/2} \frac{d^m}{d(\sin\phi)^m}\{P_k(\sin\phi)\}$$

and $P_k(\sin\phi)$ is the Legendre polynomial with argument $\sin\phi$.

m is the mass of the earth (5.983×10^{24} Kg)

k_e is the gravitational constant for the earth ($k_e^2 = 3.986 \times 10^5$ Km^3/sec^2)

r is the radial distance from the earth's center to the satellite

ϕ is the geocentric declination angle of the satellite

λ_E is the longitude of the satellite with respect to the prime meridian.

$S_{k,m}$ and $C_{k,m}$ are the harmonic coefficients for the gravitational potential such that $C_{k,0} = -J_k^{(0)}$ and $S_{k,0} = 0$ and the $J_k^{(0)}$ coefficients are the zonal harmonics.

$C_{k,m}$ and $S_{k,m}$ are termed tesseral harmonics if $m \neq k$, $m > 0$ and sectorial harmonics if $m = k$ (Ref 4:115-117).

The components of the gravitational acceleration vector along the X_R, Y_R, Z_R axes - $A_{g_{X_R}}$, $A_{g_{Y_R}}$, $A_{g_{Z_R}}$ - can now be determined by

$$(\underline{A}_g)^R \triangleq \begin{bmatrix} A_{g_{X_R}} \\ A_{g_{Y_R}} \\ A_{g_{Z_R}} \end{bmatrix} = \begin{bmatrix} \frac{\partial U}{\partial X_R} \\ \frac{\partial U}{\partial Y_R} \\ \frac{\partial U}{\partial Z_R} \end{bmatrix} \tag{2-5}$$

and the gravitational acceleration vector in the inertial frame can be determined from

$$(\underline{A}_g)^I = C_R^I (\underline{A}_g)^R \tag{2-6}$$

Lunar and Solar Perturbative Accelerations

The perturbative accelerations on the satellite due to the lunar and solar gravitational fields will be discussed in this section. Because the time elapsed during a complete tracking pass is small when compared to the inertial dynamics of the moon and sun, they will be considered stationary for the purposes of this study.

The lunar perturbative acceleration vector in the inertial frame is denoted by $(\underline{A}_m)^I$, with the components along the inertial X, Y, and Z axes denoted by Am_1, Am_2, and Am_3 respectively. The position vector of the moon in the inertial frame is denoted as

$$(\underline{Rm})^I = \begin{bmatrix} Xm \\ Ym \\ Zm \end{bmatrix} \tag{2-7}$$

The position vector of the moon relative to the vehicle is denoted by

$$(\underline{Rms})^I = (\underline{Rm})^I - (\underline{Rs})^I \triangleq \begin{bmatrix} Xm - X_1 \\ Ym - X_2 \\ Zm - X_3 \end{bmatrix}$$

and the perturbative acceleration on the vehicle (satellite) due to the moon's gravitational field is

$$(\underline{Am})^I \triangleq \mu\mathbb{C} \begin{bmatrix} \frac{Xm - X_1}{r_{ms}^3} - \frac{Xm}{r_m^3} \\ \frac{Ym - X_2}{r_{ms}^3} - \frac{Ym}{r_m^3} \\ \frac{Zm - X_3}{r_{ms}^3} - \frac{Zm}{r_m^3} \end{bmatrix} \tag{2-8}$$

where

$\mu\mathbb{C}$ = gravitational parameter of the moon (4.903×10^3 Km^3/sec^2)

$Xms = Xm - X_1$

$$Yms = Ym - X_2$$

$$Zms = Zm - X_3$$

$$r_{ms} = (X_{ms}^2 + Y_{ms}^2 + Z_{ms}^2)^{1/2}$$

$$r_m = (X_m^2 + Y_m^2 + Z_m^2)^{1/2}$$

X_1, X_2, X_3 = the satellite position in inertial frame.

In an entirely analogous manner the perturbative acceleration due to the sun's gravitational field is

$$(\underline{A}_{sun})^I \triangleq \begin{bmatrix} A_{s_1} \\ A_{s_2} \\ A_{s_3} \end{bmatrix} \tag{2-9}$$

The position vector of the sun in inertial frame is defined as

$$(\underline{R}_{sun})^I = \begin{bmatrix} X_{sun} \\ Y_{sun} \\ Z_{sun} \end{bmatrix} \tag{2-10}$$

and the perturbative acceleration on the vehicle due to the sun's gravitational field is

$$(\underline{A}_{sun})^I \triangleq \mu_{\odot} \begin{bmatrix} \frac{X_{sun} - X_1}{r_{ss}^3} - \frac{X_{sun}}{r_s^3} \\ \frac{Y_{sun} - X_2}{r_{ss}^3} - \frac{Y_{sun}}{r_s^3} \\ \frac{Z_{sun} - X_3}{r_{ss}^3} - \frac{Z_{sun}}{r_s^3} \end{bmatrix} \tag{2-11}$$

where

$\mu_{\odot}$ = gravitational parameter of the sun (1.327×10^{11} Km^3/sec^2)

$x_{ss} = X_{sun} - x_1$

$y_{ss} = Y_{sun} - x_2$

$z_{ss} = Z_{sun} - x_3$

$r_{ss} = (x_{ss}^2 + y_{ss}^2 + z_{ss}^2)^{1/2}$

$r_s = (x_s^2 + y_s^2 + z_s^2)^{1/2}$

Acceleration Due to Drag

Drag accelerations on the satellite are modeled as a function of the height above the earth's surface, the velocity of the satellite relative to the rotating atmosphere and the vehicle ballistic coefficient:

$$(\underline{A}d)^I = \frac{1}{2} \rho B |\underline{V}_a| (\underline{V}_A)^I \qquad (2\text{-}12)$$

where

$(\underline{A}d)^I$ = drag acceleration vector in inertial frame

$(\underline{V}_a)^I = \begin{bmatrix} x_4 + \omega_e x_2 \\ x_5 - \omega_e x_1 \\ x_6 \end{bmatrix}$ = velocity of satellite relative to rotating atmosphere

B = ballistic coefficient of the satellite

ρ = atmospheric density, modeled as $\rho = \rho_o e^{-\beta h}$

ρ_o = mean sea level atmospheric density (1.376229 Kg/Km^3)

β = altitude atmospheric density decay rate (1.395×10^{-4}/Km)

$h = (x_1^2 + x_2^2 + x_3^2)^{1/2} - R_o$ = height above mean earth radius

R_o = mean earth radius (6.37817×10^3 Km)

ω_e = angular rotation rate of the earth.

While the ballistic coefficient of the vehicle is generally not known, it is known that for a nonthrusting vehicle it will not change significantly during the time of a tracking pass (an attitude maneuver could affect it by changing the surface area along the velocity vector). It is assumed in this study that the ballistic coefficient can be adequately modeled as a random bias (a random variable that has 100% correlation in time)

$$\dot{B} = 0 \tag{2-13}$$

with an initial condition as a Gaussian random variable.

Tracker State Equations

While the target state equations are straightforward and represent a commonly used model for satellite dynamics, the tracker state dynamics and measurement equations are very dependent upon the modeling assumptions made in this study. Therefore, a full development of the tracker dynamic state equations and then the tracking system measurement equations will be given in this section.

The geometry of the tracker is shown in Figure 2.

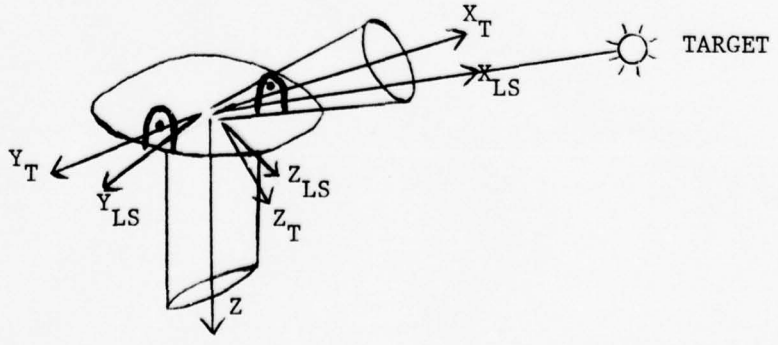

Figure 2. Tracker and Line-of-Sight Geometry

It is assumed that the tracker base is inertially stabilized such that the tracker elevation axis, Y_T, always lies in the inertial X-Y plane. The X_T axis is along the boresight of the tracker and the Z_T axis completes a right-hand orthogonal system. Assuming that the tracker base is inertially stabilized as above, the two Euler angle rotations needed to go from the inertial to the tracker frame are dependent only upon the relative position vector from the tracker to the target, expressed in inertial coordinates. The first Euler angle rotation is by an angle θ about the inertial Z axis as shown in Figure 3.

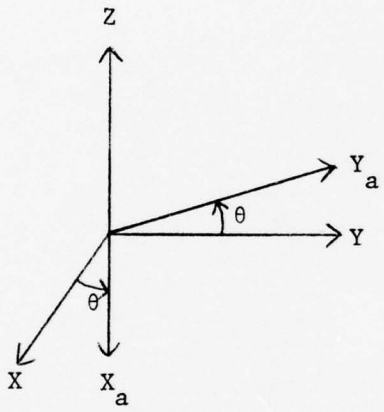

Figure 3. First Euler Angle Rotation

The subscript "a" indicates an intermediate frame and the transformation matrix C_I^a is

$$C_I^a = \begin{bmatrix} \cos\theta & \sin\theta & 0 \\ -\sin\theta & \cos\theta & 0 \\ 0 & 0 & 1 \end{bmatrix} \qquad (2\text{-}14)$$

Because of the constraint on the Y_T axis, the next Euler angle rotation is by an angle ϕ about the Y_a axis - leaving the Y_T axis in the inertial

XY plane. A planar view of this rotation is shown in Figure 4.

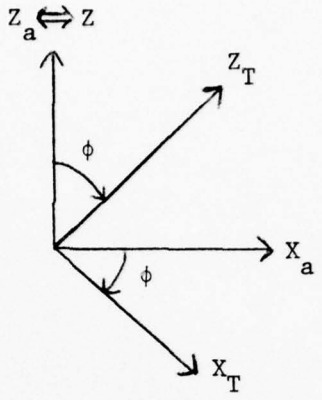

Figure 4. Planar View of Second Euler Angle Rotation

The transformation matrix between the intermediate "a" frame and the tracker "T" frame is

$$C_a^T = \begin{bmatrix} \cos\phi & 0 & -\sin\phi \\ 0 & 1 & 0 \\ \sin\phi & 0 & \cos\phi \end{bmatrix} \tag{2-15}$$

Therefore, the Euler angle transformation from the inertial to the tracker (T) frame is given by C_I^T as is shown in Figure 5.

$$C_I^T = C_a^T C_I^a = \begin{bmatrix} \cos\theta\cos\phi & \cos\phi\sin\theta & -\sin\phi \\ -\sin\theta & \cos\theta & 0 \\ \cos\theta\sin\phi & \sin\phi\sin\theta & \cos\phi \end{bmatrix} \tag{2-16}$$

The line-of-sight (LS) coordinate frame, though not directly discernible to the user, is widely used in pointing and tracking problems. The LS and T frames have the same origin; however, the LS frame has one axis

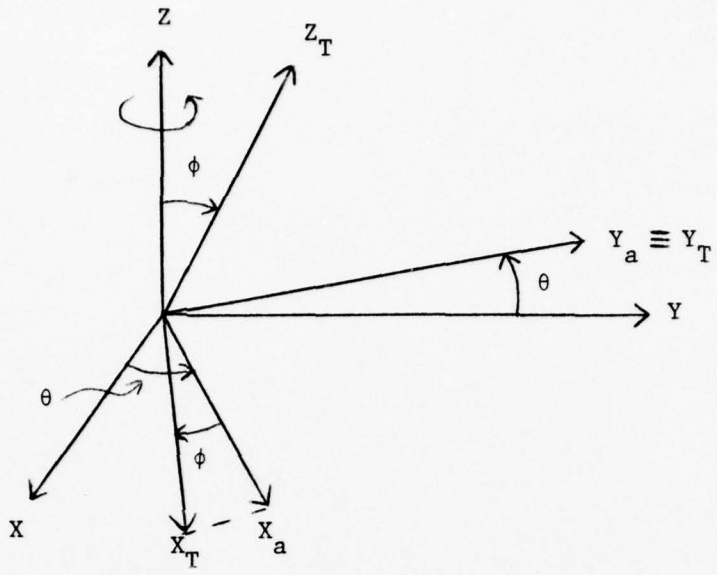

Figure 5. Inertial and Tracker Frame Orientations

pointing exactly at the target while the T frame is misaligned from this line-of-sight. In this study we will assume that the LS X-axis points directly at the target as was shown in Figure 2. For perfect tracking, the LS and T frames are aligned i.e. $C_I^T = C_I^{LS}$. Let $(\underline{R}_{ST})^I$ denote the position vector of the satellite with respect to the tracker expressed in the inertial frame:

$$(\underline{R}_{ST})^I \triangleq \begin{bmatrix} R_X \\ R_Y \\ R_Z \end{bmatrix} \tag{2-17}$$

Coordinatizing this vector in the LS frame

$$(\underline{R}_{ST})^{LS} = C_I^{LS}(\underline{R}_{ST})^I \tag{2-18}$$

However, by definition of the LS frame $(\underline{R}_{ST})^{LS} = \begin{bmatrix} R \\ 0 \\ 0 \end{bmatrix}$ where R is the range between the target and the tracker. Remembering that $C_I^{LS} \approx C_I^T$ (for perfect tracking $C_I^{LS} = C_I^T$)

$$\begin{bmatrix} R \\ 0 \\ 0 \end{bmatrix} \approx \begin{bmatrix} \cos\theta\cos\phi & \sin\theta\cos\phi & -\sin\phi \\ -\sin\theta & \cos\theta & 0 \\ \cos\theta\sin\phi & \sin\theta\sin\phi & \cos\phi \end{bmatrix} \begin{bmatrix} R_X \\ R_Y \\ R_Z \end{bmatrix} \tag{2-19}$$

then

$$-R_X\sin\theta + R_Y\cos\theta = 0 \rightarrow \frac{R_Y}{R_X} = \tan\theta$$

or

$$\left.\begin{aligned} \theta &= \tan^{-1}\left(\frac{R_Y}{R_X}\right) && R_X > 0 \\ \theta &= \tan^{-1}\frac{R_Y}{R_X} + \pi && R_X < 0 \end{aligned}\right\} \text{ Quadrant Determination} \tag{2-20}$$

Also,

$$R_X\cos\theta\sin\phi + R_Y\sin\theta\sin\phi + R_Z\cos\phi = 0$$

which implies,aafter some algebraic manipulation, that

$$\tan\phi = \frac{-R_Z}{(R_X^2 + R_Y^2)^{1/2}} \tag{2-21}$$

and therefore

$$\left.\begin{aligned} \phi &= \cos^{-1}\left[\frac{(R_X^2 + R_Y^2)^{1/2}}{(R_X^2 + R_Y^2 + R_Z^2)^{1/2}}\right] && R_Z < 0 \\ \phi &= -\phi && R_Z > 0 \end{aligned}\right\} \text{ Quadrant Determination} \tag{2-22}$$

For the suboptimal filter models used in this study it is assumed that the angles ϕ and θ will be obtained directly from resolvers. However, the relationships derived above are used in the linearized equations used for the extended Kalman Filter formulation and in generating simulated resolver data in the covariance analysis of the proposed suboptimal filters.

In practice, perfect tracking in which the tracker X axis aligns perfectly with the LS X axis will not be possible. The misalignment between the tracker and LS frames can be defined in terms of two Euler angle rotations. In a manner entirely similar to the previous derivation, the Euler angle rotations are $\delta\eta$ about the Z_T axis and $\delta\varepsilon$ about an intermediate ($Y_a \equiv Y_{LS}$) axis as shown in Figure 6 and,

$$C_T^{LS} = \begin{bmatrix} \cos\delta\eta\cos\delta\varepsilon & \sin\delta\eta\cos\delta\varepsilon & -\sin\delta\varepsilon \\ -\sin\delta\eta & \cos\delta\eta & 0 \\ \cos\delta\eta\sin\varepsilon & \sin\delta\eta\sin\delta\varepsilon & \cos\delta\varepsilon \end{bmatrix} \tag{2-23}$$

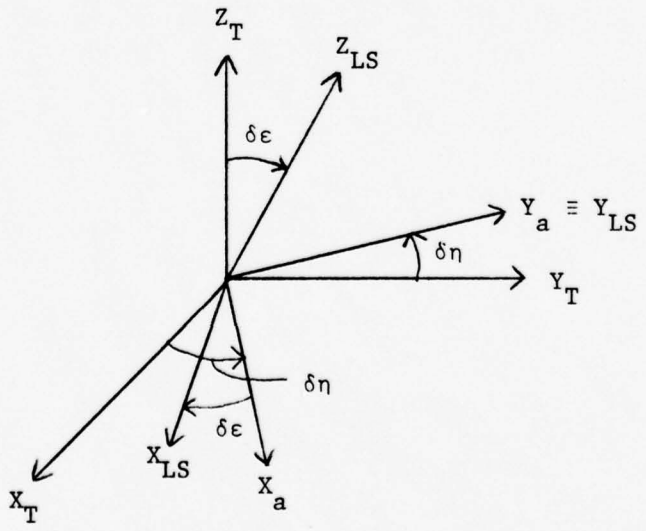

Figure 6. Tracker and Line-of-Sight Frame Orientations

It is reasonable to assume that $\delta\varepsilon$ and $\delta\eta$ are sufficiently small - even at the beginning of the track - to use the small angle approximations

$$\sin\delta\varepsilon \approx \delta\varepsilon \qquad \sin\delta\eta \approx \delta\eta$$

$$\cos\delta\varepsilon \approx 1 \qquad \cos\delta\eta \approx 1$$

In which case, Equation (2-23) becomes

$$C_T^{LS} = \begin{bmatrix} 1 & \delta\eta & -\delta\varepsilon \\ -\delta\eta & 1 & 0 \\ \delta\varepsilon & 0 & 1 \end{bmatrix} \tag{2-24}$$

We now seek relations for the time rate of change of $\delta\eta$ and $\delta\varepsilon$. The cross product matrix $[\omega_{LS}]$ for writing $[\omega_{LS}]\underline{V} = \underline{\omega}_{LS} \times \underline{V}$ is described in terms of the angular velocity of the LS frame with respect to the inertial frame coordinatized in the LS frame as the following skew symmetric form

$$[\omega_{LS}] = \begin{bmatrix} 0 & -\omega_{LS_Z} & \omega_{LS_Y} \\ \omega_{LS_Z} & 0 & -\omega_{LS_X} \\ -\omega_{LS_Y} & \omega_{LS_X} & 0 \end{bmatrix}$$

where the elements of the matrix represent angular velocities about the particular axes subscripted. In a similar manner, $[\omega_T]$, in terms of the angular velocity of the T frame with respect to inertial space coordinatized in the T frame is

$$[\omega_T] = \begin{bmatrix} 0 & -\omega_{T_Z} & \omega_{T_Y} \\ \omega_{T_Z} & 0 & -\omega_{T_X} \\ -\omega_{T_Y} & \omega_{T_X} & 0 \end{bmatrix}$$

From Broxmeyer's work we know that (Ref 13:26-27)

$$\dot{C}^T_{LS} = C^T_{LS}[\omega_{LS}] - [\omega_T]C^T_{LS}$$

Premultiplying by C^{LS}_T yields

$$C^{LS}_T \dot{C}^T_{LS} = [\omega_{LS}] - C^{LS}_T [\omega_T] C^T_{LS} \tag{2-25}$$

where - using Equation (2-24)

$$\dot{C}^T_{LS} = \begin{bmatrix} 0 & -\dot{\delta\eta} & \dot{\delta\varepsilon} \\ \dot{\delta\eta} & 0 & 0 \\ -\dot{\delta\varepsilon} & 0 & 0 \end{bmatrix}$$

Then

$$C^{LS}_T \dot{C}^T_{LS} = \begin{bmatrix} \delta\eta\dot{\delta\eta} + \delta\varepsilon\dot{\delta\varepsilon} & -\dot{\delta\eta} & \dot{\delta\varepsilon} \\ \dot{\delta\eta} & \delta\eta\dot{\delta\eta} & -\delta\eta\dot{\delta\varepsilon} \\ -\dot{\delta\varepsilon} & -\dot{\delta\eta}\delta\varepsilon & \delta\varepsilon\dot{\delta\varepsilon} \end{bmatrix} \tag{2-26}$$

If second order terms are neglected then Equation (2-26) becomes

$$C^{LS}_T \dot{C}^T_{LS} = \begin{bmatrix} 0 & -\dot{\delta\eta} & \dot{\delta\varepsilon} \\ \dot{\delta\eta} & 0 & 0 \\ -\dot{\delta\varepsilon} & 0 & 0 \end{bmatrix}$$

which is equal to

$$\omega_{LS} - C_T^{LS}\omega_T C_{LS}^T = \begin{bmatrix} 0 & -\omega_{LS_Z} & \omega_{LS_Y} \\ \omega_{LS_Z} & 0 & -\omega_{LS_X} \\ -\omega_{LS_Y} & \omega_{LS_X} & 0 \end{bmatrix} - \begin{bmatrix} 1 & \delta\eta & -\delta\varepsilon \\ -\delta\eta & 1 & 0 \\ \delta\varepsilon & 0 & 1 \end{bmatrix}$$

$$\begin{bmatrix} 0 & -\omega_{T_Z} & \omega_{T_Y} \\ \omega_{T_Z} & 0 & -\omega_{T_X} \\ -\omega_{T_Y} & \omega_{T_X} & 0 \end{bmatrix} \begin{bmatrix} 1 & -\delta\eta & \delta\varepsilon \\ \delta\eta & 1 & 0 \\ -\delta\varepsilon & 0 & 1 \end{bmatrix}$$

$$= \begin{bmatrix} 0 & (\omega_{T_Z} + \delta\varepsilon\omega_{T_X} - \omega_{LS_Z}) & (\omega_{LS_Y} - \omega_{T_Y} + \delta\eta\omega_{T_X}) \\ -(\omega_{T_Z} + \delta\varepsilon\omega_{T_X} - \omega_{LS_Z}) & 0 & (\delta\eta\omega_{T_Y} - \delta\varepsilon\omega_{T_Z} + \omega_{T_X} - \omega_{LS_X}) \\ -(\omega_{LS_Y} - \omega_{T_Y} + \delta\eta\omega_{T_X}) & -(\delta\eta\omega_{T_Y} - \delta\varepsilon\omega_{T_Z} + \omega_{T_X} - \omega_{LS_X}) & 0 \end{bmatrix}$$

Using the above equation with Equation (2-26) it is evident that

$$\left.\begin{aligned} \dot{\delta\eta} &= \omega_{LS_Z} - \omega_{T_Z} - \delta\varepsilon\omega_{T_X} \\ \dot{\delta\varepsilon} &= \omega_{LS_Y} - \omega_{T_Y} + \delta\eta\omega_{T_X} \\ \omega_{LS_X} &= \omega_{T_X} + \delta\eta\omega_{T_Y} - \delta\varepsilon\omega_{T_Z} \end{aligned}\right\} \qquad (2\text{-}27)$$

The first two equations of Equations (2-27) describe the time propagation of the error misalignment angles $\delta\varepsilon$ and $\delta\eta$. The last equation in (2-27) will prove useful in the following development of the time evolution of the line-of-sight angular velocity vector $\underline{\omega}_{LS}$.

In order to determine expressions for the time rate of change of the line-of-sight angular velocity vector, consider the position vector of

the satellite with respect to the aircraft $\underline{R}_{ST}$. Differentiating $\underline{R}_{ST}$ twice with respect to time and applying Coriolis' Theorem each time yields

$$\left.\frac{d^2\underline{R}_{ST}}{dt^2}\right|_I = \left.\frac{d^2\underline{R}_{ST}}{dt^2}\right|_{LS} + 2\underline{\omega}_{LS} \times \left.\frac{d\underline{R}_{ST}}{dt}\right|_{LS} + \left.\frac{d\underline{\omega}_{LS}}{dt}\right|_{LS} \times \underline{R}_{ST}$$

$$+ \underline{\omega}_{LS} \times (\underline{\omega}_{LS} \times \underline{R}_{ST}) \qquad (2\text{-}28)$$

where the vertical bar indicates the frame in which the differentiation takes place. Coordinatizing Equation (2-28) in the LS frame and defining the inertial acceleration of the satellite relative to the tracker along the line-of-sight X, Y, and Z axes as

$$\left(\left.\frac{d^2\underline{R}_{ST}}{dt^2}\right|_I\right)^{LS} \triangleq \begin{bmatrix} A_{rel_X} \\ A_{rel_Y} \\ A_{rel_Z} \end{bmatrix} \triangleq (\underline{A}_{rel})^{LS} = (\underline{A}_{satellite})^{LS} - (\underline{A}_{tracker})^{LS}$$

and

$$(\underline{R}_{ST})^{LS} \triangleq \begin{bmatrix} R \\ 0 \\ 0 \end{bmatrix}$$

$$\left[\left.\frac{d\underline{R}_{ST}}{dt}\right|_{LS}\right]^{LS} \triangleq \begin{bmatrix} V_r \\ 0 \\ 0 \end{bmatrix} \quad \text{where } V_r \triangleq \dot{R} = \text{range rate}$$

the following is obtained

$$\begin{bmatrix} A_{rel_X} \\ A_{rel_Y} \\ A_{rel_Z} \end{bmatrix} = \begin{bmatrix} \dot{V}_r \\ 0 \\ 0 \end{bmatrix} + 2\begin{bmatrix} 0 \\ V_r\omega_{LS_Z} \\ -V_r\omega_{LS_Y} \end{bmatrix} + \begin{bmatrix} 0 \\ R\dot{\omega}_{LS_Z} \\ -R\dot{\omega}_{LS_Y} \end{bmatrix} + \begin{bmatrix} -R(\omega^2_{LS_Y} + \omega^2_{LS_Z}) \\ R\omega_{LS_X}\omega_{LS_Y} \\ R\omega_{LS_X}\omega_{LS_Z} \end{bmatrix} \quad (2\text{-}29)$$

Examination of Equation (2-29) yields the following scalar state equations

$$\dot{\omega}_{LS_Y} = \frac{-A_{rel_Z}}{R} - \frac{2V_r\omega_{LS_Y}}{R} + \omega_{LS_X}\omega_{LS_Z} \quad (2\text{-}30)$$

$$\dot{\omega}_{LS_Z} = \frac{A_{rel_Y}}{R} - \frac{2V_r\omega_{LS_Z}}{R} - \omega_{LS_X}\omega_{LS_Y} \quad (2\text{-}31)$$

$$\dot{R} = V_r \quad (2\text{-}32)$$

$$\dot{V}_r = A_{rel_X} + R(\omega^2_{LS_Y} + \omega^2_{LS_Z}) \quad (2\text{-}33)$$

Defining $(\underline{A}_r)^T$ as the inertial acceleration of the satellite relative to the tracker, coordinatized in the tracker frame, Equation (2-24) can be used to obtain

$$(\underline{A}_{rel})^{LS} = C_T^{LS}(\underline{A}_r)^T = C_T^{LS}\begin{bmatrix} A_{r_X} \\ A_{r_Y} \\ A_{r_Z} \end{bmatrix} \quad (2\text{-}34)$$

thus, it follows that

$$A_{rel_X} = A_{r_X} + \delta\eta A_{r_Y} - \delta\varepsilon A_{r_Z} \quad (2\text{-}35)$$

$$A_{rel_Y} = A_{r_Y} - \delta\eta A_{r_X} \tag{2-36}$$

$$A_{rel_Z} = A_{r_Z} + \delta\epsilon A_{r_X} \tag{2-37}$$

Equations (2-30,31,33) now become

$$\dot{\omega}_{LS_Y} = \frac{-A_{r_Z} - \delta\epsilon A_{r_X}}{R} - \frac{2V_r \omega_{LS_Y}}{R} + \omega_{LS_X}\omega_{LS_Y} \tag{2-38}$$

$$\dot{\omega}_{LS_Z} = \frac{A_{r_Y} - \delta\eta A_{r_X}}{R} - \frac{-2V_r \omega_{LS_Z}}{R} - \omega_{LS_X}\omega_{LS_Y} \tag{2-39}$$

$$\dot{V}_r = A_{r_X} + \delta\eta A_{r_Y} - \delta\epsilon A_{r_Z} + R(\omega^2_{LS_Y} + \omega^2_{LS_Z}) \tag{2-40}$$

Using the third of Equation (2-27) to eliminate ω_{LS_X} from Equations (2-38,39) yields

$$\dot{\omega}_{LS_Y} = -\frac{A_{r_Z}}{R} - \frac{2V_r \omega_{LS_Y}}{R} + \omega_{LS_Z}\omega_{T_X} + \{\frac{-\delta\epsilon}{R} A_{r_X}$$

$$+ \omega_{LS_Z}[\delta\eta\omega_{T_Y} - \delta\epsilon\omega_{T_Z}]\} \tag{2-41}$$

$$\dot{\omega}_{LS_Z} = \frac{A_{r_Y}}{R} - 2V_r\omega_{LS_Z} - \omega_{LS_Y}\omega_{T_X} + \{\frac{-\delta\eta A_{r_X}}{R}$$

$$- \omega_{LS_Y}[\delta\eta\omega_{T_Y} - \delta\epsilon\omega_{T_Z}]\} \tag{2-42}$$

The bracketed {·} terms in Equations (2-41,42) represent effects due to the misalignment between the tracker and LS frames. For the case of perfect tracking ($\delta\epsilon=\delta\eta=0$) these terms equal zero.

Measurement Equations

The tracking system has the capability of measuring the inertial angular velocity of the tracker, the two angular deviations $\delta\varepsilon$ and $\delta\eta$, and the range between the tracker and the target. The models used in the measurement equations are developed in References 1, 6, and 7.

The inertial angular velocity of the tracker is measured in the tracker coordinate frame by three rate gyros, one mounted along each tracker axis. While the system (truth) model propagates the true line-of-sight angular velocities ω_{LS_Y} and ω_{LS_Z} [Equations (2-41,42)], measurements are available only in the tracker frame of ω_{T_X}, ω_{T_Y}, and ω_{T_Z}. Therefore, measurements of ω_{T_Y} and ω_{T_Z} are considered by the filter to be pseudo-measurements of ω_{LS_Y} and ω_{LS_Z} which are not available. The dominant effects which contribute to errors in the rate gyro measurements are scale factor errors, drift errors, g-sensitive mass unbalance errors, misalignment errors, and white noise (V_1). A suggested gyro rate measurement model (Ref 7:300) is given as (tracker x-axis only)

$$\omega_{M_X} = \omega_{Tr_X} + B_{gsf_X}\omega_{Tr_X} + \sum_{i=1}^{3} B_{gm_{X_i}} A_i + C_{g_X} + [\Delta C_{gma}\omega_{Tr}]_X + V_1 \quad (2\text{-}43)$$

where

ω_{M_X} = measured angular velocity along X_T axis.

ω_{Tr_X} = true angular velocity along X_T axis.

B_{gsf_X} = constant bias gyro scale factor.

$B_{gm_{X_i}}$ = coefficients (along X, Y, Z directions in tracker frame) of the g-sensitive mass unbalance to which the gyro is subject.

A_i = accelerations (A_{T_X}, A_{T_Y}, A_{T_Z}) of the tracker origin with respect to inertial space.

C_{g_X} = gyro drift rate along X_T axis.

ΔC_{gma} = the error angle transformation matrix resulting from the misalignments of the three gyros.

$$\Delta C_{gma} \triangleq \begin{bmatrix} 0 & -B_{gma_{12}} & B_{gma_{13}} \\ B_{gma_{21}} & 0 & -B_{gma_{23}} \\ -B_{gma_{31}} & B_{gma_{32}} & 0 \end{bmatrix}$$

$B_{gma_{ij}}$ = gyro misalignment error angles between the desired gyro coordinates and the actual gyro coordinates (mounting errors).

$[\cdot]_i$, i = X,Y,Z = i^{th} component of the vector $[\cdot]$

V_1 = additive zero mean white Gaussian noise to account for unmodeled effects such as aniso-elastic drift, quantization error, etc.

Because it shows a certain degree of time correlation, C_{g_X}, the gyro drift component along the tracker X-axis, is modeled as an exponentially time-correlated random process.

Suppose that the gyro in question has been studied in the laboratory and the drift along the X-axis has been determined to have a steady state standard deviation of σ_4 radians per second, with a process correlation time of τ_4 seconds. The question then becomes one of modeling this random variable as the output of a linear system driven by white Gaussian noise. After this is accomplished, this model is augmented to the previously modeled satellite and tracker state equations. A zero-mean exponentially time-correlated Gaussian random process of variance σ_4 and correlation time τ_4 can be modeled as the output of a first order lag with lag parameter $\beta_4 = 1/\tau_4$, driven by a zero mean white Gaussian noise of unit strength, as shown in Figure 7:

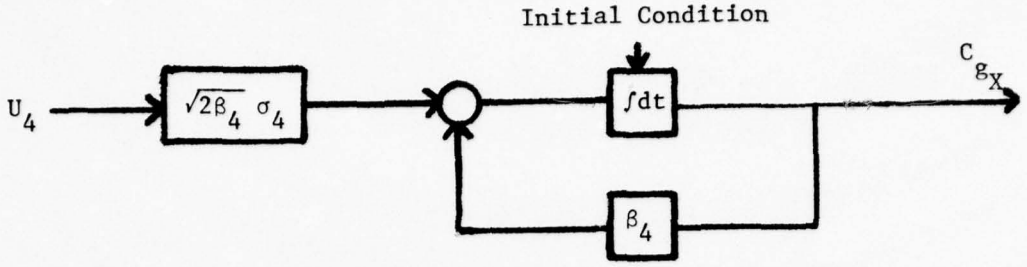

Figure 7. Gyro Drift Modeling

The state equation for C_{g_X} is

$$\dot{C}_{g_X} = -\beta_4 C_{g_X} + \sqrt{2\beta_4}\ \sigma_4 U_4 \tag{2-44}$$

The autocorrelation function of C_{g_X} is the desired decreasing exponential

$$E\{C_{g_X}(t)C_{g_X}(t+\tau)\} = \sigma_4^2 e^{-\beta_4|\tau|} \tag{2-45}$$

The remaining coefficients in the rate gyro measurement equation are modeled as random biases.

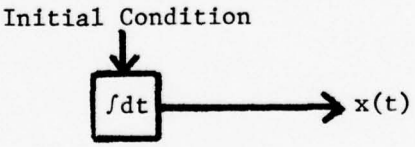

Figure 8. Random Bias Modeling

By using this model, the filter is "told" that the value of the variable does not change in time, although you do not know its magnitude apriori (Ref 3:204). This represents a reasonable model for the remaining coefficients because while they may not be constant on a long term basis, they will remain essentially constant during a ten minute tracking pass.

As seen from Figure 8, the general form of the state equation for these coefficients is $\dot{X} = 0$. The equation which describes the way the covariance propagates in time is

$$\dot{P} = 0 \tag{2-46}$$

This indicates that the variance of the coefficient does not change in time and that the initial condition on P represents the variance of the coefficient about its mean.

The measurements of the tracker angular velocity about the tracker Y and Z axes are modeled in a manner identical to ω_{M_X}. The values used for the standard deviations and the process correlation time in the gyro rate measurement model are representative of a typical aircraft rate gyro (Ref 7:302):

Quantity	Steady State Standard Deviation	Process Correlation Time
Gyro drift	1×10^{-6} rad/sec	3600 sec
Gyro scale factors	5×10^{-4}	∞
Gyro mass unbalance coefficients	3×10^{-6} rad-sec/m	∞
Gyro misalignment coefficients	1×10^{-4}	∞
Additive white Gaussian noise (V_1)	1×10^{-9} rad/sec	0

The error misalignment angles $\delta\varepsilon$ and $\delta\eta$ are measured in the tracking coordinate frames. Effects which can degrade these measurements are: deterministic scale factors, scale factor errors, angle track biases, and angle track scintillation noises. No attempt has been made to model noises that are specific to a typical radar or laser ranger. Rather,

the measurement model proposed below is representative of a large class of measurement devices (Ref 6:14)

$$\delta\varepsilon_M = K_1(\delta\varepsilon_{Tr} + S_\varepsilon) + C_{SF_\varepsilon}\delta\varepsilon_{Tr} + B_{AT_\varepsilon} + V_4 \tag{2-47}$$

$$\delta\eta_M = K_2(\delta\eta_{Tr} + S_\eta) + C_{SF_\eta}\delta\eta_{Tr} + B_{AT_\eta} + V_5 \tag{2-48}$$

where

K_1, K_2 = deterministic scale factors.

$\delta\varepsilon_{Tr}, \delta\eta_{Tr}$ = true misalignment angles.

S_ε, S_η = angle track scintillation noises.

$C_{SF_\varepsilon}, C_{SF_\eta}$ = scale factor errors.

$B_{AT_\varepsilon}, B_{AT_\eta}$ = angle track biases.

V_4, V_5 = zero mean white Gaussian noises to account for unmodeled effects.

Both the angle track scintillation noises and the scale factor errors are modeled as exponentially time correlated random variables. Scintillation noise is dependent upon various factors such as atmospheric propagation, and amplifier characteristics which change as a function of time during a typical tracking pass. Scale factor errors are a function of certain tracker variables that undergo a change with respect to time (Ref 6:15). Therefore, in a manner similar to Equation (2-44), we write

$$\begin{aligned}
\dot{S}_\varepsilon &= -\beta_1 S_\varepsilon + \sqrt{2\beta_1}\,\sigma_1 U_1 \\
\dot{S}_\eta &= -\beta_2 S_\eta + \sqrt{2\beta_2}\,\sigma_2 U_2 \\
\dot{C}_{SF_\varepsilon} &= -\beta_7 C_{SF_\varepsilon} + \sqrt{2\beta_7}\,\sigma_7 U_7 \\
\dot{C}_{SF_\eta} &= -\beta_8 C_{SF_\eta} + \sqrt{2\beta_8}\,\sigma_8 U_8
\end{aligned} \tag{2-49}$$

Where U_1, U_2, U_7, U_8 are zero mean white Gaussian noises with unit variance, and the β's and σ's represent the inverse of the process correlation time and the standard deviation of the process respectively. The angle track bias coefficients B_{AT_ε} and B_{AT_η} are modeled as random biases - initial value unknown but describable as a Gaussian random variable with mean zero and a known variance. The values used for the process standard deviations and correlation times are given below. For the purposes of this study K_1 and K_2 are assumed to equal one. (Ref 4:149)

Quantity	Steady State Standard Deviation	Process Correlation Time
Angle track scintillations (S_ε,S_η)	1×10^{-6} rad	10 sec
Angle measurement scale factor errors (C_{SF_ε},C_{SF_η})	10^{-4}	300 sec
Angle track bias (B_{AT_ε},B_{AT_η})	2×10^{-6} rad	∞
Additive white noise	1×10^{-6} rad	0

The model of the measurement of range is very similar to those of the angular deviations. Uncertainties in the measurement of range are due primarily to scintillation noise and bias errors.

$$R_M = K_R(R_{Tr} + S_R) + B_R + V_6 \tag{2-50}$$

where

K_R = deterministic scale factor.

S_R = range scintillation noise.

R_{Tr} = true range.

B_R = range bias.

V_6 = zero mean white Gaussian noise to account for unmodeled effects.

The range scintillation noise is due to atmospheric effects and errors in the digitization of the returned signal. The atmospheric effects in particular are a direct function of the elevation angle of the tracker - less scintillation error when the satellite is directly "overhead" and greater errors at the horizon. The scintillation error will show a degree of time correlation during a tracking pass and an exponentially time correlated random variable is used to model this state:

$$\dot{S}_R = -\beta_3 S_R + \sqrt{2\beta_3}\,\sigma_3 U_3 \tag{2-51}$$

where U_3 is a zero mean white Gaussian noise with unit variance, and β_3 and σ_3 are the inverse of the process correlation time and its standard deviation respectively. The range bias is modeled as a random bias. (Initial value unknown, but describable as a zero mean Gaussian random variable and known variance.) Values used for the standard deviations and correlation times are shown below (Ref 4:150).

Quantity	Steady State Standard Deviation	Process Correlation Time
Range Scintillation	.020 Km	10 sec
Range bias	.005 Km	∞
Additive white noise	.005 Km	0

Summary of State and Measurement Equations

After augmenting the satellite and tracker state equations with the noise states needed to define the measurements, the truth model contains a total of 42 states. They are repeated here for clarity.

State Equations

(1) $\dot{X}_1 = X_4$

(2) $\dot{X}_2 = X_5$

(3) $\dot{X}_3 = X_6$

} Satellite inertial position

(4) $\dot{X}_4 = A_{g_1} + A_{m_1} + A_{s_1} + A_{d_1} + W_1$

(5) $\dot{X}_5 = A_{g_2} + A_{m_2} + A_{s_2} + A_{d_2} + W_2$

(6) $\dot{X}_6 = A_{g_3} + A_{m_3} + A_{s_3} + A_{d_3} + W_3$

} Satellite inertial velocity

(7) $\dot{\omega}_{LS_Y} = \frac{-A_{r_Z}}{R} - \frac{2V_r\omega_{LS_Y}}{R} + \omega_{LS_Z}\omega_{T_X} + \left\{\frac{-\delta\varepsilon}{R} A_{r_X} + \omega_{LS_Z}\right.$

$\left.[\delta\eta\omega_{T_Y} - \delta\varepsilon\omega_{T_Z}]\right\}$ Tracker angular velocity

(8) $\dot{\omega}_{LS_Z} = \frac{A_{r_Y}}{R} - \frac{2V_r\omega_{LS_Z}}{R} - \omega_{LS_Y}\omega_{T_X} + \left\{\frac{-\delta\eta A_{r_X}}{R} - \omega_{LS_Y}\right.$

$\left.[\delta\eta\omega_{T_Y} - \delta\varepsilon\omega_{T_Z}]\right\}$ Tracker angular velocity

(9) $\dot{\delta\eta} = \omega_{LS_Z} - \omega_{T_Z} - \delta\varepsilon\omega_{T_X}$ Error misalignment angle

(10) $\dot{\delta\varepsilon} = \omega_{LS_Y} - \omega_{T_Y} + \delta\eta\omega_{T_X}$ Error misalignment angle

(11) $\dot{R} = V_r$ Range

(12) $\dot{V}_r = A_{r_X} + \delta\eta A_{r_Y} - \delta\varepsilon A_{r_Z} + R(\omega^2_{LS_Y} + \omega^2_{LS_Z})$ Range rate

(13) $\dot{X}_{13} = 0$ Satellite ballistic coefficient

(14) $\dot{S}_{\varepsilon} = -\beta_1 S_{\varepsilon} + \sqrt{2\beta_1}\,\sigma_1 U_1$

(15) $\dot{S}_{\eta} = -\beta_2 S_{\eta} + \sqrt{2\beta_2}\,\sigma_2 U_2$

} Angle track scintillation

(16) $\dot{S}_R = -\beta_3 S_R + \sqrt{2\beta_3}\,\sigma_3 U_3$ Range scintillation

(17) $\dot{C}_{g_X} = -\beta_4 C_{g_X} + \sqrt{2\beta_4}\,\sigma_4 U_4$

(18) $\dot{C}_{g_Y} = -\beta_5 C_{g_Y} + \sqrt{2\beta_5}\,\sigma_5 U_5$

(19) $\dot{C}_{g_Z} = -\beta_6 C_{g_Z} + \sqrt{2\beta_6}\,\sigma_6 U_6$

} Gyro drift

(20) $\dot{C}_{SF_{\varepsilon}} = -\beta_7 C_{SF_{\varepsilon}} + \sqrt{2\beta_7}\,\sigma_7 U_7$

(21) $\dot{C}_{SF_{\eta}} = -\beta_8 C_{SF_{\eta}} + \sqrt{2\beta_8}\,\sigma_8 U_8$

} Angle measurement scale factors

(22) $\dot{B}_{gm_{X_1}} = 0$

-- -- --

(30) $\dot{B}_{gm_{Z_3}} = 0$

} Coefficients of gyro mass unbalance (nine equations)

(31) $\dot{B}_{gma_{12}} = 0$

(32) $\dot{B}_{gma_{13}} = 0$

(33) $\dot{B}_{gma_{21}} = 0$

} Gyro misalignment coefficients
(cont'd on next page)

(34) $\dot{B}_{gma_{23}} = 0$

(35) $\dot{B}_{gma_{31}} = 0$

(36) $\dot{B}_{gma_{32}} = 0$

} Gyro misalignment coefficients (cont'd)

(37) $\dot{B}_R = 0$ Range bias

(38) $\dot{B}_{AT_\varepsilon} = 0$

(39) $\dot{B}_{AT_\eta} = 0$

} Angle track bias

(40) $\dot{B}_{gsf_X} = 0$

(41) $\dot{B}_{gsf_Y} = 0$

(42) $\dot{B}_{gsf_Z} = 0$

} Gyro scale factors

Measurement Equations

(1) $\omega_{M_X} = \omega_{Tr_X} + B_{gsf_X}\omega_{Tr_X} + \sum_{i=1}^{3} B_{gm_{X_i}} A_i + C_{g_X}$

$+ [\Delta C_{gma}\omega_{Tr}]_X + V_1$ measurement of ω_{T_X}

(2) $\omega_{M_Y} = \omega_{Tr_Y} + B_{gsf_Y}\omega_{Tr_Y} + \sum_{i=1}^{3} B_{gm_{X_i}} A_i + C_{g_Y}$

$+ [\Delta C_{gma}\omega_{Tr}]_Y + V_2$ measurement of ω_{T_Y}

$$(3)\quad \omega_{M_Z} = \omega_{Tr_Z} + B_{gsf_Z}\omega_{Tr_Z} + \sum_{i=1}^{3} B_{gm_{Z_i}} A_i + C_{g_Z}$$

$$+ [\Delta C_{gma}\omega_{Tr}]_Z + V_3 \quad \text{measurement of } \omega_{T_Z}$$

where

$$\left.\begin{aligned} A_1 &= A_{T_X} \\ A_2 &= A_{T_Y} \\ A_3 &= A_{T_Z} \end{aligned}\right\} \quad \text{Acceleration of tracker origin in tracker coordinates}$$

$$(4)\quad \delta\eta_M = K_1(\delta\eta_{Tr} + S_\eta) + C_{SF_\eta}\delta\eta_{Tr} + B_{AT_\eta} + V_4 \quad \text{measurement of } \delta\eta$$

$$(5)\quad \delta\varepsilon_M = K_2(\delta\varepsilon_{Tr} + S_\varepsilon) + C_{SF_\varepsilon}\delta\varepsilon_{Tr} + B_{AT_\varepsilon} + V_5 \quad \text{measurement of } \delta\varepsilon$$

$$(6)\quad R_M = K_R(R_{Tr} + S_R) + B_R + V_6 \quad \text{measurement of R}$$

Only measurements (2) - (6) above correspond to measurements of states of the system. There is no state equation relating the motion of the tracker about the line-of-sight X-axis.because angular velocity about the line-of-sight has no significance for purposes of tracking. Thus, ω_{T_X} is not measured because it is considered to be a system parameter.

III. Kalman Filter Formulation

Introduction

In this chapter, the propagation and update equations for both linear and extended Kalman filtering will be presented. Listed below are some of the definitions used in this chapter.

$\underline{X}(t_i)$ = system state at time t_i (n-vector)

$\hat{\underline{X}}(t_i^-)$ = filter estimate prior to incorporating a measurement at time t_i (n-vector)

$\hat{\underline{X}}(t_i^+)$ = filter estimate after incorporating a measurement at time t_i (n-vector)

$\Phi(t_{i+1},t_i)$ = state transition matrix from time t_i to time t_{i+1}

$P(t_i^-)$ = filter covariance matrix of state $\underline{X}(t_i)$, also of the error in the estimate of $\underline{X}(t_i)$, prior to incorporating a measurement at time t_i (nxn matrix)

$P(t_i^+)$ = filter covariance matrix of state $\underline{X}(t_i)$, also of the error in the estimate of $\underline{X}(t_i)$, after incorporating a measurement at time t_i (nxn) matrix

$F(t)$ = system dynamics matrix (nxn), defined for all time

$G(t)$ = system input matrix (nxs), defined for all time

$\underline{\omega}(t)$ = system dynamics white Gaussian noise s-vector, independent of $\underline{X}(t_o)$, where $E[\underline{\omega}(t)] = \underline{0}$, $E[\underline{\omega}(t)\underline{\omega}^T(\tau)] \triangleq Q(t)\delta(t - \tau)$. $\underline{\omega}(t)$ is assumed to be zero mean, Gaussian, and white (uncorrelated in time) with Q(t) an sxs positive semidefinite symmetric matrix that is in general piecewise continuous in t.

$H(t_i)$ = system observation matrix at time t_i (mxn)

$R(t_i)$ = positive definite measurement noise covariance matrix (mxm)

$\underline{Z}(t_i)$ = m vector of measurements at time t_i

$K(t_i)$ = Kalman gain matrix (nxm) defined at time t_i

$\underline{V}(t_i)$ = zero mean, white Gaussian, measurement noise sequence independent of $\underline{\omega}(t)$ and $\underline{X}(t_o)$ for all time (m vector). The statistics of $\underline{V}(t_i)$ are $E[\underline{V}(t_i)] = 0$, and

$$E[\underline{V}(t_i)\underline{V}(t_j)] = \begin{cases} \underline{R}(t_i) & t_i = t_j \\ 0 & \text{otherwise} \end{cases}$$

Linear Kalman Filter Formulation

The linear Kalman filter formulation presented in this section is for a continuous time system model with discrete time updates. Assume that the system modeling has been completed and that the state vector $\underline{X}(t)$ satisfies the vector stochastic differential equation

$$\dot{\underline{X}}(t) = F(t)\underline{X}(t) + G(t)\underline{\omega}(t) \qquad (3\text{-}1)$$

The state equation is propagated forward in time from the initial condition $\underline{X}(t_o)$. Since the exact initial condition may not be known, it is modeled as being a Gaussian random variable with mean $\underline{X}_o$ and covariance P_o.

$$E[\underline{X}(t_o)] = \hat{\underline{X}}_o, \; E\{[\underline{X}(t_o) - \hat{\underline{X}}_o][\underline{X}(t_o) - \hat{\underline{X}}_o]^T\} = P_o \tag{3-2}$$

It can be shown (Ref 3:157-163) that, under the assumption that $\underline{X}(t_o)$ is either deterministic or a Gaussian random variable, the solution $\underline{X}(t)$ to linear stochastic differential equations such as Equation (3-1) is a Gauss-Markov process, i.e. the conditional density of $\underline{X}$ at time t_i based upon all realizations of $\underline{X}$ through time t_{i-1} is both Gaussian and completely determined by the process value at t_{i-1}. Because the conditional density is Gaussian, it is completely specified by its mean and covariance (Ref 8:92). The initial covariance matrix P_o may be positive semidefinite, admitting exact knowledge of the initial conditions of some of the states.

Measurements are available at discrete time points and are assumed to be of the form of a linear combination of the states and corrupted by a white Gaussian sequence (Ref 9:2):

$$\underline{Z}(t_i) = H(t_i)\underline{X}(t_i) + \underline{V}(t_i) \tag{3-3}$$

The state estimate propagates between measurements (from time t_{i-1}^+ to time t_i^-) according to

$$\hat{X}(t_i^-) = \Phi(t_i, t_{i-1})\hat{X}(t_{i-1}^+) \tag{3-4}$$

and the covariance propagates according to

$$P(t_i^-) = \Phi(t_i,t_{i-1})P(t_{i-1}^+)\Phi^T(t_i,t_{i-1})$$

$$+ \int_{t_{i-1}}^{t_i} \Phi(t_i,\tau)G(\tau)Q(\tau)G^T(\tau)\Phi(t_i,\tau)^T d\tau \qquad (3\text{-}5)$$

At measurement time t_i, the estimate is updated according to (Ref 3:233)

$$\underline{\hat{X}}(t_i^+) = \hat{X}(t_i^-) + \underline{K}(t_i)[\underline{\zeta}_i - H(t_i)\underline{\hat{X}}(t_i^-)] \qquad (3\text{-}6)$$

$$P(t_i^+) = P(t_i^-) - K(t_i)H(t_i)P(t_i) \qquad (3\text{-}7)$$

where

$$K(t_i) = P(t_i^-)H^T(t_i)[H(t_i)P(t_i^-)H^T(t_i) + R(t_i)]^{-1} \qquad (3\text{-}8)$$

where $[\ ]^{-1}$ indicates the inverse of the bracketted matrix and $\underline{\zeta}_i$ the realized value of the measurement $\underline{Z}(t_i)$ at time t_i.

Under the assumption that the adequate system model is linear, and that the dynamic driving and measurement noises are Gaussian and white, the Kalman filter provides the optimal estimate $\underline{\hat{X}}(t_i^+)$ of the state of the system (Ref 3:66,214), relative to many optimality criteria, i.e. $\underline{\hat{X}}(t_i^+)$ is the mean, mode, and median of the conditional density of $\underline{X}(t_i)$, conditioned on the entire measurement history through time t_i. The covariance of the error committed by using $\underline{\hat{X}}(t_i^+)$ as the estimate of the state at time t_i is denoted by $P(t_i^+)$. It should be noted that for a linear estimation problem, the covariance propagation [Equations (3-5,7)],

while depending on $R(t_1)$, is independent of the measurements $\underline{z}_1$. This will no longer be the case in the extended Kalman filter formulation.

The assumption that the system can be modeled as being driven by white Gaussian noise is often well founded on two accounts. First, it has been found from practical experience that the Gaussian distribution provides a reasonable approximation to observed random behavior in certain physical systems (Ref 8:92). Secondly, the central limit theorem (Ref 8:96) states that if the random phenomenon that we observe at the macroscopic level, is due to the superposition of an extremely large number of independent random processes on the microscopic level, then the macroscopic phenomenon can be adequately modeled as a Gaussian random variable (Ref 3:40).

Extended Kalman Filter Formulation (Ref 9:179-189)

The extended Kalman Filter formulation is commonly used in estimation problems in which the adequate state and/or measurement equations are nonlinear rather than linear. Consider, as before, a system that is continuous in time with measurements at discrete sampling times. Assume that the system state satisfies the following nonlinear vector stochastic differential equation

$$\dot{\underline{X}}(t) = \underline{f}[\underline{X}(t),t] + G(t)\underline{\omega}(t) \tag{3-9}$$

where $\underline{f}(\underline{X},t)$ is a nonlinear function of the states and time [in general $\underline{f}$ could also be a function of deterministic control inputs $\underline{u}(t)$], and the vector $\underline{\omega}(t)$ of zero mean white Gaussian driving noises enters in a linear additive manner. The initial condition of $\underline{X}(t_o)$ is modeled as a Gaussian random variable with mean $\hat{\underline{X}}_o$ and covariance P_o. Noise corrupted

vector measurements of a (possibly) nonlinear function of the states and time are available at discrete times t_i as

$$\underline{Z}(t_i) = \underline{h}[\underline{X}(t_i), t_i] + \underline{V}(t_i) \tag{3-10}$$

where $\underline{V}(t_i)$ is a zero mean white Gaussian sequence with covariance kernel (Ref 9:180).

$$E[\underline{V}(t_i)\underline{V}(t_j)] = \begin{cases} R(t_i) & i = j \\ 0 & \text{otherwise} \end{cases} \tag{3-11}$$

To better understand the concepts upon which the extended Kalman filter is based, let's first look at the derivation of a linearized Kalman filter. There exists a deterministic nominal trajectory $\underline{X}_n(t)$ such that

$$\underline{X}(t) = \underline{X}_n + \delta\underline{X}(t) \tag{3-12}$$

where $\delta\underline{X}(t)$ represents the perturbation of the state from the nominal and $\dot{\underline{X}}_n(t)$ satisfies

$$\dot{\underline{X}}_n = \underline{f}[\underline{X}_n(t), t]; \quad \underline{X}_n(t_o) = \underline{X}_{n_o} \tag{3-13}$$

and $\underline{X}_{n_o}$ represents the initial condition of the state on the nominal trajectory $\underline{X}(t_o)$. Associated with the nominal trajectory is a set of deterministic measurements at t_i.

$$\underline{Z}_n(t_i) = \underline{h}[X_n(t_i), t_i] \tag{3-14}$$

From Equations (3-9,12,13) it is evident that

$$[\dot{\underline{X}}(t) - \dot{\underline{X}}_n(t)] = \underline{f}[\underline{X}(t),t] - \underline{f}[\underline{X}_n(t),t] + G(t)\underline{\omega}(t) \tag{3-15}$$

The variational equation, which is a first order approximation to Equation (3-15), is found by expanding Equation (3-15) in a Taylor series about the nominal trajectory and neglecting all but first order terms (Ref 8:58).

$$\delta\dot{\underline{X}}(t) = \underline{F}[t;\underline{X}_n(t)]\delta\underline{X}(t) + G(t)\underline{\omega}(t) \tag{3-16}$$

where $\underline{F}[t;\underline{X}_n(t)]$ is the matrix of partial derivatives of $\underline{f}$ with respect to $\underline{X}$ evaluated along the nominal trajectory $X_n(t)$

$$\underline{F}[t;\underline{X}_n(t)] \triangleq \left.\frac{\partial \underline{f}[\underline{X}_n(t),t]}{\partial \underline{X}}\right|_{\underline{X}(t) = \underline{X}_n(t)} \tag{3-17}$$

Note that $\underline{F}$ is dependent upon $\underline{X}_{n_o}$ because it is evaluated along $\underline{X}_n(t)$. In an entirely similar manner, the linearized measurement equation for the error in the measurement at time t_i is developed in the following equations

$$\underline{Z}(t_i) = Z_n(t_i) + \delta\underline{Z}(t_i) \tag{3-18}$$

then from Equations (3-10,14)

$$[\underline{Z}(t_i) - \underline{Z}_n(t_i)] = \underline{h}[\underline{X}(t_i),t_i] - \underline{h}[\underline{X}_n(t_i),t_i] + \underline{V}(t_i) \tag{3-19}$$

and

$$\underline{\delta Z}(t_i) = \underline{H}[t_i, \underline{X}(t_i)]\underline{\delta X}(t_i) + \underline{V}(t_i) \tag{3-20}$$

where $\underline{H}[t_i, \underline{X}(t_i)]$ is the matrix of partial derivatives of $\underline{h}$ with respect to $\underline{X}$ evaluated along the nominal trajectory $\underline{X}_n(t_i)$ (Ref 9:182).

$$\underline{H}[t_i, \underline{X}(t_i)] \triangleq \left. \frac{\partial \underline{h}[\underline{X}(t_i), t_i]}{\partial \underline{X}} \right|_{\underline{X}(t_i) = \underline{X}_n(t_i)} \tag{3-21}$$

As long as the partial derivative matrices $\underline{H}$ and $\underline{F}$ exist, one can apply linear filtering theory to the linearized perturbation equations, Equations (3-16,20). However, it must be kept in mind that this linearized system of equations is only valid for small perturbations about the nominal trajectory (Ref 8:59). A rule of thumb which is often applied in defining "small" perturbations is that there be approximately an order of magnitude difference between the first and second terms in the Taylor series expansions which led to Equations (3-16,20) (Ref 9:183). If the nonlinearities are too pronounced, a higher order filter incorporating more terms in the Taylor series and using higher moments of $\underline{X}(t)$ may be applied (Ref 8:190-192).

In the extended Kalman filter formulation, the validity of the assumption that deviations from the nominal trajectory are "small" is maintained by relinearizing about the trajectory emanating from $\hat{\underline{X}}(t_i^+)$ once it has been computed (Ref 9:183-184). After relinearizing about this new "nominal"

$$\hat{\delta X}(t_i^+) = 0 \tag{3-22}$$

Letting $\hat{\delta X}(t|t_i)$ = the estimate of $\delta X(t)$ at time t, $t_i^+ \leq t < t_{i+1}^-$, based upon the realizations $\underline{\zeta}_i$ of measurements $\underline{Z}(t_i)$, through time t_i, the optimal estimate of the state error $[\hat{\delta X}(t|t_i)]$ propagates forward in time according to

$$\dot{\hat{\delta X}}(t|t_i) = \underline{F}[t;X_n(t,t_i)]\hat{\delta X}(t|t_i) \tag{3-23}$$

subject to the initial condition

$$\underline{\hat{\delta X}}(t_i|t_i) = \underline{\hat{\delta X}}(t_i^+) = \underline{0} \tag{3-24}$$

where $\underline{F}(t;\underline{X}_n(t|t_i)]$ = the relinearized evaluation of $\underline{F}$, where $\underline{X}_n(t|t_i)$ is the solution to the deterministic differential equation, $\dot{\underline{X}}_n(t|t_i) = \underline{f}[\underline{X}_n(t|t_i),t]$ propagated from the new initial condition of $\hat{\underline{X}}(t_i^+)$. Thus, the solution to Equation (3-23) is $\underline{\hat{\delta X}}(t|t_i) = \underline{0}$ over the entire interval $[t_i,t_{i+1})$, and $\underline{\hat{\delta X}}(t_{i+1}^-) = \underline{\hat{\delta X}}(t_{i+1}|t_i) = \underline{0}$ (Ref 9:185). This follows from the fact that Equation (3-23) is linear.

From Equations (3-6,16), the linearized system is updated at measurement time t_{i+1}^- according to

$$\underline{\hat{\delta X}}(t_{i+1}^+) = \underline{\hat{\delta X}}(t_{i+1}^-) + K(t_{i+1})[\underline{\delta\zeta}_{i+1} - H(t_{i+1})\hat{\delta X}(t_{i+1}^-)]$$

$$= K(t_{i+1})\underline{\delta\zeta}_{i+1} = K(t_{i+1})[\underline{\zeta}_{i+1} - \underline{h}[\underline{X}_n(t_{i+1}|t_i),t_{i+1}]] \tag{3-25}$$

Matrices evaluated along the most recent nominal trajectory $\underline{X}_n(t|t_i)$ are used to compute the Kalman filter gains $K(t_{i+1})$.

We now combine these results to achieve the final extended Kalman filter algorithm. Because $\underline{\hat{\delta X}}(t|t_i) = \underline{0}$ over the interval from t_i to t_{i+1} the best estimate of $\underline{X}(t)$ over this interval is the solution to (Ref 9:185)

$$\dot{\underline{\hat{X}}}(t|t_i) = \underline{f}[\underline{\hat{X}}(t|t_i),t] \tag{3-26}$$

with initial condition

$$\underline{\hat{X}}(t_i|t_i) = \underline{\hat{X}}(t_i^+) \tag{3-27}$$

At the next update time, t_{i+1}, from Equation (3-12)

$$\underline{\delta X}(t_{i+1}) = \underline{X}(t_{i+1}) - \underline{X}_n(t_{i+1}) \tag{3-28}$$

and the estimate of $\underline{\hat{\delta X}}(t_{i+1})$ is given by

$$\underline{\hat{\delta X}}(t_{i+1}^+) = \underline{\hat{X}}(t_{i+1}) - \underline{\hat{X}}(t_{i+1}|t_i) \tag{3-29}$$

where $\underline{\hat{X}}(t_{i+1}|t_i)$ is the solution to Equation (3-26) integrated forward from the initial condition of $\underline{\hat{X}}(t_i^+)$. Using the fact that the update for the state perturbation is given by Equation (3-25), the update equation for the state estimate at time t_{i+1} is given by (Ref 9:186)

$$\underline{\hat{X}}(t_{i+1}^+) = \underline{\hat{X}}(t_{i+1}|t_i) + K(t_{i+1})[\underline{\zeta}_{i+1} - \underline{h}[\underline{\hat{X}}(t_{i+1}|t_i),t_{i+1}]] \tag{3-30}$$

The covariance is propagated between t_i^+ and t_{i+1}^- by integrating

$$\dot{P}(t|t_i) = \underline{F}[t;\hat{\underline{X}}(t|t_i)]P + PF^T[t;\hat{\underline{X}}(t,t_i)]$$

$$+ G(t)Q(t)G^T(t) \tag{3-31}$$

from the initial conditions

$$\hat{\underline{X}}(t_i|t_i) \triangleq \hat{\underline{X}}(t_i^+),\ P(t_i|t_i) \triangleq P(t_i^+)$$

and is updated according to

$$P(t_{i+1}^+) = P(t_{i+1}^-) - K(t_{i+1})\underline{H}[t_{i+1},\hat{\underline{X}}(t_{i+1}^-)]P(t_{i+1}^-) \tag{3-32}$$

where

$$K(t_{i+1}) = P(t_{i+1}^-)H^T[t_{i+1},\hat{\underline{X}}(t_{i+1}^-)]\{H[t_{i+1},\hat{\underline{X}}(t_{i+1}^-)]P(t_{i+1}^-)$$

$$\cdot H^T[t_{i+1},\hat{X}(t_{i+1}^-)] + R(t_{i+1})\}^{-1} \tag{3-33}$$

Note that the Kalman gains and covariance propagation are no longer independent of the state estimate - and thus of the measurements - as they were in the linear estimator.

The next chapter of this study will present the development of a covariance analysis as a method for evaluating the performance of a reduced order filter. In a covariance analysis, the covariances of the filter and truth models are propagated without generating the actual filter estimate $\hat{\underline{X}}(t)$. However, as shown previously, the covariance propagation in an extended Kalman filter is dependent upon the state estimate through the partial derivative matrices $\underline{F}$ and $\underline{H}$. An approximate

covariance analysis can be accomplished by linearizing instead along a nominal reference trajectory $\underline{X}_n(t)$, i.e. $\underline{F}$ and H are evaluated using $\underline{X}_n(t)$ (Ref 9:186). Because a covariance analysis is viewed as a first step (to be followed by a Monte Carlo analysis) in determining the feasibility of a filter for a linear system model, it is of utmost importance that the results obtained using a linearized system model be viewed as tentative because deviations between $\underline{X}_n(t)$ and $\hat{\underline{X}}(t|t_i)$ may lead to a significant degradation in actual performance.

A covariance analysis costs much less in time and money than a Monte Carlo analysis and, in light of the above discussion, it still represents a viable first step in the analysis of a proposed extended Kalman filter design. It is to be viewed as a small scale analysis, assuming deviations from the a priori nominal are small - $\hat{\underline{X}}(t|t_i) \simeq \underline{X}_n(t)$. The partial derivative matrices $\underline{F}$ and $\underline{H}$ [Equations (3-16,20)] for the system model developed in Chapter II are described in Appendix A.

IV. Covariance Analysis of a Reduced Order Filter Model

In Chapter II the truth (system) model state and measurement equations were developed for the satellite tracker. The term "truth" model, though widely used in the literature, is slightly misleading in that it implies that the true system dynamics and measurements are exactly modeled. This is, of course, incorrect in that there is no way of predicting exactly what the actual system performance will be. Rather, the 42-state "truth" model is an attempt to account for the dominant system disturbances. When the speed and memory capabilities of airborne computer systems are examined, it becomes readily apparent that it would not be possible to implement the filter based upon this truth model. Therefore, as in most Kalman filter applications, suboptimal (reduced order) filter models are proposed to perform the task within the existing hardware and software capabilities. Several such designs are proposed in Chapter V. The obvious question becomes, how do you evaluate a suboptimal filter design? One widely used method is the covariance analysis. A covariance analysis provides a direct comparison between the covariance of the errors committed by the reduced order filter and the filter based on the truth model for a linear system. It also provides a comparison for the errors that the filter commits and the errors it "thinks" it commits.

However, a covariance analysis is viewed as only a first step in the evaluation of a proposed filter design. While the covariance equations provide RMS filter performance data directly, they do not represent a system simulation (Ref 3:361). Once the covariance analysis has proven the feasibility of the filter design, a Monte Carlo simulation is usually performed which uses the filter mechanization equations to process simulated data. While a Monte Carlo analysis is a better indicator of

expected filter performance, it is more costly in terms of time and money.

Covariance Analysis Equations

In this section, the covariance analysis equations will be briefly presented. The error states will be formulated by subtracting value of the optimal estimate of states in the filter from the values of these same states as provided by the truth model. A new state vector will then be formed by augmenting this error state vector with the suboptimal filter state vector. The result will be in the form of a linear system driven by white Gaussian noise and will allow us to apply linear analysis techniques to the augmented system to determine the covariance propagation and update equations for the augmented state. In practice, the estimates from the filter would be used in a closed loop control system. To simplify the developments presented here, control inputs will not be considered. The developments are based extensively on several reports prepared by Air Force Avionics Laboratory personnel (Ref 10,11).

Consider the truth model equations to be of the form

$$\dot{\underline{X}}_s(t) = F_s(t)\underline{X}_s(t) + G_s(t)\underline{\omega}_s(t) \qquad (4\text{-}1)$$

where

$\underline{X}_s$ is an n_1 state vector for the truth model

F_s is an $n_1 x n_1$ system dynamics matrix

G_s is an $n_1 x s_1$ gain matrix

$\underline{\omega}_s$ is an s_1 vector of zero mean white Gaussian noise inputs with variance $E[\underline{\omega}_s(t)\underline{\omega}_s^T(\tau)] = Q_s\delta(t - \tau)$.

Equation (4-1) is considered to represent the linearized error state equation - Equation (3-16) - for the truth model.

Consider also a reduced order filter model that satisfies the following state equation

$$\dot{\underline{X}}_f(t) = F_f\underline{X}_f(t) + G_f(t)\underline{\omega}_f(t) \tag{4-2}$$

where

$\underline{X}_f$ is an n_2 vector denoting the filter state ($n_2 < n_1$ in general)

F_f is an $n_2 x n_2$ filter dynamics matrix

G_f is an $n_2 x s_2$ gain matrix

$\underline{\omega}_f$ is an s_2 vector of zero mean white Gaussian noise inputs with variance $E[\underline{\omega}_f(t)\underline{\omega}_f^T(\tau)] = Q_f\delta(t - \tau)$.

System and filter model measurements will be considered to be available as discrete time sequences corrupted by zero mean white Gaussian noise sequences. For the system, measurements are modeled as

$$\underline{Z}_s(t_i) = H_s(t_i)\underline{X}_s(t_i) + \underline{V}_s(t_i) \tag{4-3}$$

where

$\underline{Z}_s(t_i)$ is an m vector of discrete time measurements

$H_s(t_i)$ is an $m x n_1$ system measurement matrix

$\underline{V}_s(t_i)$ is an m vector of zero mean white Gaussian noise sequences with variance $E[\underline{V}_s(t_i)\underline{V}_s(t_j)] = R_s(t_i)\delta_{ij}$

The filter's model for these same measurements is

$$\underline{Z}_f(t_i) = H_f(t_i)\underline{X}_f(t_i) + \underline{V}_f(t_i) \tag{4-4}$$

where

$\underline{Z}_f(t_i)$ is an m vector of discrete time measurements

$H_f(t_i)$ is an mxn_2 filter measurement matrix

$\underline{V}_f(t_i)$ is an m vector of zero mean white Gaussian noise sequences with variance $E[\underline{V}_f(t_i)\underline{V}_f^T(t_i)] = R_f\delta_{ij}$

Because the covariance analysis equations are only applicable to a linear system, Equation (4-4) is replaced by Equation (3-20), the linearized measurement error equation for the filter. The filter state estimate and covariance $(\hat{X}_f, P_f)$ are propagated and updated according to Equations (3-4) to (3-8), with the exception that the filter state estimate uses the realizations of the measurements provided by the system model - $\underline{\zeta}_s(t_i)$

$$\hat{\underline{X}}_f(t_i^+) = \hat{X}_f(t_i) + K_f(t_i)[\underline{\zeta}_s(t_i) - H_f(t_i)\hat{\underline{X}}_f(t_i^-)] \tag{4-5}$$

In order to develop the equations relating the statistical behavior of the actual error, the following definition of the actual estimation error is made (Ref 10:16). The error $\underline{e}(t)$ is defined as an n_2 vector expressing the error committed by using a particular filter and is evaluated as

$$\underline{e}(t) \triangleq \underline{X}_s(t) - T\hat{\underline{X}}_f(t) \tag{4-6}$$

where

$$T \triangleq [\underline{I} \vdots \underline{0}]^T$$

with

$\underline{I}$ = n_2xn_2 identity matrix

$\underline{0}$ = $(n_1-n_2)xn_2$ null matrix

What Equation (4-6) implies, of course, is that the first n_2 states of the system model are identical to the entire set of states in the filter. In practice, the filter model is usually the truth model with selected states removed. If this is not the case, T may be appropriately redefined without changing the final results (Ref 4:56).

The objective of the covariance analysis is to examine the time propagation of the covariance of $\underline{e}(t)$

$$P_{ee}(t) \triangleq E[\underline{e}(t)\underline{e}^T(t)]$$

Defining the augmented state vector $\underline{Y}(t)$ as

$$\underline{Y}(t) \triangleq \begin{bmatrix} \underline{e}(t) \\ \hline \underline{X}_f(t) \end{bmatrix} \tag{4-7}$$

then it can be shown that $\underline{Y}(t)$ satisfies the following stochastic differential equation

$$\dot{\underline{Y}}(t) = F(t)\underline{Y}(t) + G(t)\underline{\omega}_s(t) \tag{4-8}$$

where

$$F(t) \triangleq \begin{bmatrix} F_s(t) & F_s(t)T - TF_f(t) \\ 0 & F_f(t) \end{bmatrix}$$

$$G(t) \triangleq \begin{bmatrix} G_s \\ 0 \end{bmatrix}$$

and the second moment propagates according to

$$\dot{P}(t) = F(t)P(t) + P(t)F^T(t) + G(t)Q_s(t)G(t) \tag{4-9}$$

where

$$P(t) \triangleq \begin{bmatrix} P_{ee}(t) & P_{12}(t) \\ P_{21}(t) & P_f(t) \end{bmatrix}$$

The augmented state vector $\underline{Y}(t)$ is updated at a measurement according to (Ref 10:18)

$$\underline{Y}(t_i^+) = \begin{bmatrix} \underline{e}(t_i^+) \\ \hat{X}_f(t_i^+) \end{bmatrix} = \begin{bmatrix} I - TK_f(t_i)H_s(t_i) & TK_f(t_i)[H_f(t_i) - H_s(t_i)T] \\ K_f(t_i)H_s(t_i) & I + K_f(t_i)H_s(t_i)T - K_f(t_i)H_f(t_i) \end{bmatrix}$$

$$\begin{bmatrix} \underline{e}(t_i^-) \\ \hat{\underline{X}}_f(t_i^-) \end{bmatrix} + \begin{bmatrix} -TH_f(t_i) \\ K_f(t_i) \end{bmatrix} \underline{V}_s(t_i) \tag{4-10}$$

or

$$\underline{Y}(t_i^+) = A(t_i)\underline{Y}(t_i^-) + B(t_i)\underline{V}_s(t_i)$$

and the covariance is updated according to

$$P(t_i^+) = A(t_i)P(t_i^-)A^T(t_i) + B(t_i)R_s(t_i)B^T(t_i) \tag{4-11}$$

As stated before, the state equations for both truth and filter models must be linear before a covariance analysis can be performed. This is

accomplished by linearizing about a nominal trajectory. The usefulness of the results of the analysis depend upon the validity of assumption of linearity. To preserve this assumption, it is important to keep the interval between measurements small with respect to system time constants, and to keep the perturbations small about the assumed nominal trajectory. Effects of violating these conditions can be evaluated only through a subsequent Monte Carlo analysis.

V. Reduced Order Filter Models

Introduction

The purpose of this chapter is to develop the two reduced order system models for which covariance analyses were performed in this study. In all cases, the reduced order system model should be computationally simpler than the truth model, as this is usually the criterion which prevents the implementation of the filter based upon the truth model. How this simplification takes place is due to the decisions, skill, prior experience, etc. of the designer. In many cases, simplification is accomplished by deleting states from the truth model that represent nondominant effects in the problem under study. Typically, this is accomplished with a corresponding increase in strengths of noises driving the system to account for the neglected effects. For instance, while neglecting gyro drift rates as sources of error in a navigation filter may significantly degrade performance of the filter, the deletion of these states may not be deleterious in a tracking problem of ten minutes of duration. In addition to the deletion of states, another technique that is used is to delete terms in the state equations that are less than a third or a quarter of the size of the other terms in the expression, i.e. in addition to deleting nondominant states, we also delete nondominant terms in the remaining state equations. Careful judgment must be exercised in this latter case because these small cross coupling terms may be extremely important in meeting certain performance criteria for the system.

The first reduced order filter (hereafter referred to as Filter I) model represents a simplification to the truth model based upon the two criteria discussed above - deletion of states and nondominant terms. The second reduced order filter (Filter II) was suggested by the Air Force

Avionics Laboratory specifically for this study. The main thrust of this filter is to use what is known about the dominant dynamical modes of the vehicle being tracked to aid in the simplification of the truth model.

Filter I State Equation Development

The truth model developed in Chapter II has 42 states. The first 12 of these states model the satellite and tracker dynamics. State 13 was included to model the effect of atmospheric drag and the remainder of the states were included to model uncertainties in the measuring devices for angular tracking rates, tracker angular deviations from the line-of-sight and range.

Consider first the simplication of the first six of the state equations. They are repeated below for convenience

$$\dot{X}_1 = X_4 \tag{5-1}$$

$$\dot{X}_2 = X_5 \tag{5-2}$$

$$\dot{X}_3 = X_6 \tag{5-3}$$

$$\dot{X}_4 = A_{g_1} + A_{m_1} + A_{s_1} + A_{d_1} + W_1 \tag{5-4}$$

$$\dot{X}_5 = A_{g_2} + A_{m_2} + A_{s_2} + A_{d_2} + W_2 \tag{5-5}$$

$$\dot{X}_6 = A_{g_3} + A_{m_3} + A_{s_3} + A_{d_3} + W_3 \tag{5-6}$$

where

$\underline{A}_g$ = acceleration due to full gravity

$\underline{A}_m$ = perturbative acceleration due to the moon's gravitational field

$\underline{A}_s$ = perturbative acceleration due to the sun's gravitational field

$\underline{A}_d$ = acceleration due to atmospheric drag

W_i = zero mean white Gaussian driving noise, with variance

$$E\{W_1(t)W_1(\tau)\} = (3 \times 10^{-12} \text{ Km/sec}^2)^2 \, \delta(t - \tau)$$

As can be seen by the data presented on page 10 of this study, the dominant effect is that of the earth's gravitational field. The two body point mass acceleration accounts for all but (-2.0×10^{-9} Km/sec) of the effect (-7.55×10^{-6} Km/sec^2) due to full gravity (Ref 4:66). Therefore, the filter model chosen for the satellite dynamics is the basic two body point mass acceleration model. While this model would certainly be a poor choice for long tracking passes (long in the sense that the pass represents a significant portion of the orbital period), it is a reasonable model for the profile under test for which the typical tracking pass represents only 1/20th of the orbital period. The increase in uncertainty due to the reduced accuracy in the dynamics model is accounted for by increasing the strengths of the driving noises W_1, W_2, and W_3. Thus, the following relations are obtained:

$$\dot{X}_1 = X_4 \tag{5-7}$$

$$\dot{X}_2 = X_5 \tag{5-8}$$

$$\dot{X}_3 = X_6 \tag{5-9}$$

$$\dot{X}_4 = \frac{-\mu_\oplus X_1}{r_v^3} + W_1 \tag{5-10}$$

$$\dot{X}_5 = \frac{-\mu_\oplus X_2}{r_v^3} + W_2 \tag{5-11}$$

$$\dot{X}_6 = \frac{-\mu_\oplus X_3}{r_v^3} + W_3 \tag{5-12}$$

where

$\mu_\oplus$ = the earth's gravitational constant

$r_v = \sqrt{X_1^2 + X_2^2 + X_3^2}$ is the distance from the earth's center to the satellite

and W_1, W_2, W_3 were initially assigned one sigma values of 2×10^{-9} Km/sec, based upon the above analysis of the size of the unmodeled acceleration terms.

Consider now the tracker angular velocity state equations

$$\dot{\omega}_{LS_Y} = \frac{-A_{r_Z}}{R} - \frac{2V_r \omega_{LS_Y}}{R} + \omega_{LS_Z}\omega_{T_X} + \{\frac{-\delta\varepsilon}{R} A_{r_X}$$

$$+ \omega_{LS_Z}[\delta\eta\omega_{T_Y} - \delta\varepsilon\omega_{T_Z}]\} \tag{5-13}$$

$$\dot{\omega}_{LS_Z} = \frac{A_{r_Y}}{R} - \frac{2V_r \omega_{LS_Z}}{R} - \omega_{LS_Y}\omega_{T_X} + \{\frac{-\delta\eta}{R} A_{r_X}$$

$$- \omega_{LS_Y}[\delta\eta\omega_{T_Y} - \delta\varepsilon\omega_{T_Z}]\} \tag{5-14}$$

The bracketted terms {•} result from the fact that the tracker and line-of-sight frames are not coincident and differ by the two small Euler angles $\delta\varepsilon$ and $\delta\eta$. For high accuracy tracking, the small angular deviations $\delta\eta$ and $\delta\varepsilon$ will have magnitudes on the order of 10^{-5} radians or less (Ref 3:67). For the particular tracking profile used in this study, the bracketted terms are on the order of 10^{-11} radians/sec^2 while the smallest values of $\dot{\omega}_{LS_Y}$ and $\dot{\omega}_{LS_Z}$ are $\approx 10^{-6}$ radians/sec^2. Thus, in the reduced order filter model the bracketted terms are neglected and replaced by a zero mean white Gaussian driving noise to account for the increased uncertainty in the dynamics model:

$$\dot{\omega}_{LS_Y} = \frac{-A_{r_Z}}{R} - \frac{2V_r}{R}\omega_{LS_Y} + \omega_{LS_Z}\omega_{T_X} + W_4 \tag{5-15}$$

$$\dot{\omega}_{LS_Z} = \frac{A_{r_Y}}{R} - \frac{2V_r}{R}\omega_{LS_Z} - \omega_{LS_Y}\omega_{T_X} + W_5 \tag{5-16}$$

Initially, before the covariance analysis was tuned to give the best performance, W_4 and W_5 were assigned one-sigma values of 10^{-11} radians/sec^2, based upon the values of the bracketted terms that were dropped.

The remaining state equations are:

$$\dot{\delta\eta} = \omega_{LS_Z} - \omega_{T_Z} - \delta\varepsilon\omega_{T_X} \tag{5-17}$$

$$\dot{\delta\varepsilon} = \omega_{LS_Y} - \omega_{T_Y} + \delta\eta\omega_{T_X} \tag{5-18}$$

$$\dot{R} = V_r \tag{5-19}$$

$$\dot{V}_r = A_{r_X} + \delta\eta A_{r_Y} - \delta\varepsilon A_{r_Z} + R(\omega^2_{LS_Y} + \omega^2_{LS_Z}) \tag{5-20}$$

Equation (5-20) may be simplified using the same criteria as for Equations (5-13,14). For high accuracy tracking, the terms containing $\delta\eta$ and $\delta\varepsilon$ will be approximately five orders of magnitude smaller than $\dot{V}_r$. Therefore, in the proposed filter model, these two terms are dropped and replaced by a zero mean white Gaussian driving noise (W_6) of strength equal to (1×10^{-16} Km/sec^2):

$$\dot{V}_r = A_{r_X} + R(\omega^2_{LS_Y} + \omega^2_{LS_Z}) + W_6 \tag{5-21}$$

Filter I Measurement Equation Development

The measurement equations for the truth model are summarized at the end of Chapter II on page 37. In each case, the measurement is considered to be the sum of the state which is a realization of one stochastic process, and the noises are realizations or samples of other stochastic processes by our model. For instance, consider the measurement of the inertial angular velocity of the tracker along the tracker Y axis

$$\omega_{M_Y} = \omega_{Tr_Y} + B_{gsf_Y}\omega_{Tr_Y} + \sum_{i=1}^{3} B_{gm_{Y_i}} A_i + C_{g_Y} + [\Delta C_{gma}\omega_{Tr}]_Y + V_2 \tag{5-22}$$

where $\omega_{Tr} \triangleq [\omega_{Tr_X}\ \omega_{Tr_Y}\ \omega_{Tr_Z}]^T$ represents the true angular velocity of the tracker coordinatized in the tracker frame (it should be recalled that ω_{M_Y} and ω_{M_Z} are considered to be pseudomeasurements of the line-of-sight angular velocities ω_{LS_Y} and ω_{LS_Z} which are not directly measurable). The second through fifth terms in Equation (5-22) are stochastic models of the dominant noise processes that corrupt a rate gyro measurement. The last term, V_2, is a zero mean white Gaussian noise sequence added to account for errors in the modeling assumptions and unmodeled higher

order effects. B_{gsf_Y}, $B_{gm_{Y_1}}$, $B_{gm_{Y_2}}$, $B_{gm_{Y_3}}$ and the elements of the matrix ΔC_{gma} are all modeled as random biases, i.e. $\dot{X}(t) = 0$. For lack of better information they are modeled as zero mean with a variance determined from experimental evidence. Each of these stochastic processes is then multiplied times a deterministic quantity - the resulting product in each case being a random process. $\underline{\omega}_{Tr}$ at a given time is modelable as a sample value at that time from a stochastic process. The inertial acceleration of the tracker origin in tracker coordinates

$$(\underline{A}_T)^T = \begin{bmatrix} A_1 \\ A_2 \\ A_3 \end{bmatrix} = \begin{bmatrix} A_{T_X} \\ A_{T_Y} \\ A_{T_Z} \end{bmatrix}$$

is assumed to be a deterministic system parameter in this study for both Filter I and II. Note that both filters would require "ownship" accelerations in order to determine the relative acceleration in the tracker frame. The component of the gyro drift along the tracker Y axis, C_{g_Y}, is modeled as an exponentially time-correlated random process. In the filter measurement model, it is assumed that the total effect of all of the corruptive effects in each of the truth model measurement equations can be replaced by a single zero-mean white Gaussian noise sequence. The filter measurement model, for each state, consists of the "true value" plus an additive white noise to account for modeling uncertainties. For the state we chose as an example,

$$\omega_{M_Y} = \omega_{Tr_Y} + V_2 \qquad (5\text{-}23)$$

This approach to modeling the measurements leads to the simplest filter implementation. If the performance should prove to be poor using this model, the variance of V_2 could be increased to indicate additional uncertainty in the assumed measurement model. If performance remains poor, this would be an indication that some of the effects appearing in the truth model measurement equations must be added - at the expense of a higher dimensioned filter - to the filter measurement equations.

Summary of Filter I State and Measurement Equations

The state and measurement equations for the Filter I reduced order system model are summarized below. The development of the linearized dynamics and measurement matrices $\underline{F}$ and $\underline{H}$ for Filter I is given in Appendix B.

State Equations

(1) $\dot{X}_1 = X_4$

(2) $\dot{X}_2 = X_5$

(3) $\dot{X}_3 = X_6$

(4) $\dot{X}_4 = \frac{-\mu_\oplus X_1}{r_v^3} + W_1$

(5) $\dot{X}_5 = \frac{-\mu_\oplus X_2}{r_v^3} + W_2$

(6) $\dot{X}_6 = \frac{-\mu_\oplus X_3}{r_v^3} + W_3$

$$(7)\quad \dot{\omega}_{LS_Y} = \frac{-A_{r_Z}}{R} - \frac{2V_r\omega_{LS_Y}}{R} + \omega_{LS_Z}\omega_{T_X} + W_4$$

$$(8)\quad \dot{\omega}_{LS_Z} = \frac{A_{r_Y}}{R} - \frac{2V_r\omega_{LS_Z}}{R} - \omega_{LS_Y}\omega_{T_X} + W_5$$

$$(9)\quad \dot{\delta\eta} = \omega_{LS_Z} - \omega_{T_Z} - \delta\varepsilon\omega_{T_X}$$

$$(10)\quad \dot{\delta\varepsilon} = \omega_{LS_Y} - \omega_{T_Y} + \delta\eta\omega_{T_X}$$

$$(11)\quad \dot{R} = V_r$$

$$(12)\quad \dot{V}_r = A_{r_X} + R(\omega^2_{LS_Y} + \omega^2_{LS_Z})$$

Measurement Equations

$$(1)\quad \omega_{M_Y} = \omega_{Tr_Y} + V_1$$

$$(2)\quad \omega_{M_Z} = \omega_{Tr_Z} + V_2$$

$$(3)\quad \delta\eta = \delta\eta_{Tr} + V_3$$

$$(4)\quad \delta\varepsilon = \delta\varepsilon_{Tr} + V_4$$

$$(5)\quad R = R_{Tr} + V_5$$

The original (untuned) one sigma of the measurement noises are:

Noise	One Sigma Value
V_1	5.0×10^{-6} rad/sec
V_2	5.0×10^{-6} rad/sec
V_3	2.5×10^{-6} rad
V_4	2.5×10^{-6} rad
V_5	2.2×10^{-2} Km

Filter II State Equation Development

The underlying concept for the development of the filter model proposed in this section is to delete the satellite inertial position and velocity states [X(1) → X(6)]. Other information already available in the remaining six states and INS data will then be used to determine the acceleration of the satellite relative to the tracker $(\underline{A}_T)^T$ based upon the knowledge that the dominant acceleration of the satellite can be described by a two body point mass gravity model. This approach to the satellite tracking problem was suggested for inclusion in this study by U. S. Air Force Avionics Laboratory personnel.

Figure 9 represents a typical tracker line-of-sight-satellite geometry.

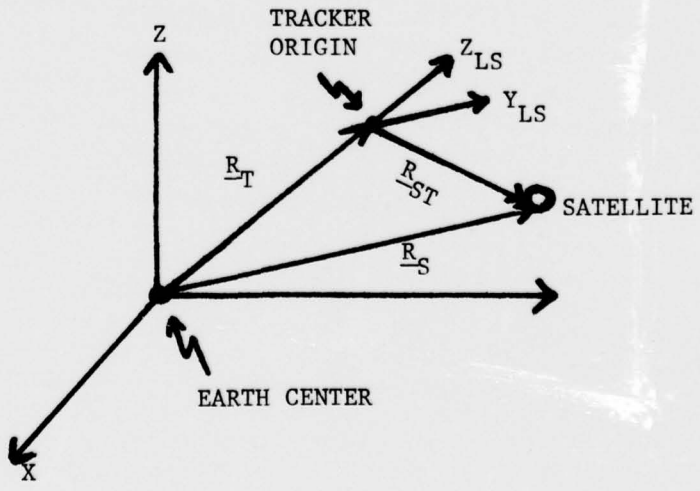

Figure 9. Typical Tracker Line-of-Sight-Satellite Geometry

where

(X,Y,Z) is the geocentric equatorial inertial frame

(X_{LS},Y_{LS},Z_{LS}) is the tracker line-of-sight frame, with X_{LS} pointing at the satellite

$\underline{R}_T$ is the vector from the center of the earth to the tracker

$\underline{R}_S$ is the vector from the center of the earth to the satellite

$\underline{R}_{ST}$ is the vector from the origin of the tracker system to the satellite along the line-of-sight X axis

When the satellite inertial position and velocity states are deleted from the Filter I model, the following information remains available to formulate a new filter model:

θ,ϕ - precise resolver measurements of the tracker azimuth and elevation angles.

$C_I^{LS}(\theta,\phi)$ - the transformation matrix from the inertial to the line-of-sight frames as a function of θ and ϕ.

$(\underline{A}_T)^T$ - high precision measurements of the tracker acceleration with respect to inertial space in tracker coordinates, determined from the outputs of three accelerometers - one mounted along each of the tracker axes.

$R_M,\omega_{M_Y},\omega_{M_Z},\delta\varepsilon_M,\delta\eta_M$ - noise corrupted measurements of range, tracker angular rates, and angular deviations as discussed in Chapter II.

The formulation of the state equations for Filter II is different from Filter I in that filter estimates of the satellite inertial position are no longer available to calculate $(\underline{A}_r)^T$ - the inertial acceleration of the satellite with respect to the tracker in the tracker frame. The components of $(\underline{A}_r)^T$ along the tracker X, Y, and Z axes are used by the filter in estimating the tracker angular rates and the range rate per Equations (2-40,41,42). As in the Filter I formulation, terms containing $\delta\varepsilon$ and $\delta\eta$, in these equations are neglected to yield

$$\dot{\omega}_{LS_Y} = \frac{-A_{r_Z}}{R} - \frac{2V_r\omega_{LS_Y}}{R} + \omega_{LS_Z}\omega_{T_X} + W_4 \tag{5-24}$$

$$\dot{\omega}_{LS_Z} = \frac{A_{r_Y}}{R} - \frac{2V_r\omega_{LS_Z}}{R} - \omega_{LS_Y}\omega_{T_X} + W_5 \tag{5-25}$$

$$\dot{V}_r = A_{r_X} + R(\omega^2_{LS_Y} + \omega^2_{LS_Z}) \tag{5-26}$$

Consider the following development of the acceleration of the satellite with respect to the tracker $(\underline{A}_{rel})^{LS}$ expressed in the line-of-sight frame. From Figure

$$(\underline{R}_S)^I = (\underline{R}_T)^I + (\underline{R}_{ST})^I \tag{5-27}$$

where the superscript "I" again indicates coordinatization in the inertial frame. From the definition of the line-of-sight (LS) frame (the line-of-sight X axis - X_{LS} - points exactly at the target), we know that the position vector of the satellite relative to the tracker $(\underline{R}_{ST})^{LS}$ lies along X_{LS}

$$(\underline{R}_{ST})^{LS} \triangleq \begin{bmatrix} R \\ 0 \\ 0 \end{bmatrix}$$

where R is the range between the tracker origin and the satellite. It follows that

$$(\underline{R}_{ST})^{I} = C_{LS}^{I}(\underline{R}_{ST})^{LS} \tag{5-28}$$

From Equation (5-27) is is seen that the inertial acceleration of the satellite with respect to the tracker expressed in inertial coordinates $(\ddot{\underline{R}}_{ST})^{I}$ is

$$(\ddot{\underline{R}}_{ST})^{I} = (\ddot{\underline{R}}_{S})^{I} - (\ddot{\underline{R}}_{T})^{I} \tag{5-29}$$

Elementary astrodynamics tells us that we can model the inertial acceleration of the satellite $(\ddot{\underline{R}}_{S})^{I}$ as

$$(\ddot{\underline{R}}_{S})^{I} = \frac{-\mu_{\oplus}(\underline{R}_{S})^{I}}{|(\underline{R}_{S})^{I}|^{3}}$$

and Equation (5-29) becomes

$$(\ddot{\underline{R}}_{ST})^{I} = \frac{-\mu_{\oplus}(\underline{R}_{S})^{I}}{|(\underline{R}_{S})^{I}|^{3}} - (\ddot{\underline{R}}_{T})^{I} \tag{5-30}$$

where from Equations (5-27,28)

$$(\underline{R}_{S})^{I} = (\underline{R}_{T})^{I} + C_{LS}^{I}(\underline{R}_{ST})^{LS} \tag{5-31}$$

It is evident at this point that if the tracker inertial position $(\underline{R}_T)^I$ were made available from an INS on the aircraft, then the acceleration of the satellite relative to the tracker expressed in LS coordinates [which is $(\underline{A}_{rel})^{LS}$] can be found by

$$(\underline{A}_{rel})^{LS} \triangleq (\ddot{\underline{R}}_{ST})^{LS} = C_I^{LS}(\ddot{\underline{R}}_{ST})^I = C_I^{LS}\left[\frac{-\mu_\oplus(\underline{R}_S)^I}{|(\underline{R}_S)^I|^3} - (\ddot{\underline{R}}_T)^I\right]$$

$$= C_I^{LS}\left\{-\mu_\oplus\left[\frac{(\underline{R}_T)^I + C_{LS}^I(\underline{R}_{ST})^{LS}}{|(\underline{R}_S)^I|^3}\right] - (\ddot{\underline{R}}_T)^I\right\}$$

$$= \frac{-\mu_\oplus C_I^{LS}(\underline{R}_T)^I + (\underline{R}_{ST})^{LS}}{|(\underline{R}_S)^I|^3} - (\ddot{\underline{R}}_T)^{LS} \qquad (5\text{-}32)$$

Under out assumption that $\delta\varepsilon$ and $\delta\eta$ are small, the tracker and line-of-sight frames are nearly aligned. It follows that the acceleration vector of the satellite relative to the tracker coordinatized in the tracker frame - $(\underline{A}_r)^T$ - is well approximated by $(\underline{A}_{rel})^{LS}$. Also, the acceleration of the tracker with respect to inertial space expressed in the LS frame - $(\ddot{\underline{R}}_T)^{LS}$ - is well approximated by the inertial acceleration of the tracker in the tracker frame $(\ddot{\underline{R}}_T)^T$ which is derived from the outputs of the accelerometers. Equation (5-32) can now be expressed as

$$(\underline{A}_r)^T = \frac{-\mu_\oplus\left[C_I^{LS}(\underline{R}_T)^I + (\underline{R}_{ST})^{LS}\right]}{|(\underline{R}_S)^I|^3} - (\ddot{\underline{R}}_T)^T \qquad (5\text{-}33)$$

Equation (5-33) is readily implementable as all parameters in it are available:

C_I^{LS} is a known function of the resolver angles ϕ and θ

$(\underline{R}_T)^I$ is provided by the INS

$$(\underline{R}_{ST})^{LS} = \begin{bmatrix} R \\ 0 \\ 0 \end{bmatrix}$$ where R is the range

$(\ddot{\underline{R}}_T)^T$ is derived from the output of the accelerometers

$$(\underline{R}_S)^I = (\underline{R}_T)^I + C_{LS}^I (\underline{R}_{ST})^{LS}$$

Therefore, for Filter II, the form of the state equations for $\dot{\omega}_{LS_Y}$, $\dot{\omega}_{LS_Z}$, and $\dot{V}_r$ remain as given in Equations (5-24,25,26) with the components of $(\underline{A}_r)^T$

$$(\underline{A}_r)^T \triangleq \begin{bmatrix} A_{r_X} \\ A_{r_Y} \\ A_{r_X} \end{bmatrix}$$

determined by the corresponding components of Equation (5-33).

Filter II Measurement Equations

The measurement equations for Filter II remain the same as for Filter I.

VI. Results and Discussion

Introduction

The purpose of this chapter is to present the results of the covariance analysis performed on the Filter I and II models, and subsequently to discuss and interpret these results. Special emphasis will be given to expected actual filter performance. Prior to presenting the results, the tracking profile used in the covariance analysis and the philosophy used to tune the filters will be discussed, since they have a direct bearing on the performance achieved in the study.

At the initialization of the tracking profile, the aircraft/tracker lies on the Greenwich meridian at a geocentric latitude of 30° north. For the duration of the 200 second tracking pass, the tracker moves at a constant speed of 0.3 Km/sec eastward while maintaining the same geocentric latitude. The satellite is in a 200 Km circular, near polar orbit, and it is a relatively small vehicle with a ballistic coefficient of 1.5 and a solar pressure coefficient equal to that of a vehicle with a projected surface area towards the sun of $10m^2$. Initially, the satellite lies essentially on the prime meridian and is approaching a descending node (descending towards the equator), as shown in Figure 10.

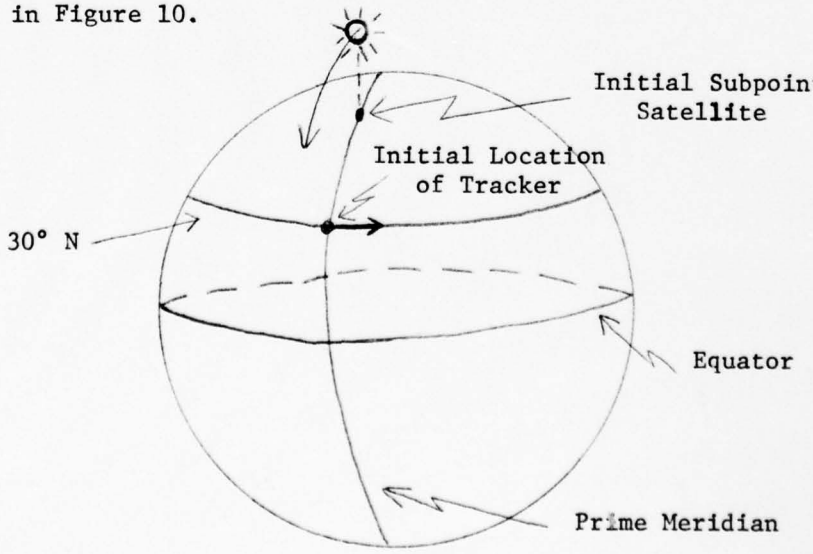

Figure 10. Satellite/Tracker Geometry

Pertinent tracking information for the profile used in this study is summarized below. The angles θ and ϕ, which define the coordinate transformation from the inertial to the line-of-sight frame (see Chapter II), may also be used to describe the tracker azimuth and elevation angles - $(-\phi)$ being the elevation angle and θ the azimuth angle (0° azimuth being defined as the condition in which the x_{LS} axis is parallel to the inertial X axis).

Parameter	Initial Value (t = 0)	Final Value (t = 200 secs)
Elevation angle of tracker $(-\phi)$	56.5°	74.7°
Azimuth angle of tracker (θ)	180.0°	222.1°
ω_{LS_Y}	-9.58×10^{-4} rad/sec	-18.91×10^{-3} rad/sec
ω_{LS_Z}	2.57×10^{-4} rad/sec	55.9×10^{-3} rad/sec

The time history of ω_{LS_Y} and ω_{LS_Z} are given in Figures 11 and 12. Note that both curves are nonlinear with ω_{LS_Z} being especially so. This is to be expected from the geometry of this tracking profile. As the track progresses, the tracker moves in a plane perpendicular to the orbit plane of the satellite. Therefore, it is expected that the inertial angular velocity about the line-of-sight Y axis - the elevation axis of the tracker - $-\omega_{LS_Y}$ would first accelerate and then slow down as the satellite approaches its zenith with respect to the tracker. On the other hand, the time rate of change of the tracker azimuth angle - ω_{LS_Z} - is expected to continually accelerate until the satellite is coplanar with the tracker - an azimuth angle of 270°. Thus, while the tracking profile used was not representative of worst case conditions, it does present a highly nonlinear angular rate history with which to evaluate each filter's estimation capability.

Briefly stated, for a filter to be well "tuned" through a covariance analysis, the filter error variance should follow the "true" system error

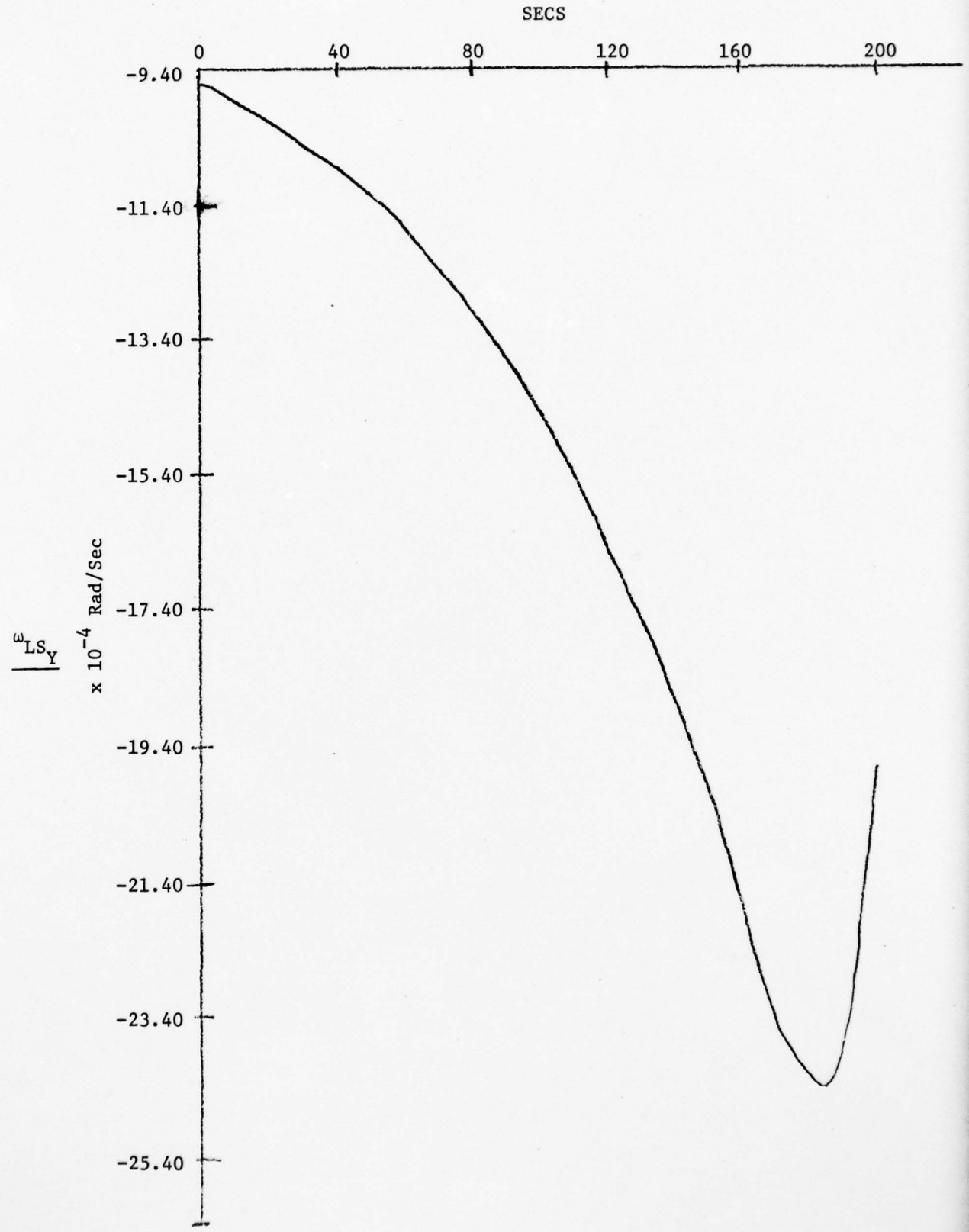

Figure 11. ω_{LS_Y} Time History

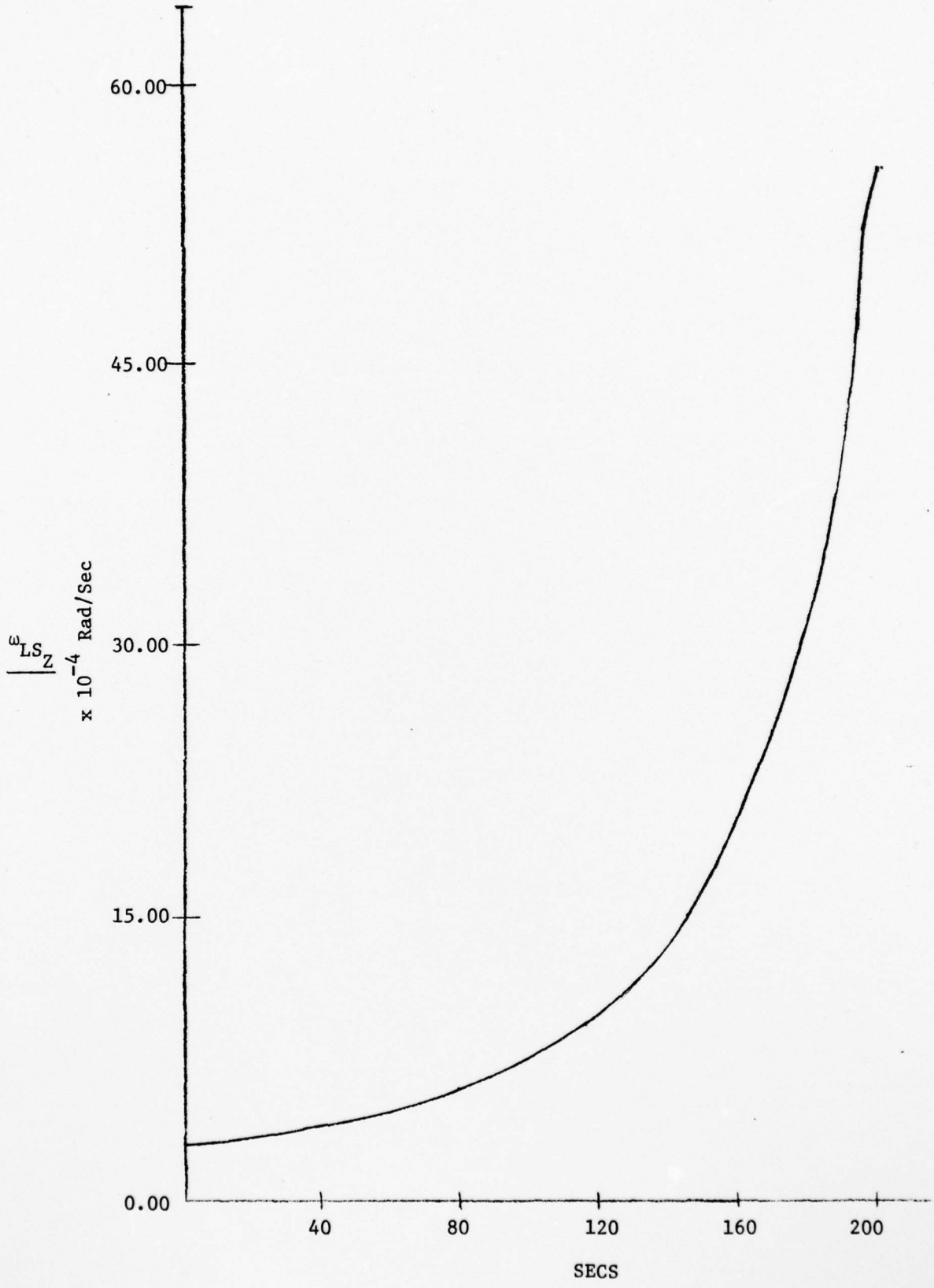

Figure 12. ω_{LS_Z} Time History

variance as closely as possible without underestimating it. Typically, this results in the generation of the lowest possible system error variances. This is accomplished by varying the strengths of the state dynamics and measurement noises in the filter until the desired "tuning" is achieved. By using constant noises in an extended Kalman filter, we are faced with the possibility of divergence, in which the error variance of a filter state approaches steady state while the error variance of the system

$$P_S(t) = P_{ee}(t) \triangleq E\{[\underline{X}_S(t) - T\hat{\underline{X}}_f(t)][\underline{X}_S(t) - T\hat{\underline{X}}_f(t)]^T\}$$

grows without bound. This happens because the filter is weighting its internal model too heavily. This is what Jazwinski has termed "learning the wrong state too well" (Ref 14:301-302). Such divergence characteristics can be remedied to some extent by admitting time varying (such as piecewise-constant) noise strengths in the model upon which the filter is based. However, as mentioned before, the scope of this study was confined to achieving adequate tracking performance over a reasonable time interval with the use of a single set of noise strengths. Decreased dynamic noise strengths would allow a "tighter" tuning during the initial period while increased strengths would remove (or at least postpone) the onset of divergence. In eventual implementation, time-varying strengths, possibly set adaptively since their "best" evaluation would be trajectory dependent, could enhance filter performance (Ref 9:155).

Filter I Results

This section will present the results of the covariance analysis performed on Filter I. They should be considered as representative of the filter's capabilities but not final. Further tuning may be possible and should be performed if specific limits of the capability of the

filter are under question. Moreover, a Monte Carlo analysis would be required to evaluate large scale filter performance.

The one sigma values for the errors committed by the filter in the estimation of the satellite inertial position and velocity (states $X_1 \rightarrow X_6$) are plotted in Figures 13-24. Each of the satellite inertial position states exhibited an initial upward transient followed by a period in which the error variance decreased. This very slow transient response was due to the weak coupling between the satellite and tracker state equations (no direct measurements of any of the satellite states were available in this formulation). The error plots for the satellite inertial velocity states (Figures 19-24) show a steadily decreasing error for all states.

Figures 25 and 26 are the plots for the standard deviation of the errors in the estimates of ω_{LS_Y} and ω_{LS_Z}. The errors committed by the filter and the system are given on the same plot so as to facilitate comparison. The filter's inability to follow the system closely when time-invariant noises are employed is evident in Figure 25. However, this plot does indicate that the filter can provide a conservative estimate (the filter overestimates its own errors) of ω_{LS_Y} in spite of the nonlinear nature of the ω_{LS_Y} time history. The filter performed nearly as well over the tracking period in estimating the error in its own ω_{LS_Z} estimate, again performing as a conservative estimator. Note, however, that divergence between the filter and system is very evident for the last 50 seconds of the track. Though the filter's estimate of the error is slowly increasing, it is placing too much emphasis on its internal dynamics model and is not able to follow the highly nonlinear behavior of ω_{LS_Z} towards the end of the tracking profile. As shown in Figures 27-30, the filter follows the system very well for the error misalignment angles, range and range rate states. Divergence in the

estimate of $\delta\eta$ can be seen near the end of the track. This is directly attributable to the coupling between $\delta\eta$ and ω_{LS_Z} (the estimate of which is diverging at the end of the track) in the state equation

$$\dot{\delta\eta} = \omega_{LS_Z} - \omega_{T_Z} - \delta\varepsilon\omega_{T_X} \tag{6-1}$$

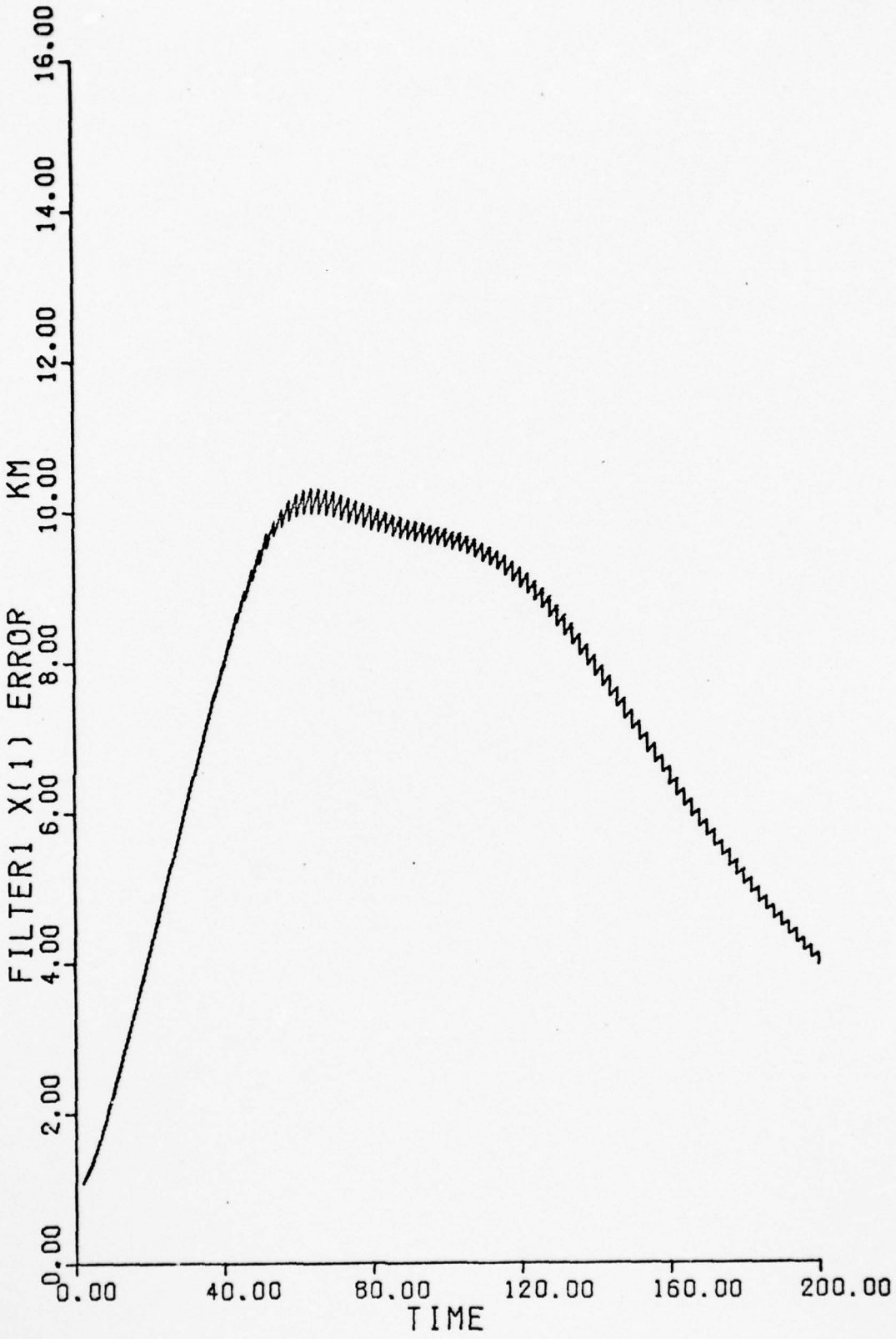

Figure 13. Filter I, Filter Error Standard Deviation - State X_1

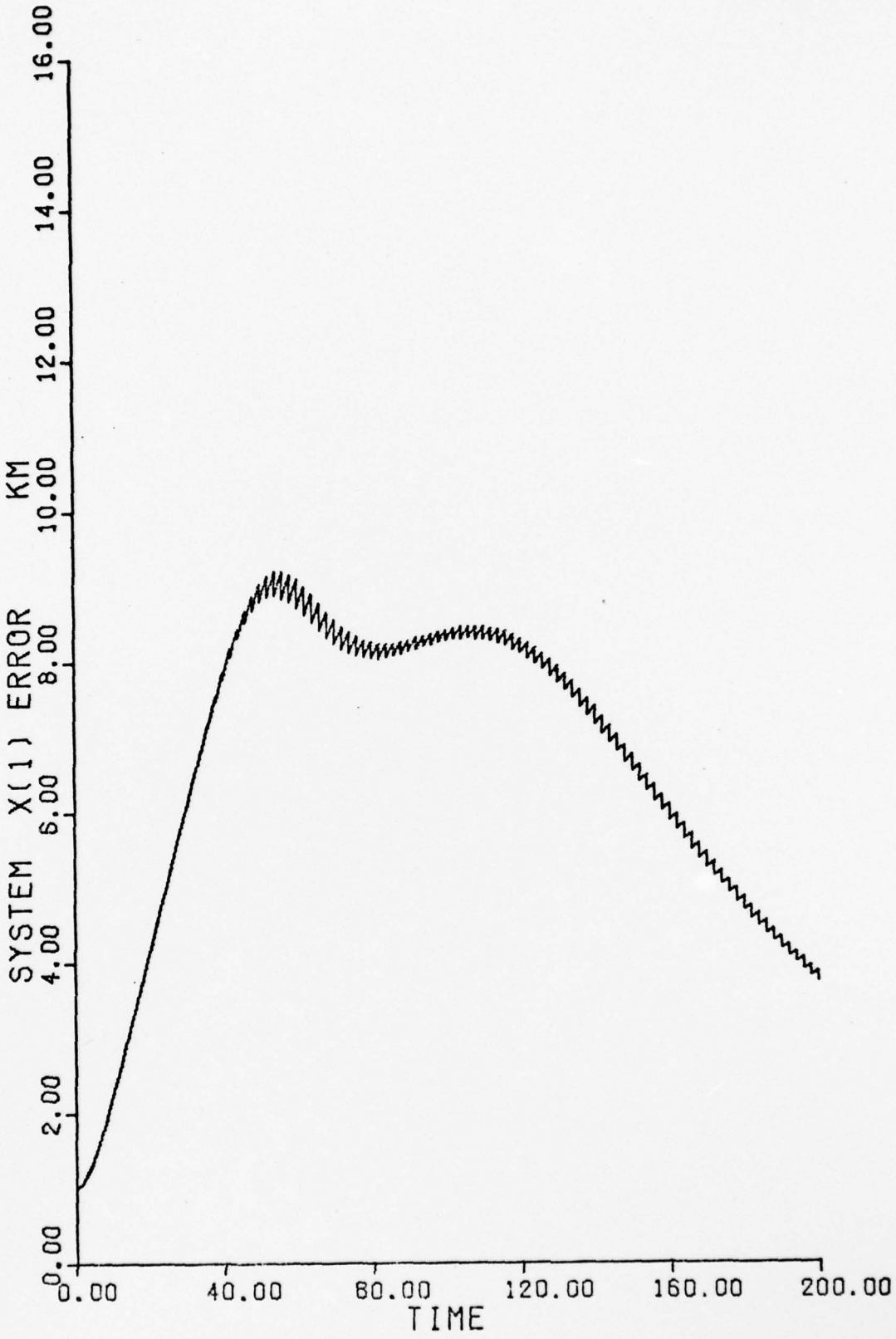

Figure 14. Filter I, System Error Standard Deviation - State X_1

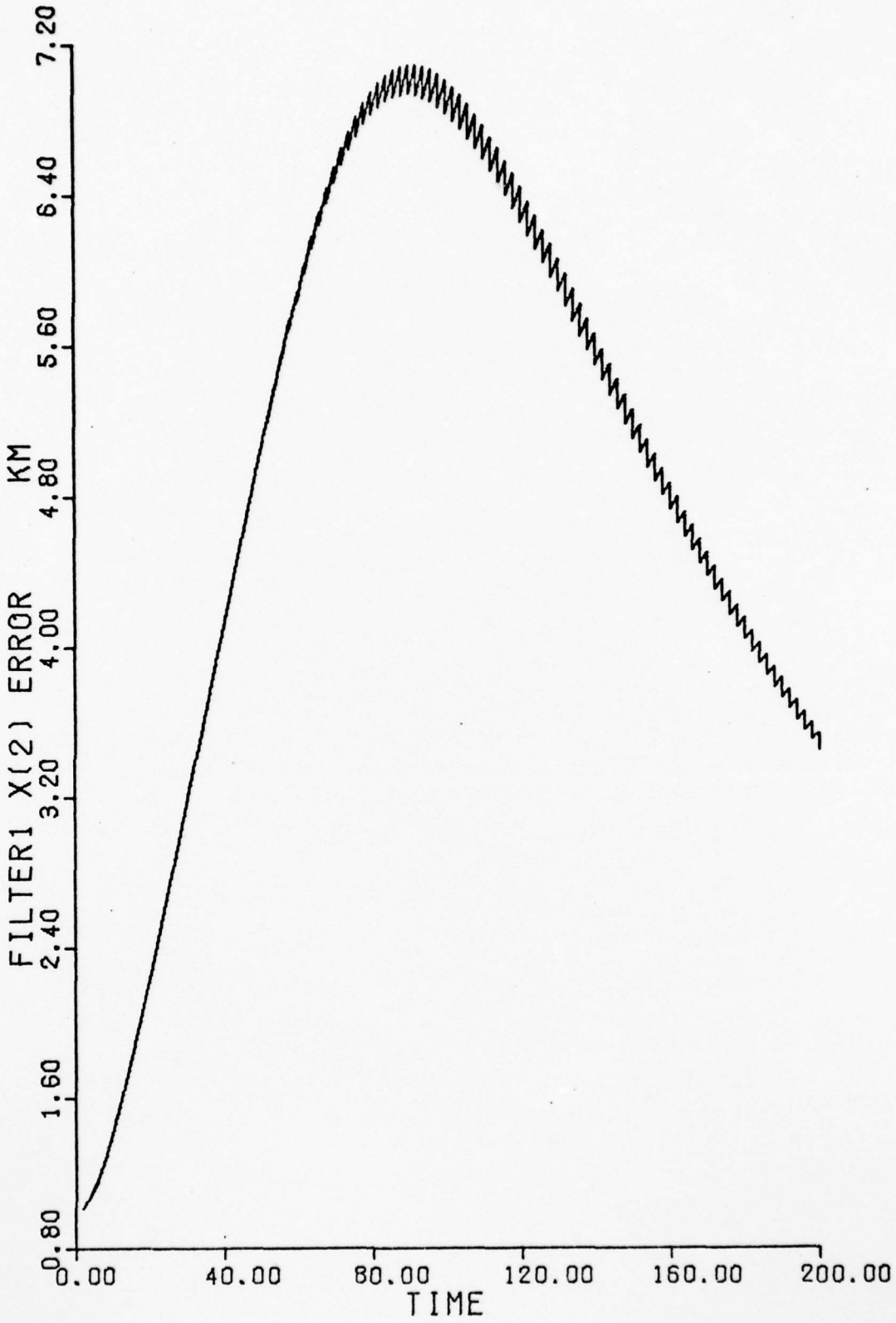

Figure 15. Filter I, Filter Error Standard Deviation - State X_2

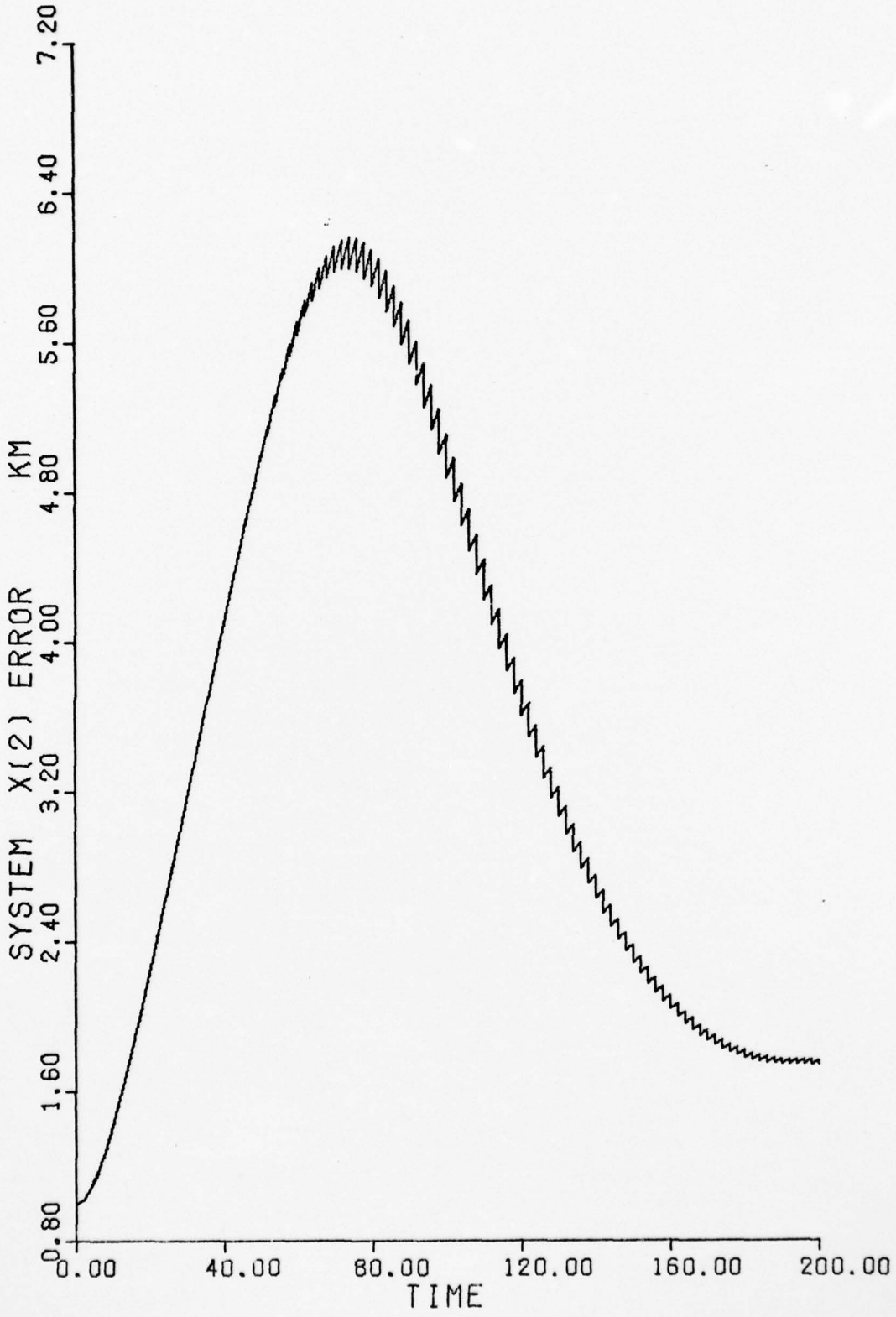

Figure 16. Filter I, System Error Standard Deviation - State X_2

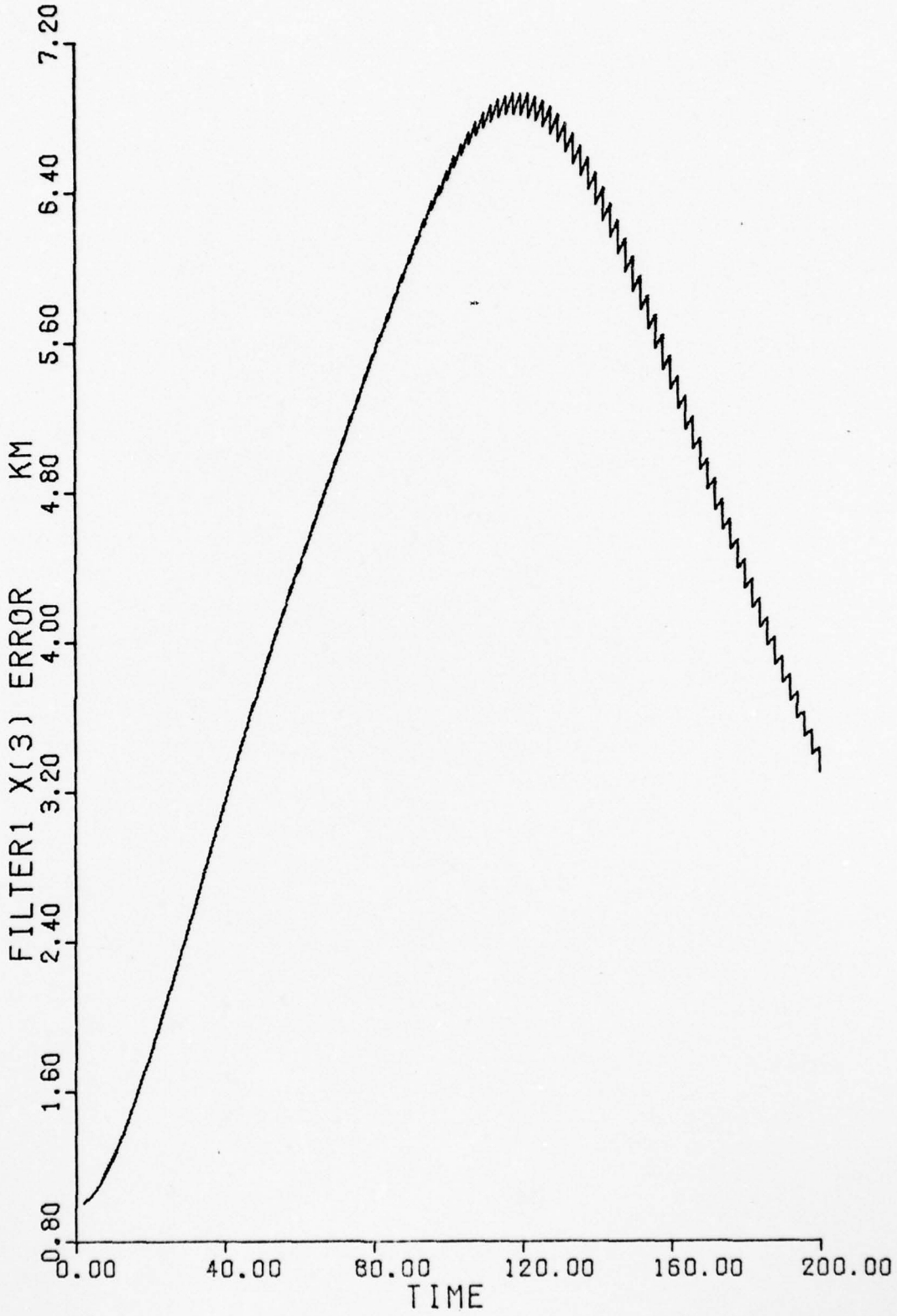

Figure 17. Filter I, Filter Error Standard Deviation - State X_3

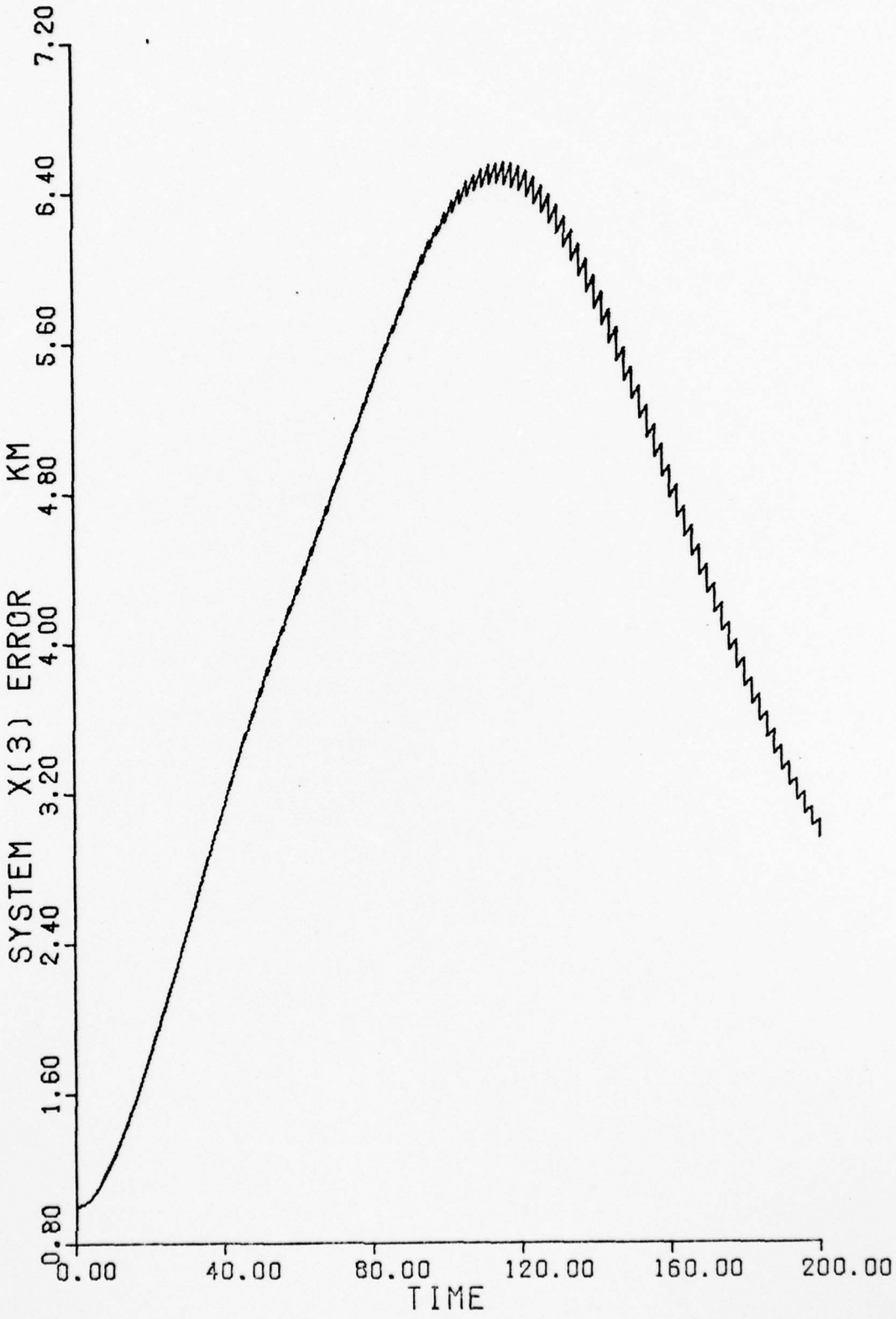

Figure 18. Filter I, System Error Standard Deviation - State X_3

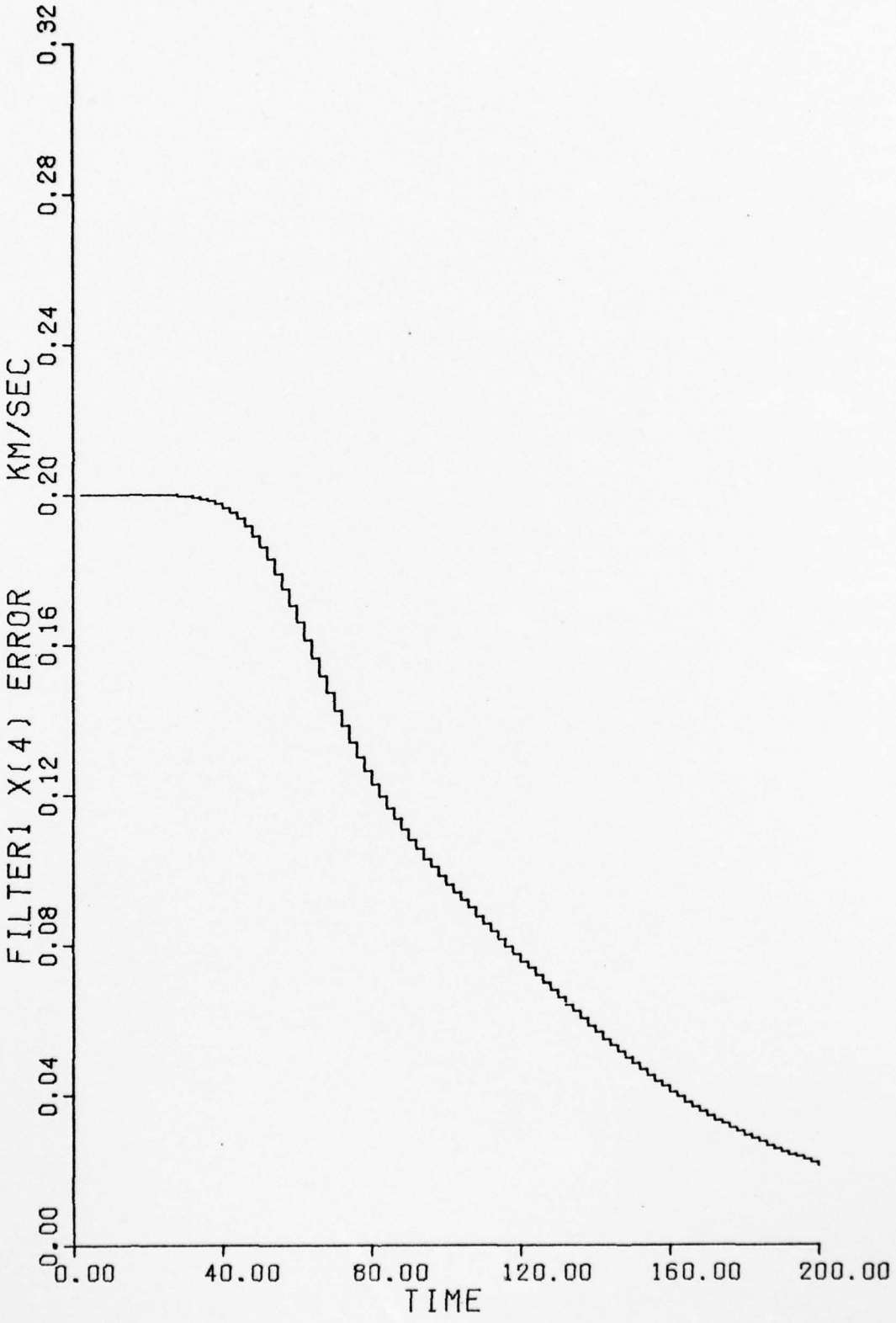

Figure 19. Filter I, Filter Error Standard Deviation - State X_4

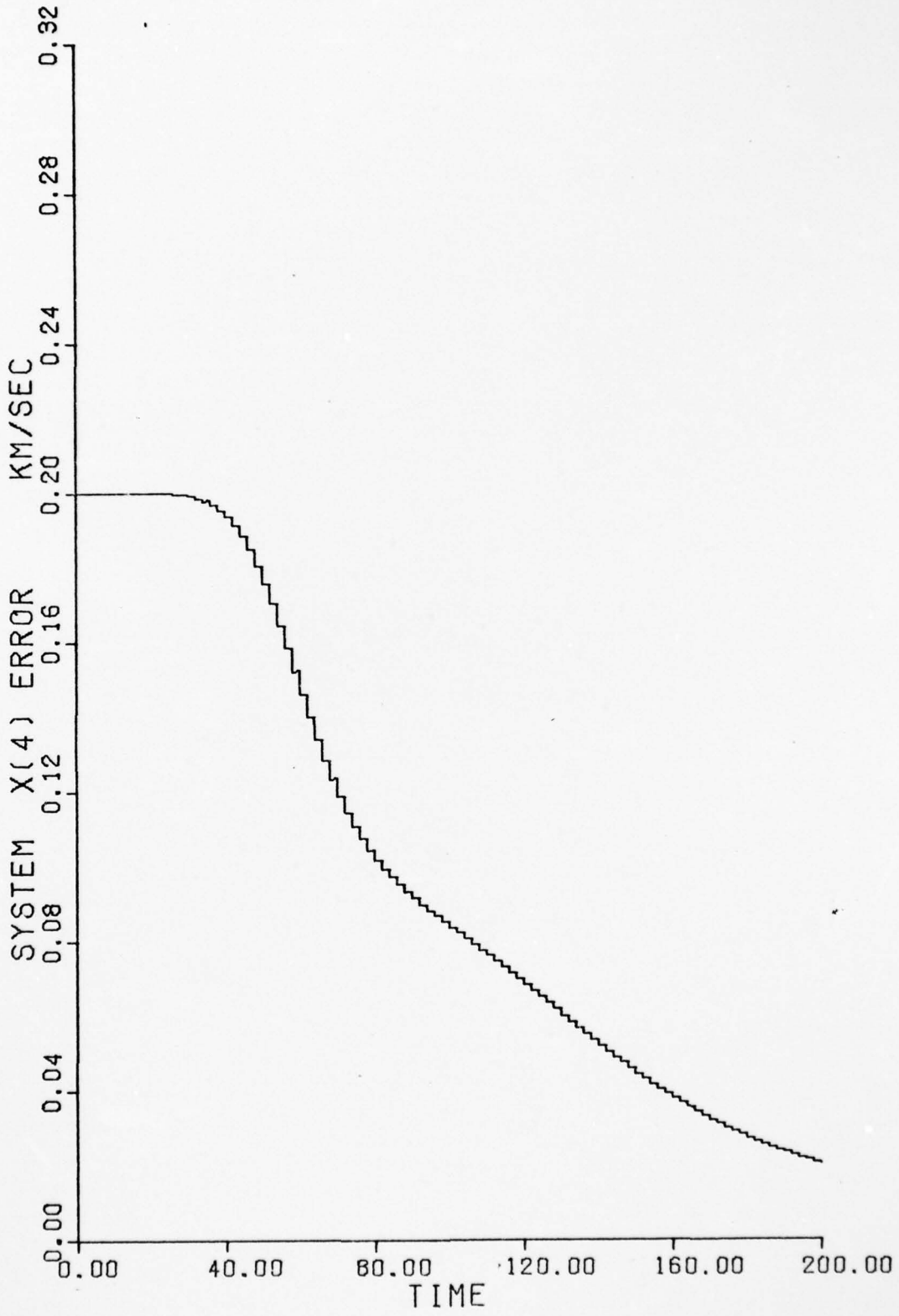

Figure 20. Filter I, System Error Standard Deviation - State X_4

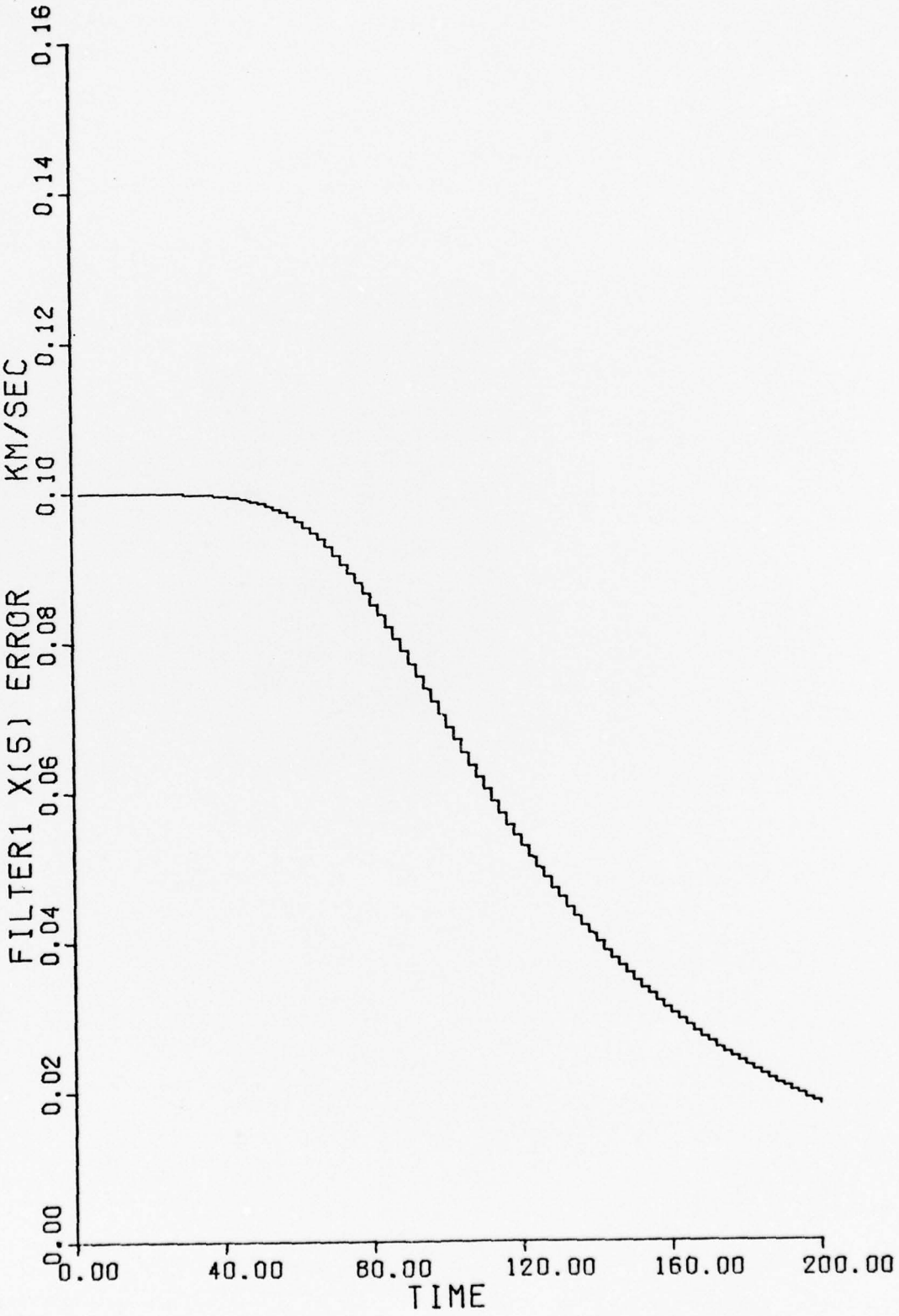

Figure 21. Filter I, Filter Error Standard Deviation - State X_5

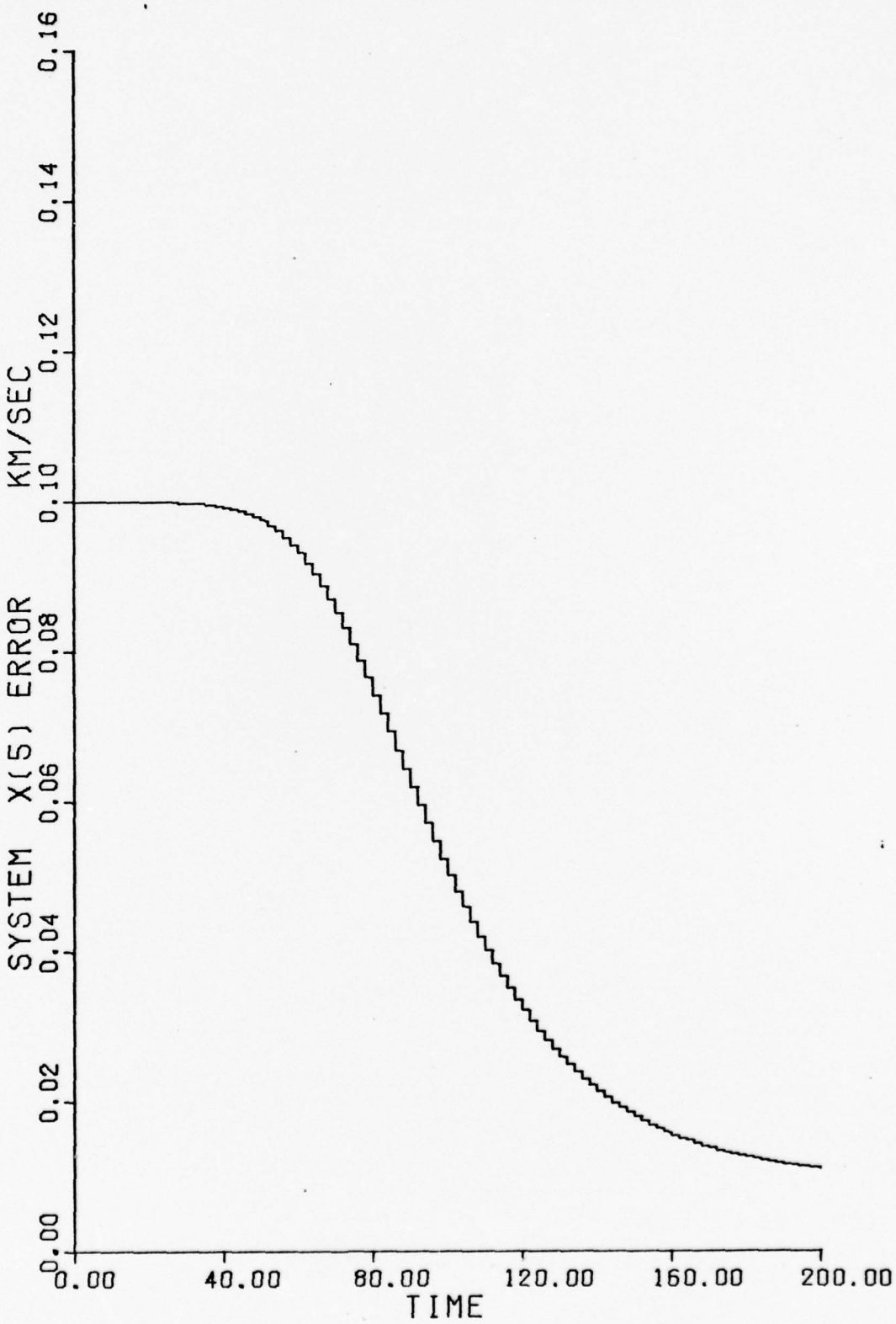

Figure 22. Filter I, System Error Standard Deviation - State X_5

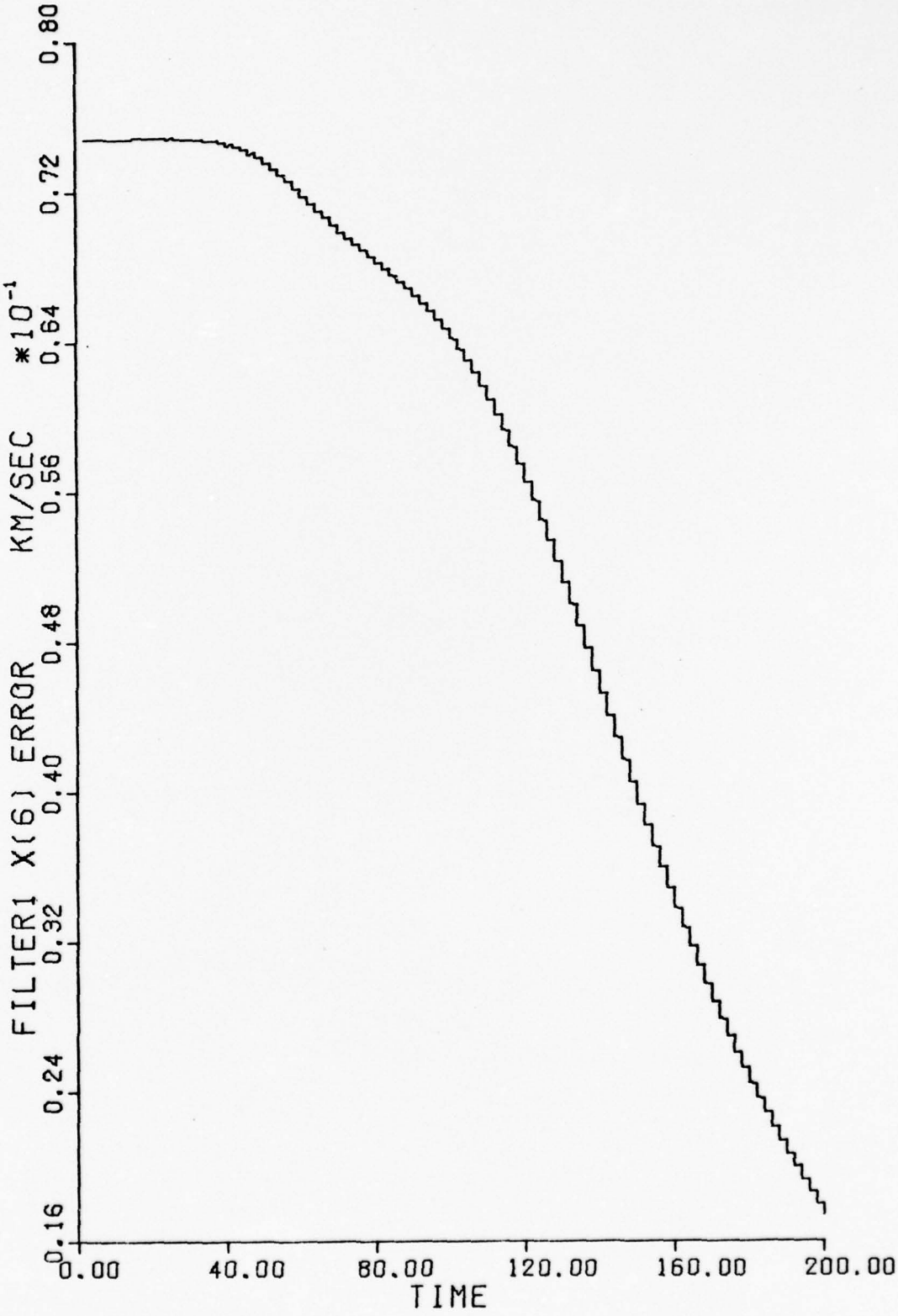

Figure 23. Filter I, Filter Error Standard Deviation - State X_6

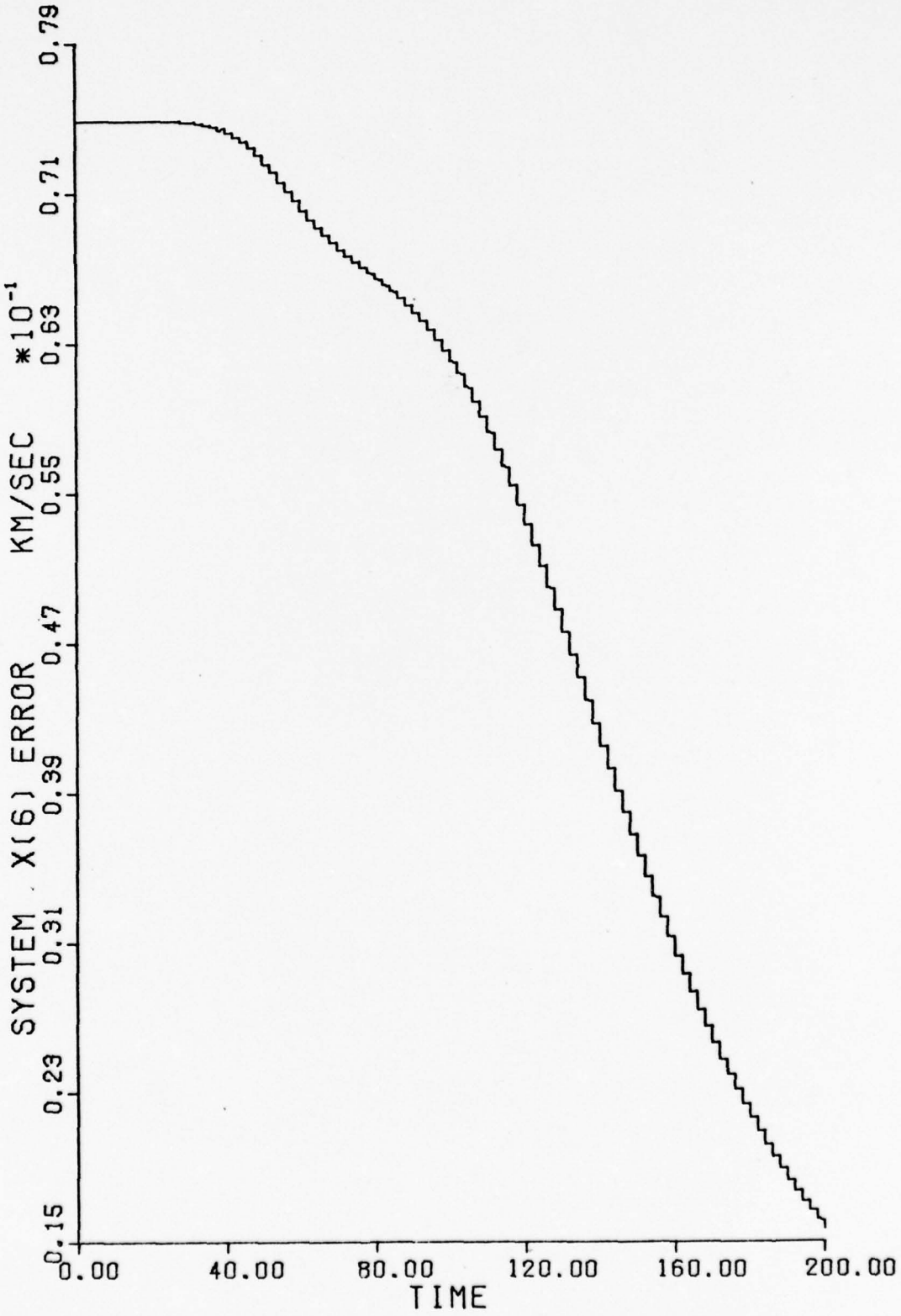

Figure 24. Filter I, System Error Standard Deviation - State X_6

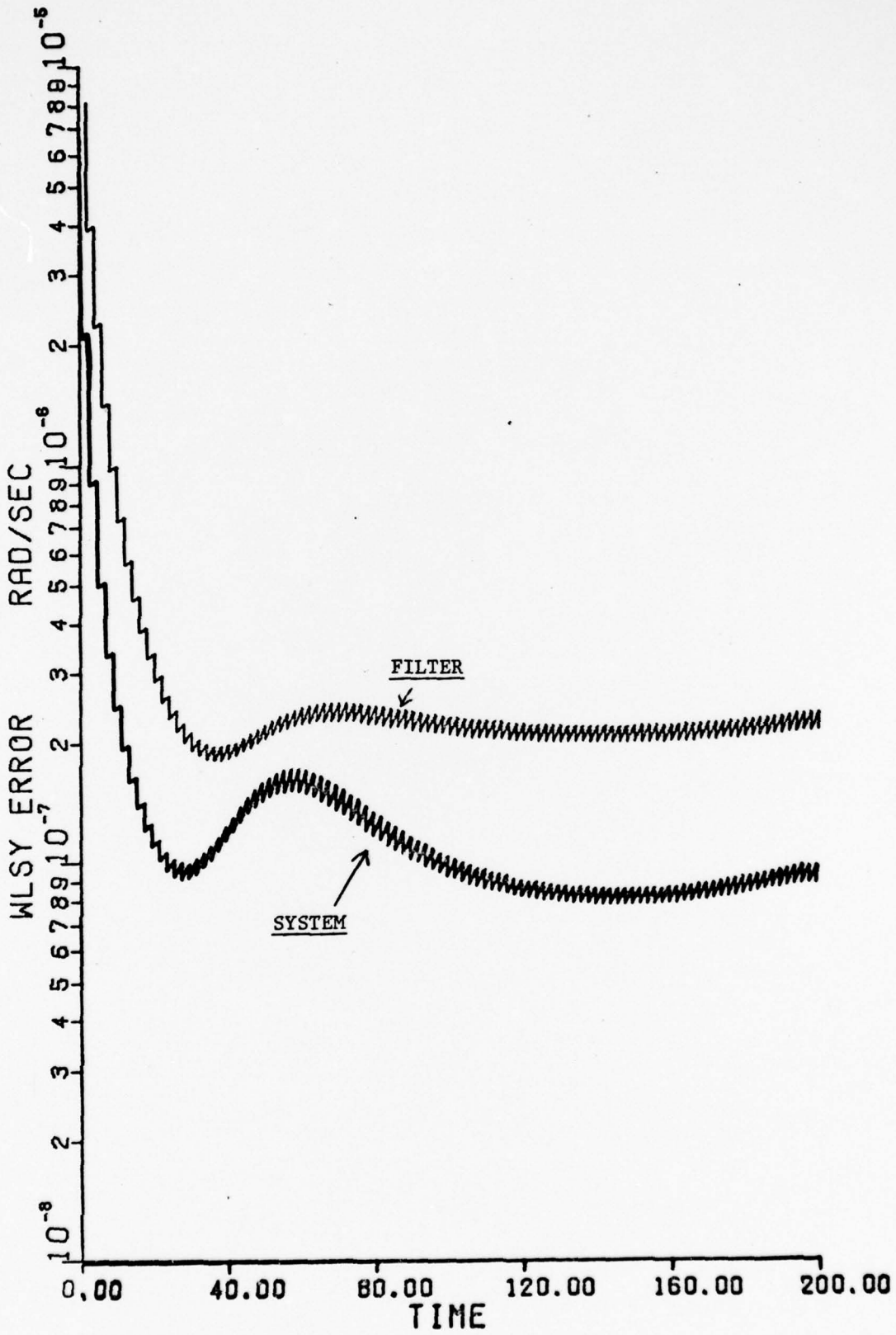

Figure 25. Filter I, Error Standard Deviation of ω_{LS_Y} Estimate

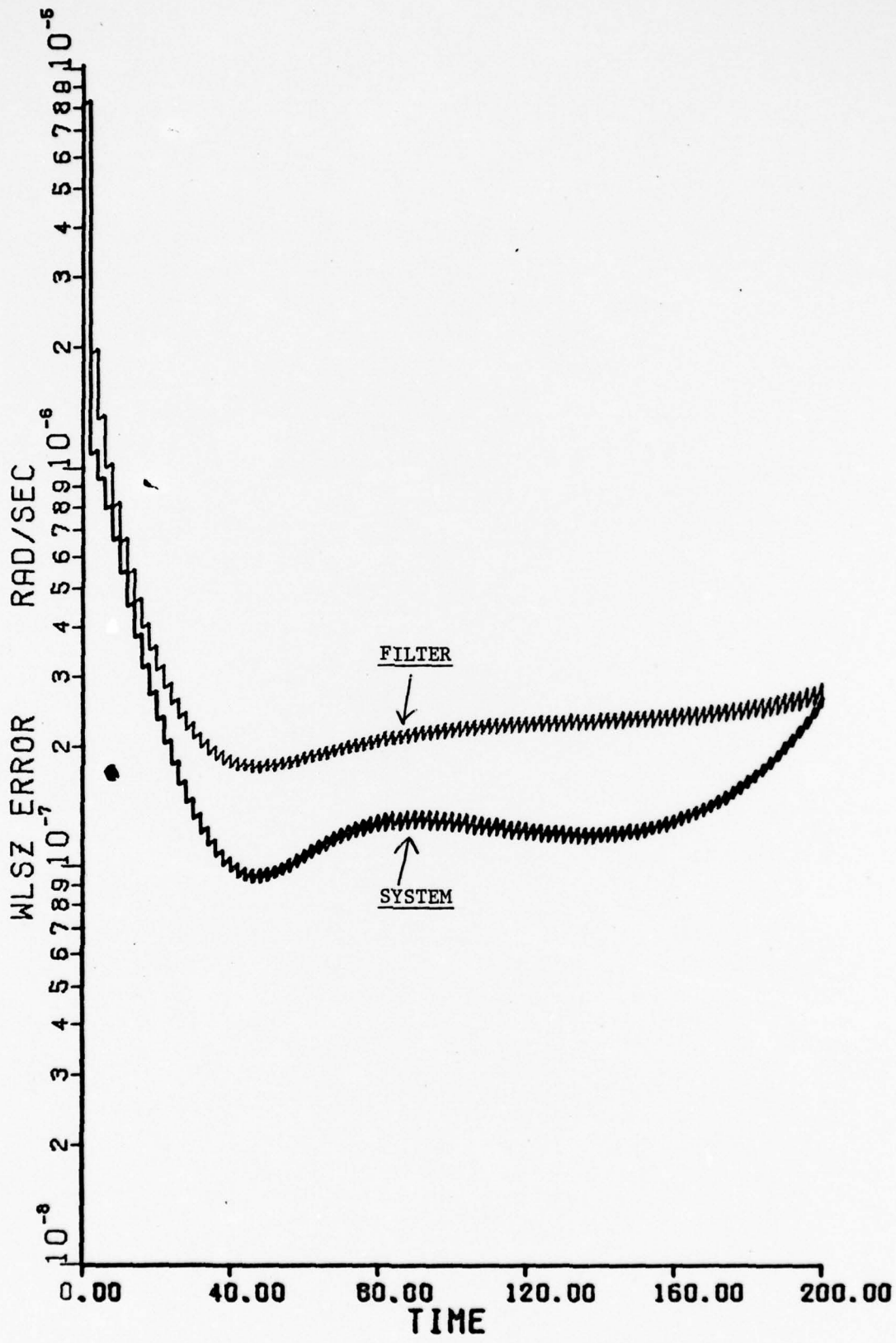

Figure 26. Filter I, Error Standard Deviation of ω_{LS_Z} Estimate

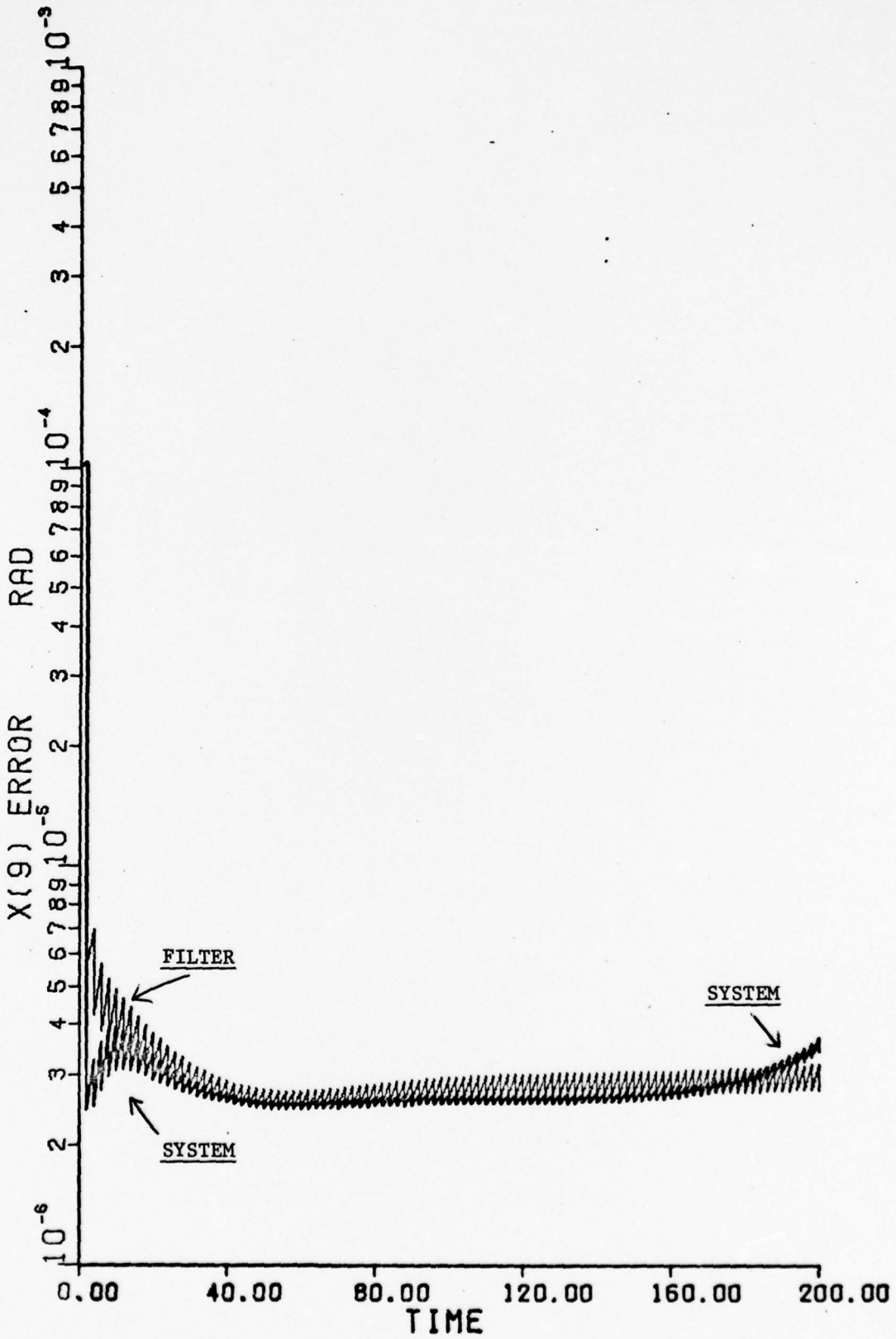

Figure 27. Filter I, Error Standard Deviation of $\delta\eta$ Estimate

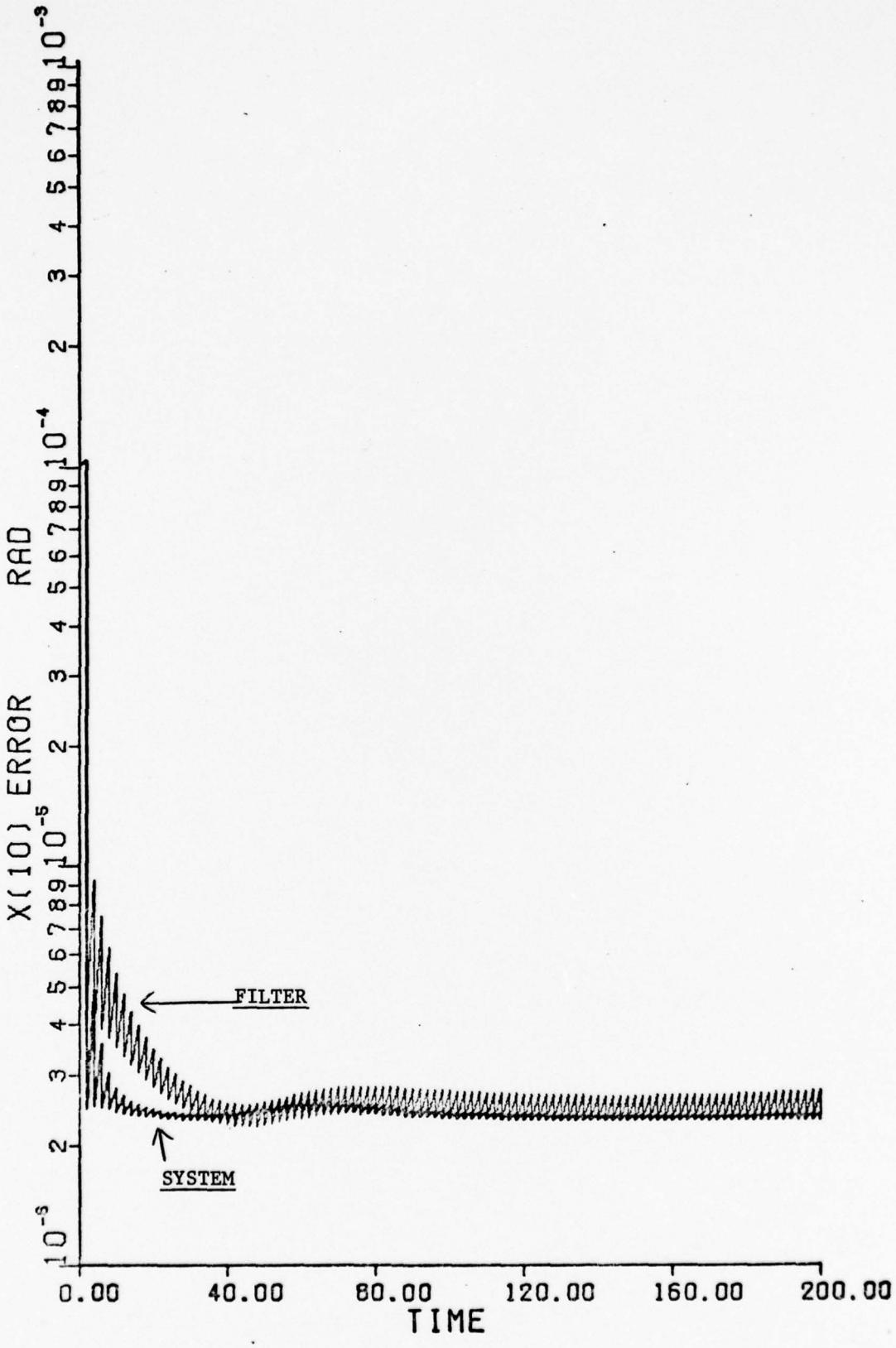

Figure 28. Filter I, Error Standard Deviation of $\delta\epsilon$ Estimate

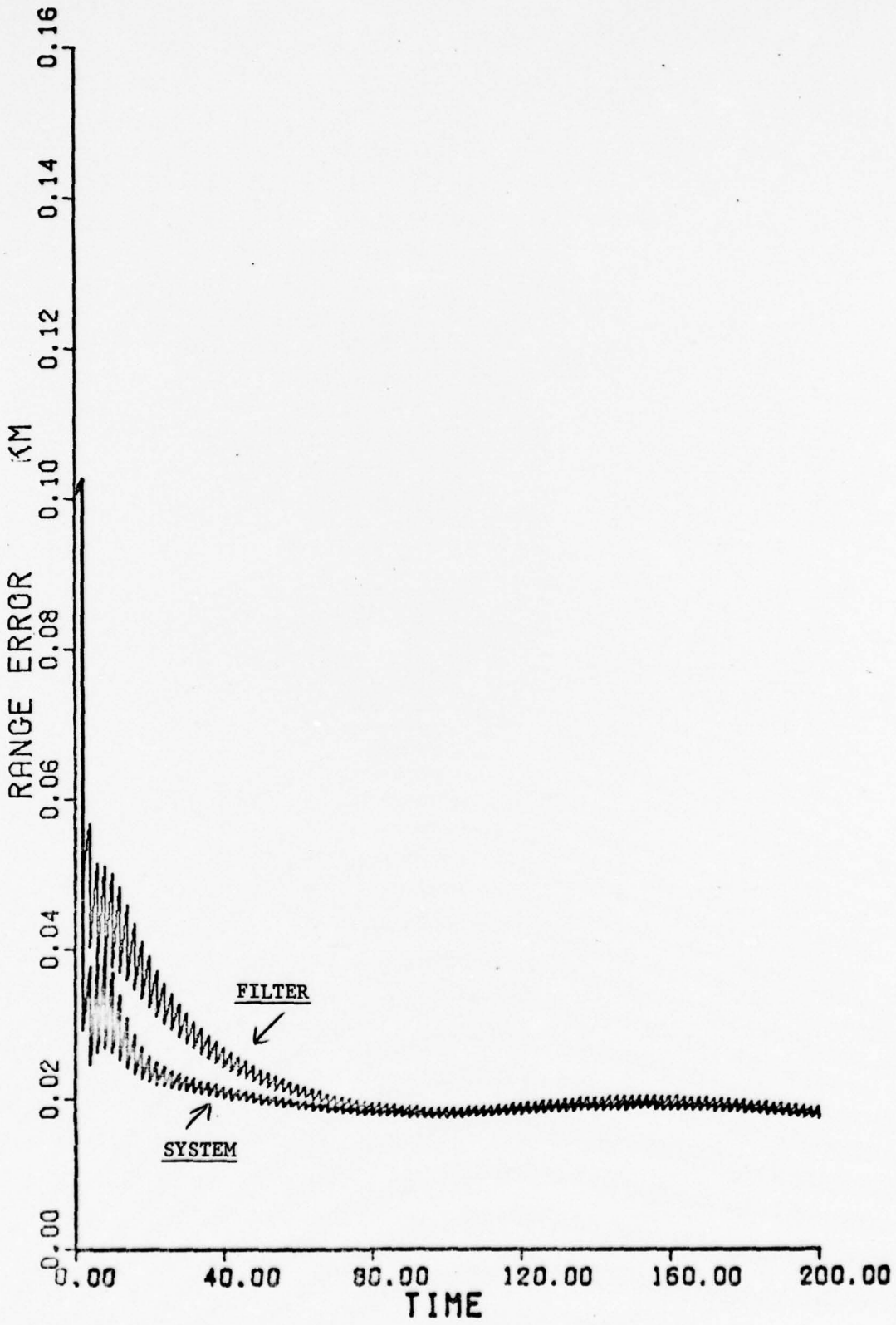

Figure 29. Filter I, Error Standard Deviation of Range Estimate

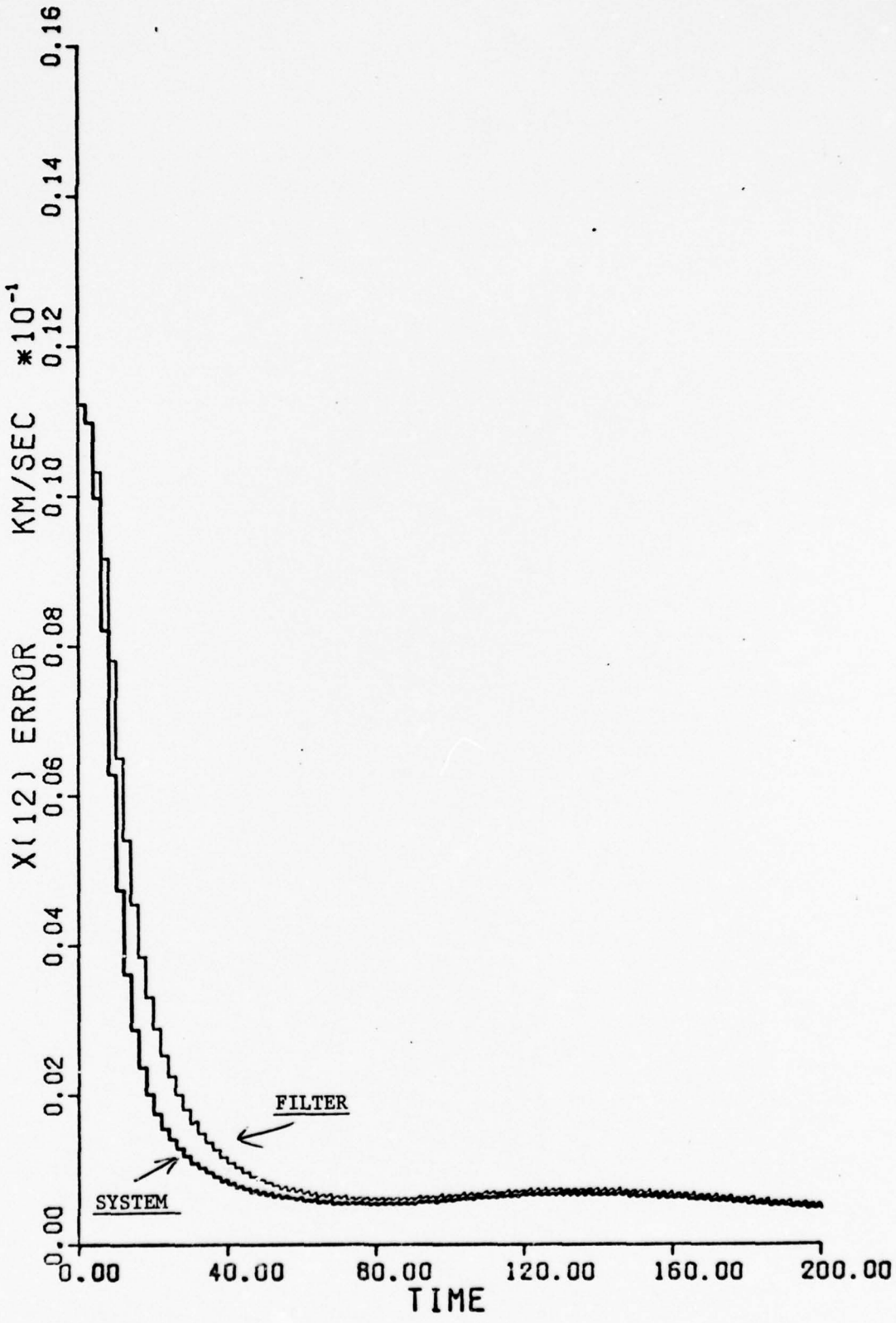

Figure 30. Filter I, Error Standard Deviation of Range Rate Estimate

Filter II Results

Plots of the standard deviation of the error estimates for the six state Filter II model are shown in Figures 31-36. The filter was unable to follow the system for the total tracking profile for any state. Consequently, it was decided to tune the filter to provide the best possible performance over the first 100 seconds of the tracking pass. The "best possible performance" is defined here as minimizing the area between the filter and system curves while insuring that the filter doesn't underestimate its own errors. These plots represent a fairly well tuned filter in that every attempt by the author to force the filter to follow the system's initial transient resulted in divergence occuring before 100 seconds. As in the case for ω_{LS_Z} in Filter I, the results indicate that Filter II can provide a conservative estimate of all of the states, i.e. with computed error variances at least as large as "true" system errors, over the first 100 seconds of the tracking profile. That the divergence of this filter may not be due solely to the nonlinearities inherent in the profile under study will be discussed in the next section.

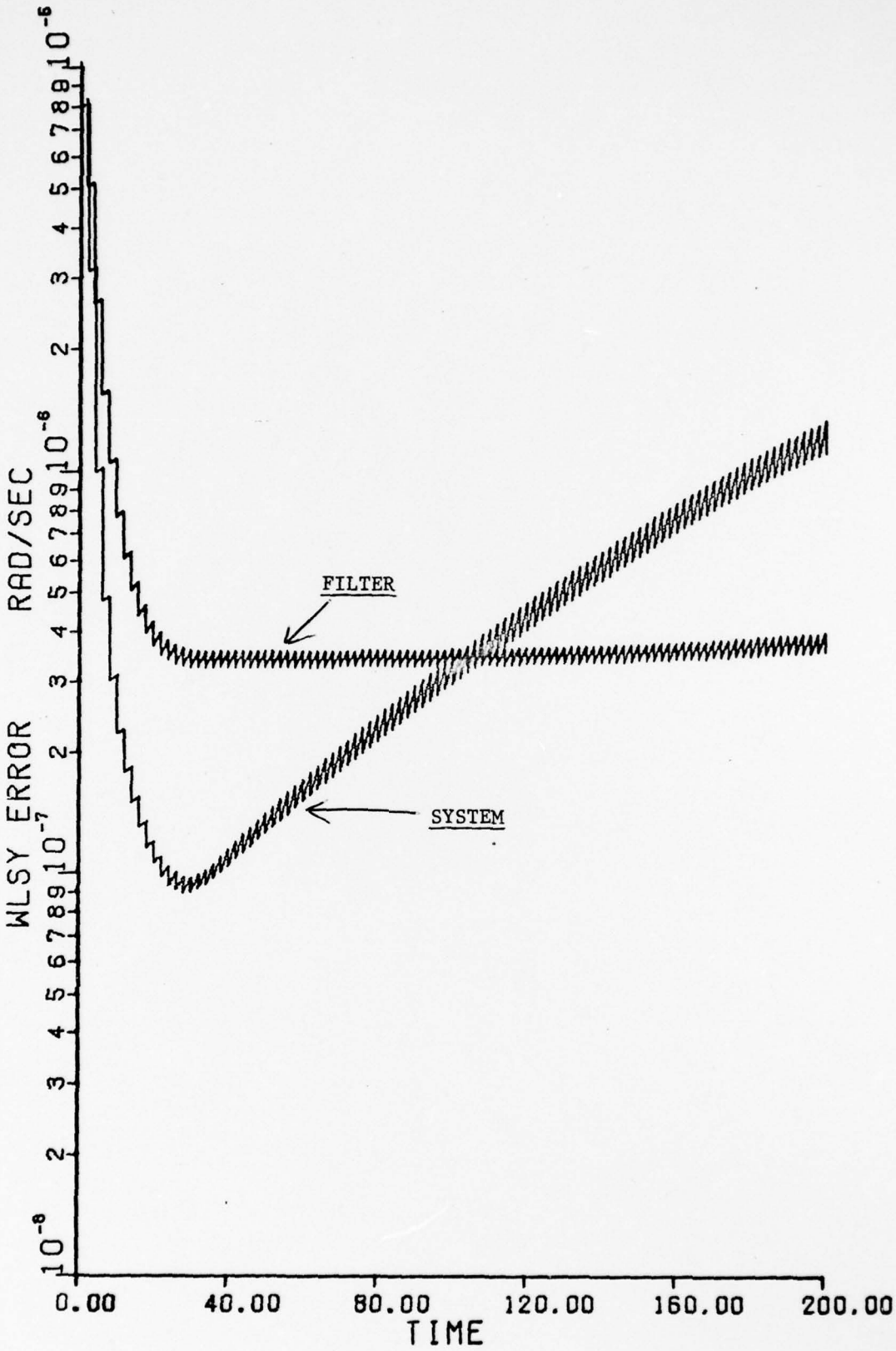

Figure 31. Filter II, Error Standard Deviation of ω_{LS_Y} Estimate

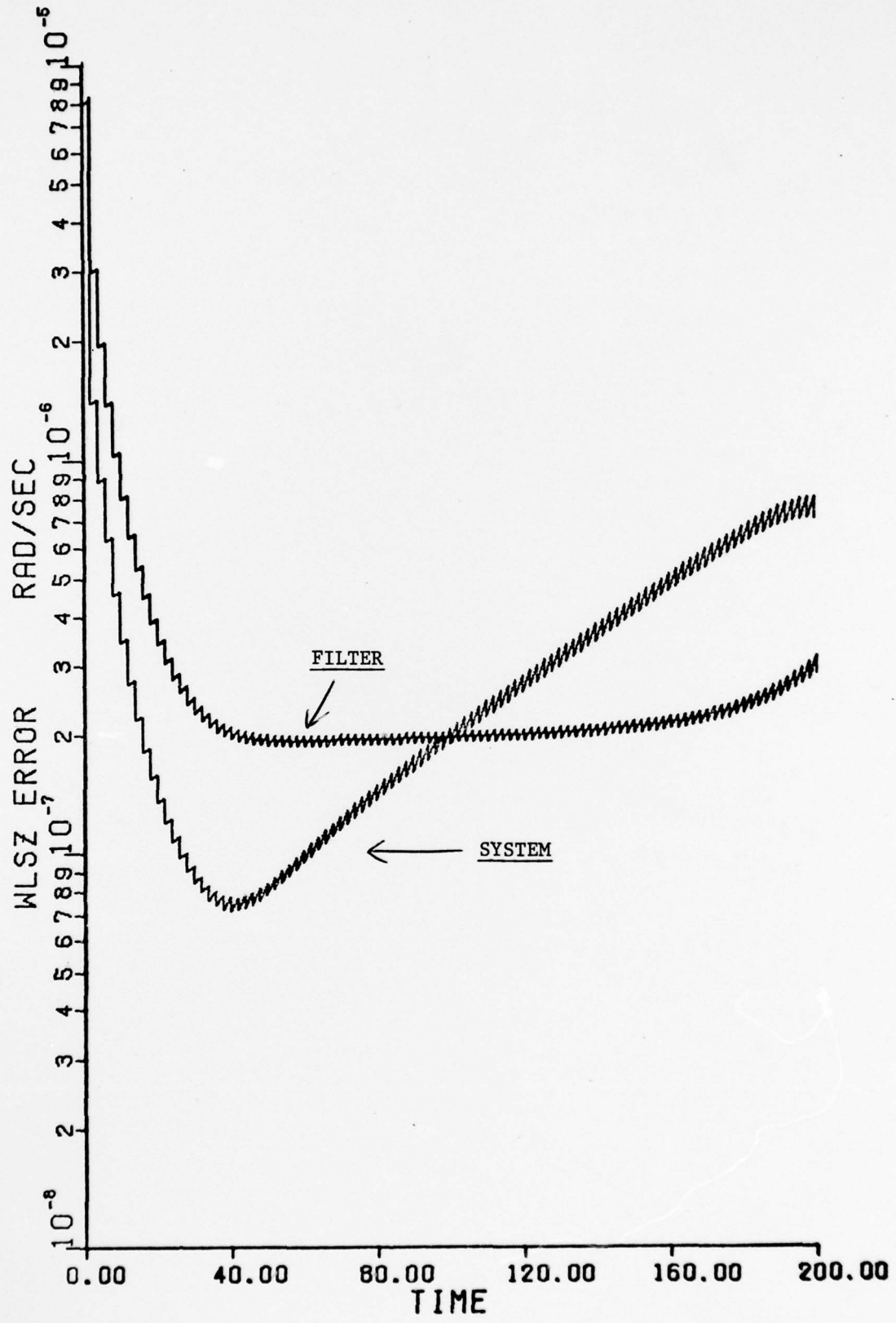

Figure 32. Filter II, Error Standard Deviation of ω_{LS_Z} Estimate

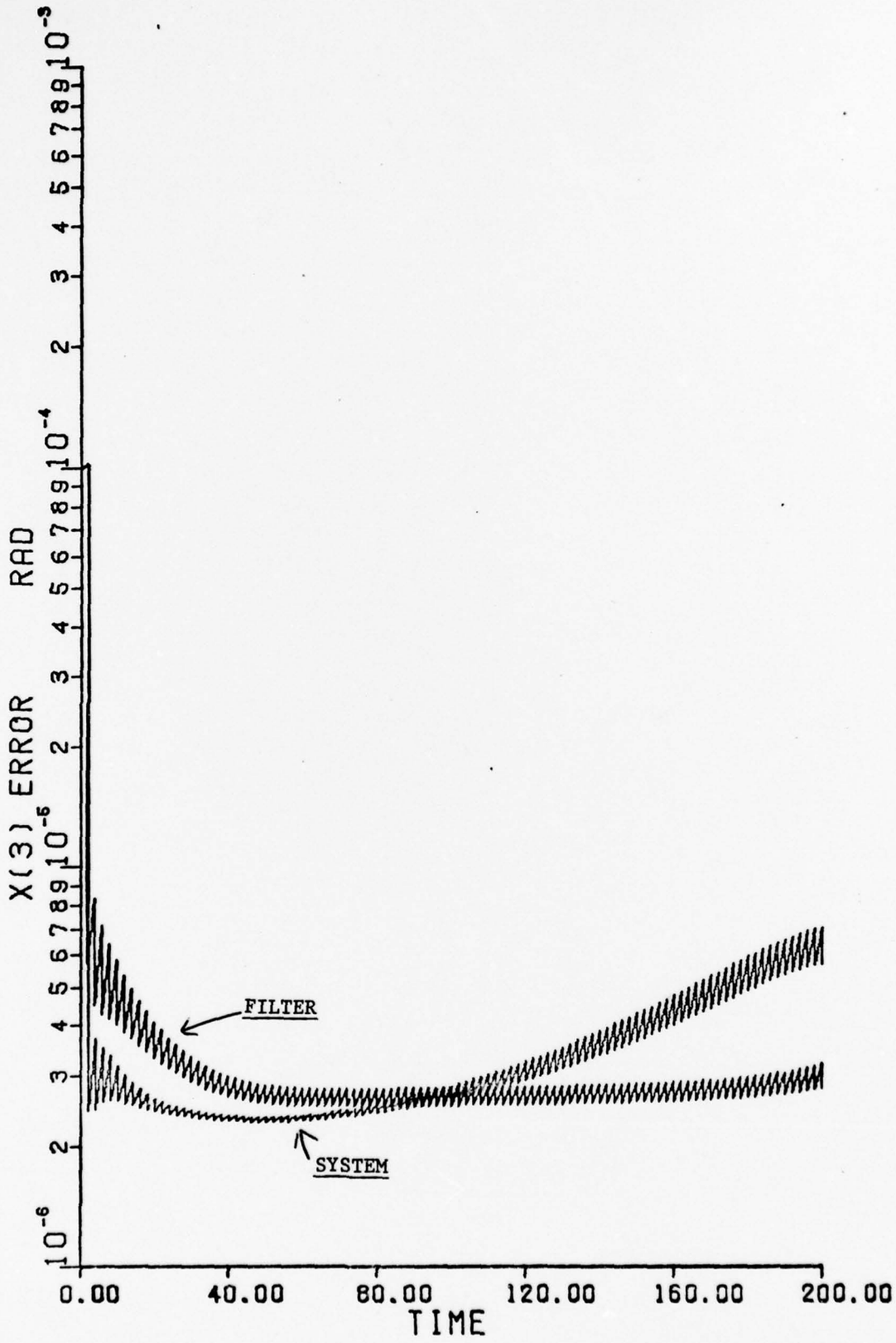

Figure 33. Filter II, Error Standard Deviation of $\delta\eta$ Estimate

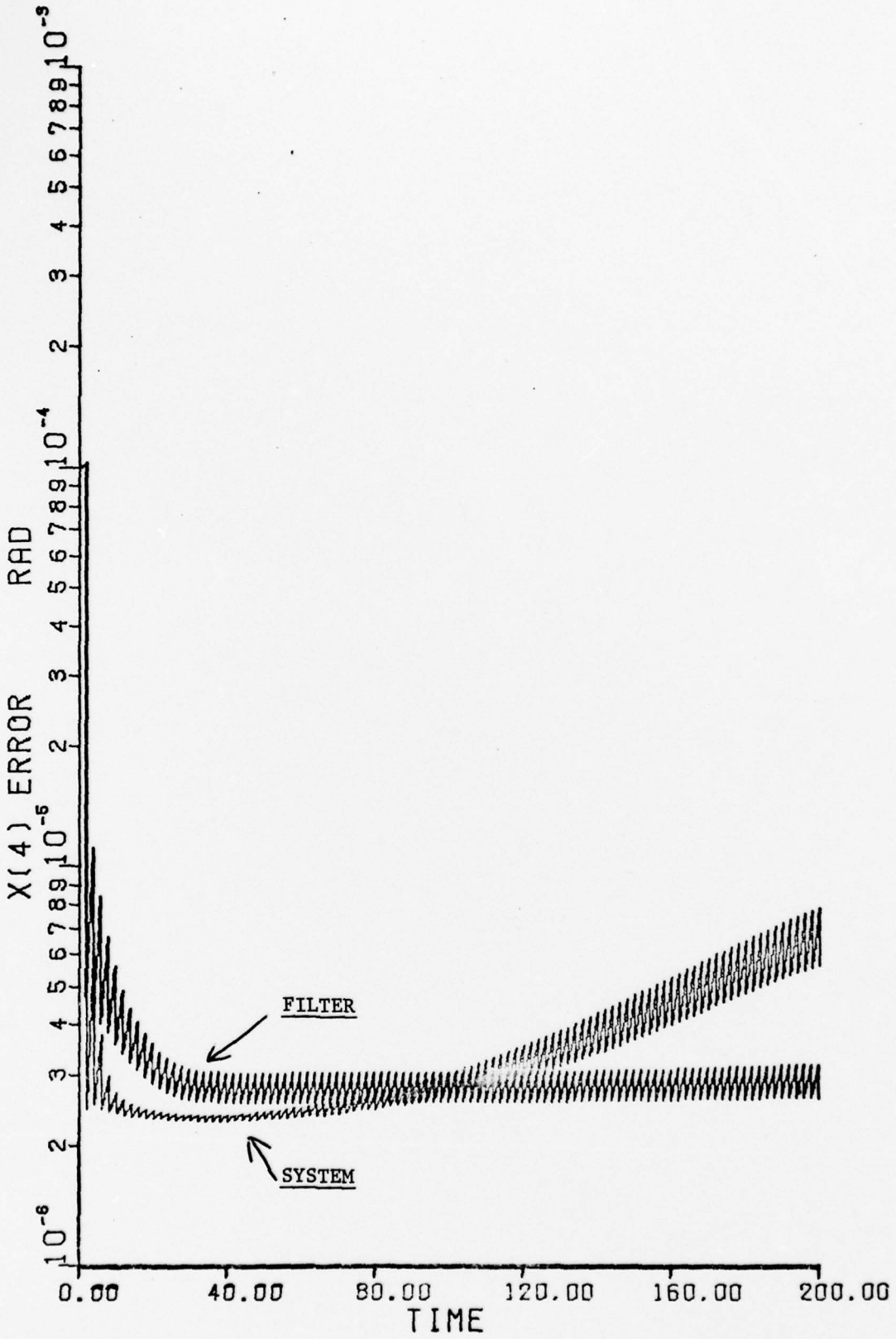

Figure 34. Filter II, Error Standard Deviation of $\delta\varepsilon$ Estimate

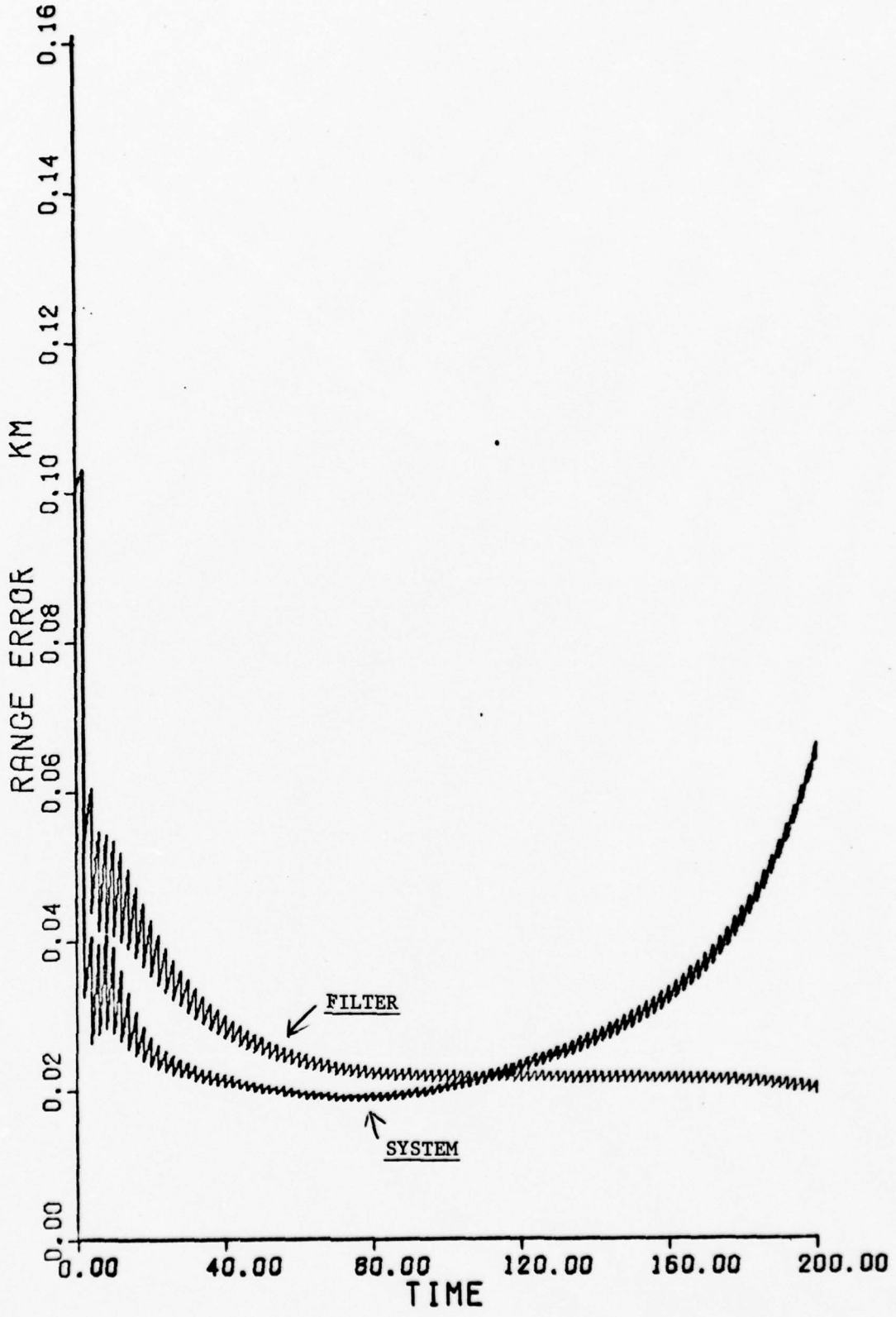

Figure 35. Filter II, Error Standard Deviation of Range Estimate

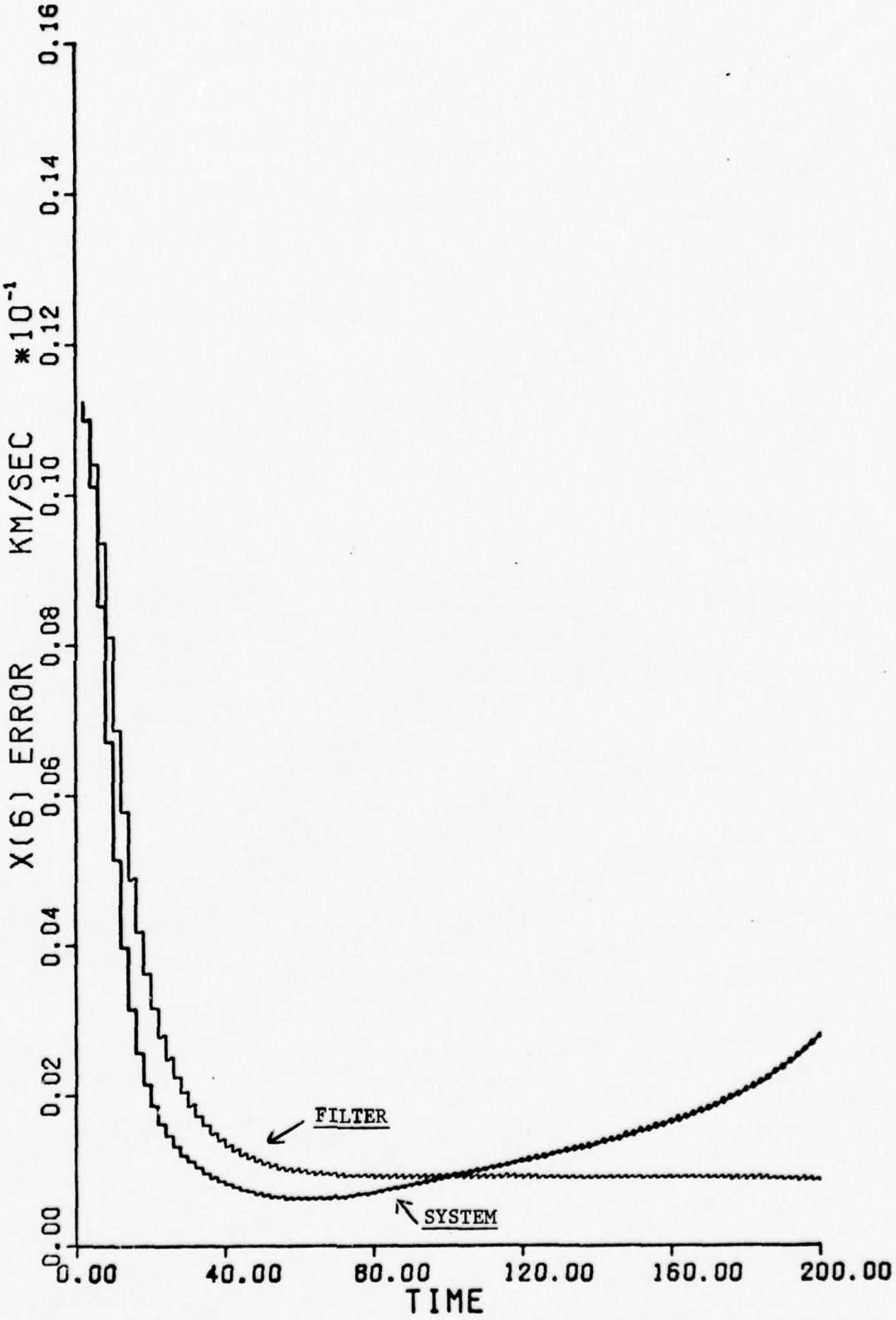

Figure 36. Filter II, Error Standard Deviation of Range Rate Estimate

Discussion and Interpretation of Results

The author considers the results presented in the last section to be informative but rather misleading for both proposed filter models. The above judgment is based upon a comparison of the results (which are dependent upon the limitations inherent to a covariance analysis) with expected actual filter performance.

Consider the calculation of the inertial acceleration of the satellite with respect to the tracker, coordinatized in the tracker frame, $(\underline{A}_T)^T$, for Filter I. We know that

$$(\underline{A}_T)^T = (\underline{A}_S)^T - (\underline{A}_T)^T = C_I^T(\underline{A}_S)^I - (\underline{A}_T)^T$$

$$= C_I^T \begin{bmatrix} \dot{X}_4 \\ \dot{X}_5 \\ \dot{X}_6 \end{bmatrix} - (\underline{A}_T)^T \qquad (6\text{-}2)$$

where $(\underline{A}_T)^T$ is available to the filter from accelerometer measurements. But, the accelerations $\dot{X}_4$, $\dot{X}_5$, and $\dot{X}_6$ are functions of $X_1 \rightarrow X_6$ and in actual implementation would be calculated using the most recent estimates, $\hat{X}_1(t_i^+) \rightarrow \hat{X}_6(t_i^+)$, provided by the filter. But, in fact, the estimates of the satellite inertial position and velocity states will be rather poor because of 1) the weak coupling with the tracker states, and 2) the inadequate satellite dynamics model used in the Filter I formulation. As shown by Meyers (Ref 15:346), a satellite dynamics model that does not include at least the J2 gravitational potential term - which models the effects of the earth's oblateness - will cause rapid divergence of the state estimate in an extended Kalman filter. The good results obtained for Filter I, therefore, are in all likelihood due to the fact that for

a covariance analysis, $\hat{\underline{X}}$ is not available and all time varying expressions ($\dot{X}_4 \rightarrow \dot{X}_6$, $(\underline{A}_r)^T$, and $\partial(\underline{A}_r)^T/\partial X_1 \rightarrow X_3$) are evaluated along a predetermined nominal trajectory $\underline{X}_n$. Therefore, if Filter I were implemented, one would expect that, on the average, the filter would perform worse than the results of this study imply.

The results do indicate that we could expect this reduced order system model to perform well if the satellite acceleration state equations for $\dot{X}_4$, $\dot{X}_5$, and $\dot{X}_6$ were more accurately modeled to insure that the filter estimates $\hat{X}_1 \rightarrow \hat{X}_6$ do not diverge from the actual trajectory when the filter is implemented. Besides adding the J2 gravitational potential term, modeling of the atmospheric drag acceleration is suggested, since results have shown that this effect is on the order of J2 when satellite orbital altitudes are less than 500 miles (16,247). The ballistic coefficient need not be added as another filter state. In most satellite tracking situations, a good estimate of this parameter will already be available and can be entered by the operator from keyboard as a system parameter. Should these changes be made to the Filter I model, a Monte Carlo analysis should be performed to evaluate large-scale filter performance. A covariance analysis would probably give results very similar to those presented here for the tracker states and would prove very little about eventual actual filter performance.

The results for Filter II were not as good as originally expected. However, an examination of the Filter II formulation (see Chapter V) reveals a probable cause for the divergence of this filter. Both filters were evaluated using the same perturbation truth model, which itself was evaluated along a highly accurate nominal trajectory - $\underline{X}_n$. Whereas $(\underline{A}_r)^T$ in the Filter I and truth model representations were evaluated along $\underline{X}_n$ (which led to misleading results as discussed above) using a

highly accurate model for X_4, X_5, and X_6, $(\underline{A}_r)^T$ in the Filter II formulation was calculated online according to Equation (5-33)

$$(\underline{A}_r)^T = (\underline{A}_S)^{LS} - (\underline{A}_T)^T = -\mu_{\oplus} \frac{[C_I^{LS}(\underline{R}_T)^I + (\underline{R}_{ST})^{LS}]}{|(\underline{R}_S)^I|^3} - (\underline{A}_T)^T \qquad (6\text{-}3)$$

In all likelihood the second filter formulation probably diverged in the covariance analysis for the same reason that the first filter would diverge if actually implemented - insufficient satellite dynamics information. There exists a good possibility that Filter II
better if the J2 and atmospheric drag terms discussed earlier were added to the onboard computation of $(\underline{A}_r)^T$; time limitations prevented the author from exploring these possibilities. The addition of the atmospheric drag terms to the filter would require a differencing technique applied to the satellite inertial position information to obtain the inertial velocity estimates since explicit estimates of these parameters are not available in the Filter II formulation.

Recommendations for Future Study

Several simplifying assumptions were made in order to limit the scope of this study and are candidates for inclusion in future work.

1. The resolver measurements of the angles ϕ and θ were considered to be perfect. These parameters should be modeled stochastically and included in a future filter analysis to determine the sensitivity of the filter's performance to these variables.

2. The sensitivity of a filter's performance to both accelerometer and inertial position measurement noise corruption should be studied in future work.

3. A time varying Q profile as an ad-hoc function of the angular rates and/or range data could be obtained after studying a number of representative trajectories.

4. An adaptive Q technique based upon the real time evaluation of the innovations (residuals) sequence(s) could be studied.

As a follow on to this work, the author highly recommends that the Filter II formulation be reevaluated using the changes suggested in the last section - the addition of J2 and possibly atmospheric drag accelerations to the satellite dynamics model - in a Monte Carlo analysis. The Filter II formulation may require as little as 50% of the computer memory requirements for Filter I (Ref 3:346) - though this may be increased a little by the differencing technique required to determine X_4, X_5, and X_6. Should the Filter II formulation continue to diverge - as well it might in a highly nonlinear angular rate scenario, time varying or adaptive noise techniques should be explored.

The feasibility of the Filter II formulation has been proven in this study. Any subsequent studies should necessarily contain tradeoff analyses with the overall objective being to meet the required system performance specifications with the simplest (least demanding in terms of computation and memory requirements) filter model.

Bibliography

1. Pearson, John B. and Edwin B. Stear, Kalman Filter Applications in Airborne Radar Tracking, IEEE Transactions, Vol. AES-10, No. 3, May 1974.

2. Gelb, A., editor, Applied Optimal Estimation, 1974, The Analytic Sciences Corporation, The M.I.T. Press, Massachusetts Institute of Technology, Cambridge, Massachusetts.

3. Maybeck, Peter S., "Stochastic Estimation and Control Systems: Part I", Unpublished class notes, Wright-Patterson Air Force Base: Air Force Institute of Technology, 1975.

4. Mitchell, R. A. K., High Accuracy Aircraft to Satellite Tracking Using an Extended Kalman Filter, Thesis, Wright-Patterson Air Force Base: Air Force Institute of Technology, 1974.

5. Baker, Robert M. L., Jr., and Maud W. Makemson, An Introduction to Astrodynamics, 2nd Ed., New York, London, Academic Press, 1967,

6. Asher, Robert B. and David H. Watjen, Kalman Filtering for Precision Pointing and Tracking Applications, AF Avionics Laboratory, Wright-Patterson AFB, AFAL Technical Report to be published.

7. Kayton, Myron and Walter R. Fried, Avionics Navigation Systems, New York, John Wiley & Sons, 1969.

8. Meditch, J. S., Stochastic Optimal Linear Estimation and Control, New York, McGraw-Hill, 1969.

9. Maybeck, Peter S., "Stochastic Estimation and Control Systems: Part II", Unpublished class notes. Wright-Patterson Air Force Base: Air Force Institute of Technology, 1975.

10. Hamilton, Edward L., The General Covariance Analysis Program (GCAP). An Efficient Implementation of the Covariance Analysis Equations, Unpublished computer program guide, Wright-Patterson Air Force Base, Air Force Avionics Laboratory.

11. Hamilton, E. L., et al, An Efficient Covariance Analysis Computer Program Implementation, Proceedings of the IEEE 1976 National Aerospace and Electronics Conference (NAECON '76), pages 340-345, IEEE Inc., New York, New York.

12. Pollard, Joseph J., Orbital Parameter Determination by Weighted Least Square Error and Kalman Filtering Methods, Thesis submitted for the degree of Master of Science, Air Force Institute of Technology, WPAFB, 1973.

13. Broxmeyer, Charles, Inertial Navigation Systems, New York, McGraw-Hill, 1964.

14. Jazwinski, A. H., Stochastic Processes and Filtering Theory, Academic Press, Inc., New York, 1970.

15. Meyers, K. A. and B. D. Tapley, Dynamical Model Compensation for Near-Earth Satellite Orbit Determination, AIAA Journal, Vol 13, No. 3, pages 343-349, March 1975.

16. Pon, Wing Y., Mathematical Theory for the Advanced Orbit Determination and Ephemeris Generation System, DATA Dynamics, Inc., September 1973.

Appendix A

Linearization of the Truth Model State and Measurement Equations

The purpose of this appendix is to develop the partial derivative matrices, F_S nnd H_S, for the truth model dynamics and measurement equations defined in the summary to Chapter II. The results presented here are different than those in Mitchell's previous work (Ref 4) in four respects.

1) The accelerometer measurement noise states and solar pressure acceleration state have been deleted, reducing the number of states from 61 to 42.

2) The measurement equations have not been substituted into the state dynamics equations before linearizing - in the truth model the actual dynamics are modeled.

3) The partials of the drag acceleration have been changed to reflect the fact that the inertial velocity vector of the satellite relative to the atmosphere is

$$(\underline{V}_a)^I \triangleq \begin{bmatrix} X_4 + \omega_e X_2 \\ X_5 - \omega_e X_1 \\ X_6 \end{bmatrix}$$

and not

$$(\underline{V}_a)^I = \begin{bmatrix} X_4 + \omega_e X_2 \\ X_5 - \omega_e X_1 \\ X_3 \end{bmatrix}$$

as was used extensively in Appendix B of Mitchell's work.

4) The gravitational forces in the rotating frame are calculated according to

$$A_{g_{X_r}} = \frac{\partial U}{\partial X_R}$$

$$A_{g_{Y_r}} = \frac{\partial U}{\partial Y_R}$$

$$A_{g_{Z_r}} = \frac{\partial U}{\partial Z_R}$$

where U is the gravitational potential defined in Equation (2-4). The gravitational forces in the inertial frame are then found by

$$(\underline{A}_g)^I = C_R^I (\underline{A}_g)^R$$

In order to linearize the state equations for the extended Kalman filter formulation, the second partials U with respect to X_1, X_2, and X_3 must be found. The method used to accomplish this is a one sided differencing technique suggested by Pollard (Ref 12) with a differencing step size of one meter. The differencing is accomplished in the rotating coordinate system. Letting U_{2_R} indicate the matrix of second partials of the gravity potential with respect to the rotating frame

$$U_{2_R} = \begin{bmatrix} \frac{\partial 2_U}{\partial X_R^2} & \frac{\partial 2_U}{\partial X_R Y_R} & - - - \\ | & & \\ | & & \\ - - - - - - & & \frac{\partial^2 U}{\partial Z_R^2} \end{bmatrix} \qquad \text{(A-1)}$$

then the matrix of the second partial derivatives taken with respect to the inertial nonrotating earth centered coordinate (I) frame U_{2_I} can be found using the following similarity transformation (Ref 13:28)

$$U_{2_I} = (C_I^R)^T \, U_{2_R} \, C_I^R \tag{A-2}$$

This is as opposed to the following form that was used by Mitchell.

$$U_{2_I} = C_I^R U_{2_R} (C_I^R)^T$$

It is easy to become confused because Broxmeyer defines C_I^R as the coordinate transformation from the rotating to the inertial frame (Ref 13:22) - the opposite of the convention used in this and Mitchell's work. The following definitions are used in this appendix.

X_1, X_2, X_3 = satellite inertial position vector

X_4, X_5, X_6 = satellite inertial velocity vector

X_M, Y_M, Z_M = moon's inertial (earth centered) position vector

X_S, Y_S, Z_S = sun's inertial (earth centered) position vector

r_V = distance from earth center to satellite

r_S = distance from earth center to sun

r_M = distance from earth center to moon

ρ = atmospheric density of altitude h

ρ_o = mean sea level atmospheric density

V_a = velocity of satellite relative to the rotating atmosphere

r_{ms} = distance from satellite to moon

r_{ss} = distance from satellite to sun

ω_e = earth rotation rate

$\mu_\odot$ = sun's gravitational constant

$\mu_\mathbb{C}$ = moon's gravitational constant

System F Matrix

Given the following nonlinear state equation

$$\dot{\underline{X}}(t) = \underline{f}_s(\underline{X}(t),t) + G_s(t)\ \underline{\omega}_s(t)$$

the matrix of partial derivatives of the dynamics with respect to the states is defined as

$$F_s(t) = \left.\frac{\partial \underline{f}_s(t)}{\partial \underline{X}}\right|_{\underline{X}_n(t)}$$

where $\underline{X}_n(t)$ is the nominal reference state trajectory. The determination of this matrix is very straightforward except for the partials of the relative acceleration vector. The inertial acceleration of the satellite relative to the tracker expressed in tracker coordinates $(\underline{A}_r)^T$ is determined from

$$(\underline{A}_r)^T \triangleq C_I^T[(\ddot{\underline{R}}_S)^I - (\ddot{\underline{R}}_T)^I] \tag{A-3}$$

but

$$(\ddot{\underline{R}}_S)^I \triangleq \begin{bmatrix} \dot{X}_4 \\ \dot{X}_5 \\ \dot{X}_6 \end{bmatrix}$$

and

$$(\ddot{\underline{R}}_T)^I \triangleq \begin{bmatrix} XA(1) \\ XA(2) \\ XA(3) \end{bmatrix}$$

and thus

$$(\underline{A}_r)^T = \begin{bmatrix} A_{r_X} \\ A_{r_Y} \\ A_{r_Z} \end{bmatrix} \approx C_I^{LS} \begin{bmatrix} \dot{X}_4 - XA(1) \\ \dot{X}_5 - XA(2) \\ \dot{X}_6 - XA(3) \end{bmatrix} \tag{A-4}$$

Choosing A_{r_X} as an example to work with, it follows that

$$A_{r_X} = C_I^{LS}(1,1)[\dot{X}_4 - XA(1)] + C_I^{LS}(1,2)[\dot{X}_5 - XA(2)]$$

$$+ C_I^{LS}(1,3)[\dot{X}_6 - XA(3)]$$

and

$$\frac{\partial A_{r_X}}{\partial X_1} = C_I^{LS}(1,1)\left[\frac{\partial \dot{X}_4}{\partial X_1}\right] + C_I^{LS}(1,2)\left[\frac{\partial \dot{X}_5}{\partial X_1}\right] + C_I^{LS}(1,3)\left[\frac{\partial \dot{X}_6}{\partial X_1}\right] \qquad \text{(A-5)}$$

where $\dot{X}_4$, $\dot{X}_5$, and $\dot{X}_6$ are defined in Equation (2-2), and $\frac{\partial C_I^{LS}}{\partial X} = 0$, $\frac{\partial \underline{XA}}{\partial X} = 0$ because they are not functions of the states. The inertial X_4 acceleration is defined as

$$\dot{X}_4 = A_{g_1} + A_{d_1} + A_{m_1} + A_{s_1} + W_1 \qquad \text{(A-6)}$$

then

$$\frac{\partial \dot{X}_4}{\partial X_1} = \frac{\partial A_{g_1}}{\partial X_1} + \frac{\partial A_{d_1}}{\partial X_1} + \frac{\partial A_{m_1}}{\partial X_1} + \frac{\partial A_{s_1}}{\partial X_1} \qquad \text{(A-7)}$$

The first term in Equation (A-4) can be determined using the relationship previously derived that

$$U_{2_I} = (C_I^R)^T U_{2_R} C_I^R$$

where in particular $\frac{\partial A_{g_1}}{\partial X_1} = U_{2_I}(1,1)$. Equation (A-7) can now be written as

$$\frac{\partial \dot{X}_4}{\partial X_1} = U_{2_I}(1,1) + \frac{\partial A_{d_1}}{\partial X_1} + \frac{\partial A_{m_1}}{\partial X_1} + \frac{\partial A_{s_1}}{\partial X_1}$$

In a similar manner we define

$$\frac{\partial \dot{X}_5}{\partial X_1} = U_{2_I}(2,1) + \frac{\partial A_{d_1}}{\partial X_1} + \frac{\partial A_{m_1}}{\partial X_1} + \frac{\partial A_{s_1}}{\partial X_1}$$

$$\frac{\partial \dot{X}_6}{X_1} = U_{2_I}(3,1) + \frac{\partial A_{d_1}}{\partial X_1} + \frac{\partial A_{m_1}}{\partial X_1} + \frac{\partial A_{s_1}}{\partial X_1}$$

In the results that follow $\frac{\partial A_{r_X}}{\partial X_j} = Q_{1_j}$, $j = 1,3$; $\frac{\partial A_{r_Y}}{\partial X_j} = Q_{2_j}$, $j = 1,3$;

$\frac{\partial A_{r_Z}}{\partial X_j} = Q_{3_j}$, $j = 1,3$.

Now F_S for the truth model is

$$F_S = \left[\begin{array}{c|cc} F_1(13 \times 13) & & 0(13 \times 29) \\ \hline & F_2(8 \times 8) & 0(8 \times 21) \\ 0(29 \times 13) & & \\ & 0(21 \times 8) & 0(21 \times 21) \end{array}\right]$$

Where the figures in the brackets indicate the dimensions of the various submatrices.

$$F_1 = \left[\begin{array}{ccc|ccc|ccccccc} 0(3\times 3) & & & I(3\times 3) & & & 0(3\times 7) & & & & & & \\ \hline f_1 & f_2 & f_3 & f_4 & f_5 & f_6 & & & & & & & f_7 \\ f_8 & f_9 & f_{10} & f_{11} & f_{12} & f_{13} & & & 0(3\times 6) & & & & f_{14} \\ f_{15} & f_{16} & f_{17} & f_{18} & f_{19} & f_{20} & & & & & & & f_{21} \\ \hline g_1 & g_2 & g_3 & & & & g_4 & g_5 & g_6 & g_7 & g_8 & g_9 & 0 \\ g_{10} & g_{11} & g_{12} & & & & g_{13} & g_{14} & g_{15} & g_{16} & g_{17} & g_{18} & 0 \\ 0 & 0 & 0 & 0(6\times 3) & & & 0 & g_{19} & 0 & g_{20} & 0 & 0 & 0 \\ 0 & 0 & 0 & & & & g_{21} & 0 & g_{22} & 0 & 0 & 0 & 0 \\ 0 & 0 & 0 & & & & 0 & 0 & 0 & 0 & 0 & 0 & 0 \\ g_{24} & g_{25} & g_{26} & & & & g_{27} & g_{28} & g_{29} & g_{30} & g_{31} & 0 & 0 \\ \hline \multicolumn{13}{c}{0(1\times 13)} \end{array}\right]$$

with

$$f_1 = u(1,1) + \left\{\frac{0.5X_{13}Va\beta\rho X_1(X_4 + WEX_2)}{r_v}\right\}$$

$$+\left\{\frac{0.5X_{13}WE\rho(X_5 - WEX_1)(X_4 + WEX_2)}{Va}\right\}$$

$$-\frac{\mu\odot}{r_{vs}^3} + \frac{3\mu_{\odot}(x_s - X_1)^2}{r_{vs}^5} - \frac{\mu\,\mathbb{C}}{r_{vm}^3} + \frac{3\mu_{\mathbb{C}}(x_m - X_1)^2}{r_{vm}^5}$$

$$f_2 = u(1,2) + \left\{\frac{0.5X_{13}Va\beta\rho X_2(X_4 + WEX_2)}{r_v}\right\}$$

$$-\left\{\frac{0.5X_{13}WE\rho(X_4 + WEX_2)^2}{V_a}\right\} - \left\{0.5X_{13}\rho WEVa\right\}$$

$$+\left\{\frac{3\mu_{\odot}(x_s - X_1)(y_s - X_2)}{r_{vs}^5}\right\} + \left\{\frac{3\mu_{\mathbb{C}}(x_m - X_1)(y_m - X_2)}{r_{vm}^5}\right\}$$

$$f_3 = u(1,3) + \left\{\frac{0.5X_{13}Va\beta\rho X_3(X_4 + WEX_2)}{r_v}\right\}$$

$$+\left\{\frac{3\mu_{\odot}(x_s - X_1)(z_s - X_3)}{r_{vs}^5}\right\} + \left\{\frac{3\mu_{\oplus}(x_m - X_1)(z_m - X_3)}{r_{vm}^5}\right\}$$

$$f_4 = -0.5X_{13}\rho\left\{\frac{(X_4 + WEX_2)^2}{Va} + Va\right\}$$

$$f_5 = \frac{-0.5X_{13}\rho(X_4 + WEX_2)(X_5 - WEX_1)}{Va}$$

$$f_6 = \frac{-0.5X_{13}\rho(X_4 + WEX_2)X_6}{Va}$$

$$f_7 = -0.5\rho V_a(X_4 + WEX_2)$$

$$f_8 = u(2,1) + \left\{\frac{0.5X_{13}Va\beta\rho X_1(X_5 - WEX_1)}{r_v}\right\}$$

$$+\left\{\frac{0.5X_{13}WE\rho(X_5 - WEX_1)^2}{Va}\right\}$$

$$+\left\{0.5X_{13}Va\rho WE\right\} + \left\{\frac{3\mu_{\odot}(y_s - x_2)(x_s - X_1)}{r_{vs}^5}\right\}$$

$$+\left\{\frac{3\mu_{\oplus}(y_m - X_2)(x_m - X_1)}{r_{vm}^5}\right\}$$

$$f_9 = u(2,2) + \left\{\frac{0.5X_{13}Va\beta\rho X_2(X_5 - WEX_1)}{r_v}\right\}$$

$$- \left\{\frac{0.5X_{13}WE\rho(X_5 - WEX_1)(X_4 + WEX_2)}{Va}\right\}$$

$$- \frac{\mu\odot}{r_{vs}^3} + \frac{3\mu_\odot(y_s - X_2)^2}{r_{vs}^5} - \frac{\mu\text{☾}}{r_{vm}^3}$$

$$+ \frac{3\mu_{\text{☾}}(y_m - X_2)^2}{r_{vm}^5}$$

$$f_{10} = u(2,3) + \left\{\frac{0.5X_{13}Va\beta\rho X_3(X_5 - WEX_1)}{r_v}\right\}$$

$$+ \left\{\frac{3\mu_\odot(y_s - X_2)(z_s - X_3)}{r_{vs}^5}\right\}$$

$$+ \left\{\frac{3\mu_{\text{☾}}(y_m - X_2)(z_m - X_3}{r_{vm}^5}\right\}$$

$$f_{11} = \frac{-(X_4 + WEX_2)(X_5 - WEX_1)0.5X_{13}\rho}{Va}$$

$$f_{12} = -0.5X_{13}\rho\left\{\frac{(X_5 - WEX_1)^2}{Va} + Va\right\}$$

$$f_{13} = -0.5X_{13}\rho(X_5 - WEX_1)X_6$$

$$f_{14} = -0.5\rho Va(X_5 - WEX_1)$$

$$f_{15} = u(3,1) + \left\{\frac{0.5X_{13}\beta\rho X_1 VaX_6}{r_v}\right\}$$

$$+\left\{\frac{0.5X_{13}\rho WEX_6(X_5 - WEX_1)}{Va}\right\}$$

$$+\left\{\frac{3\mu_{\odot}(z_s - X_3)(x_s - X_1)}{r_{vs}^5}\right\} + \left\{\frac{3\mu_{\text{☾}}(z_m - X_3)(x_m - X_1)}{r_{vm}^5}\right\}$$

$$f_{16} = u(3,2) + \left\{\frac{0.5X_{13}\beta\rho X_2 VaX_6}{r_v}\right\}$$

$$-\left\{\frac{0.5X_{13}\rho WEX_6(X_4 + WEX_2)}{Va}\right\}$$

$$+\left\{\frac{3\mu_{\odot}(z_s - X_3)(y_s - X_2)}{r_{vs}^5}\right\}$$

$$+\left\{\frac{3\mu_{\text{☾}}(z_m - X_3)(y_m - X_2)}{r_{vm}^5}\right\}$$

$$f_{17} = u(3,3) + \left\{\frac{0.5X_{13}\beta\rho VaX_3X_6}{r_v}\right\} - \frac{\mu_{\odot}}{r_{vs}^3} + \frac{3\mu_{\odot}(z_s - X_3)^2}{r_{vs}^5}$$

$$- \frac{\mu_{\text{☾}}}{r_{vm}^3} + \frac{3\mu_{\text{☾}}(z_m - X_3)^2}{r_{vm}^5}$$

$$f_{18} = \frac{-0.5X_{13}\rho(X_4 + WEX_2)X_6}{Va}$$

$$f_{19} = \frac{-0.5X_{13}\rho(X_5 - WEX_1)X_6}{Va}$$

$$f_{20} = \frac{-0.5X_{13}\rho X_6^2}{Va} - 0.5X_{13}\rho V_a$$

$$f_{21} = -0.5\rho VaX_6$$

$$g_1 = \frac{-Q_{31}}{R} - \frac{\delta\varepsilon Q_{11}}{R}$$

$$g_2 = \frac{-Q_{32}}{R} - \frac{\delta\varepsilon Q_{12}}{R}$$

$$g_3 = \frac{-Q_{33}}{R} - \frac{\delta\varepsilon Q_{13}}{R}$$

$$g_4 = \frac{-2V_r}{R}$$

$$g_5 = \omega_{T_X} + \delta\eta\omega_{T_Y} - \delta\varepsilon\omega_{T_Z}$$

$$g_6 = \omega_{LS_Z}\omega_{T_Y}$$

$$g_7 = \frac{-A_{r_X}}{R} - \omega_{LS_Z}\omega_{T_Z}$$

$$g_8 = \frac{A_{r_Z}}{R^2} + \frac{2V_r\omega_{LS_Y}}{R^2} + \frac{\delta\varepsilon A_{r_X}}{R^2}$$

$$g_9 = \frac{-2\omega_{LS_Y}}{R}$$

$$g_{10} = \frac{Q_{21}}{R} - \frac{\delta\eta Q_{11}}{R}$$

$$g_{11} = \frac{Q_{22}}{R} - \frac{\delta\eta Q_{12}}{R}$$

$$g_{12} = \frac{Q_{23}}{R} - \frac{\delta\eta Q_{13}}{R}$$

$$g_{13} = -\omega_{T_X} - \delta\eta\omega_{T_Y} + \delta\epsilon\omega_{T_Z}$$

$$g_{14} = \frac{-2V_r}{R}$$

$$g_{15} = \frac{-A_{r_X}}{R} - \omega_{LS_Y}\omega_{T_Y}$$

$$g_{16} = \omega_{LS_Y}\omega_{T_Z}$$

$$g_{17} = \frac{-A_{r_Y}}{R^2} + \frac{2V_r\omega_{LS_Z}}{R^2} - \frac{\delta\eta A_{r_X}}{R^2}$$

$$g_{18} = \frac{-2\omega_{LS_Z}}{R}$$

$$g_{19} = 1$$

$$g_{20} = -\omega_{T_X}$$

$$g_{21} = 1$$

$$g_{22} = \omega_{T_X}$$

$$g_{23} = 1$$

$$g_{24} = Q_{11} + \delta\eta Q_{21} - \delta\varepsilon Q_{31}$$

$$g_{25} = Q_{12} + \delta\eta Q_{22} - \delta\varepsilon Q_{32}$$

$$g_{26} = Q_{13} + \delta\eta Q_{23} - \delta\varepsilon Q_{33}$$

$$g_{27} = 2R\omega_{LS_Y}$$

$$g_{28} = 2R\omega_{LS_Z}$$

$$g_{29} = A_{r_Y}$$

$$g_{30} = -A_{r_Z}$$

$$g_{31} = \omega^2_{LS_Y} + \omega^2_{LS_Z}$$

$$F_2 = \begin{bmatrix} -\beta_1 & & & & & & & \\ & -\beta_2 & & & & & & \\ & & -\beta_3 & & & \underline{0} & & \\ & & & -\beta_4 & & & & \\ & \underline{0} & & & -\beta_5 & & & \\ & & & & & -\beta_6 & & \\ & & & & & & -\beta_7 & \\ & & & & & & & -\beta_8 \end{bmatrix}$$

System H_S Matrix

Given the nonlinear measurement equation

$$\underline{Z}_S(t_i) = \underline{h}_S[\underline{X}(t_i), t_i] + \underline{V}_S(t_i)$$

$H_S(t_i)$ is defined as

$$H_S(t_i) \triangleq \left.\frac{\partial \underline{h}_S[\underline{X}(t_i), t_i]}{\partial \underline{X}}\right|_{\underline{X}_n(t_i)}$$

where $\underline{X}_n(t_i)$ is the nominal reference trajectory. Assuming that the constants K_1, K_2, and K_R are all unity, then $H_S(t_i)$ is given by

$$H_S(t) \triangleq \left[\begin{array}{c|c|c} H_{S_1}(5 \times 14) & H_{S_2}(5 \times 14) & H_{S_3}(5 \times 14) \end{array}\right]$$

$$H_{S_1} = \left[\begin{array}{c|cccccccc} & 1 & 0 & 0 & 0 & 0 & 0 & 0 & 0 \\ & 0 & 1 & 0 & 0 & 0 & 0 & 0 & 0 \\ 0(6 \times 6) & 0 & 0 & 1 & 0 & 0 & 0 & 0 & 0 \\ & 0 & 0 & 0 & 1 & 0 & 0 & 0 & 1 \\ & 0 & 0 & 0 & 0 & 1 & 0 & 0 & 0 \end{array}\right]$$

$$H_{S_2} = \left[\begin{array}{cccccccccccccc} 0 & 0 & 0 & 1 & 0 & 0 & 0 & 0 & 0 & 0 & AT_X & AT_Y & AT_Z & 0 \\ 0 & 0 & 0 & 0 & 1 & 0 & 0 & 0 & 0 & 0 & 0 & 0 & 0 & AT_X \\ 1 & 0 & 0 & 0 & 0 & 0 & \delta\eta & 0 & 0 & 0 & 0 & 0 & 0 & 0 \\ 0 & 0 & 0 & 0 & 0 & \delta\epsilon & 0 & 0 & 0 & 0 & 0 & 0 & 0 & 0 \\ 0 & 1 & 0 & 0 & 0 & 0 & 0 & 0 & 0 & 0 & 0 & 0 & 0 & 0 \end{array}\right]$$

$$
H_{S_3} = \begin{bmatrix}
0 & 0 & 0 & 0 & W_{T_X} & -W_{T_Z} & 0 & 0 & 0 & 0 & 0 & W_{T_Y} & 0 \\
AT_Y & AT_Z & 0 & 0 & 0 & 0 & -W_{T_X} & W_{T_Y} & 0 & 0 & 0 & 0 & 0 & W_{T_Z} \\
0 & 0 & 0 & 0 & 0 & 0 & 0 & 0 & 0 & 0 & 1 & 0 & 0 & 0 \\
0 & 0 & 0 & 0 & 0 & 0 & 0 & 0 & 0 & 1 & 0 & 0 & 0 & 0 \\
0 & 0 & 0 & 0 & 0 & 0 & 0 & 0 & 1 & 0 & 0 & 0 & 0 & 0
\end{bmatrix}
$$

Appendix B

Linearization of Filter I Model State and Measurement Equations

The purpose of this appendix is to develop the F and H matrices for the Filter I (12 state) model developed in Chapter V. The terms used in this development are given in the beginning of Appendix A.

Filter I Model F-Matrix

$$F \triangleq \left.\frac{\partial f[X(t),t]}{\partial \underline{X}}\right|_{\underline{X}_n(t)}$$

$$F = \begin{bmatrix} F_1(6 \times 6) & 0(6 \times 6) \\ F_2(6 \times 6) & F_3(6 \times 6) \end{bmatrix}$$

where

$$F_1 = \begin{bmatrix} 0(3 \times 3) & I(3 \times 3) \\ U_{2_I}(3 \times 3) & 0(3 \times 3) \end{bmatrix}$$

and

$$U_{2_I} = \begin{bmatrix} \frac{-\mu_\oplus}{r_v^3} + \frac{3\mu_\oplus X_1^2}{r_v^5} & \frac{3\mu_\oplus X_1 X_2}{r_v^5} & \frac{3\mu_\oplus X_3 X_1}{r_v^5} \\ \frac{3\mu_\oplus X_3 X_1}{r_v^5} & \frac{-\mu_\oplus}{r_v^3} + \frac{3\mu_\oplus X_2^2}{r_v^5} & \frac{3\mu_\oplus X_2 X_1}{r_v^5} \\ \frac{3\mu_\oplus X_3 X_1}{r_v^5} & \frac{3\mu_\oplus X_2 X_3}{r_v^5} & \frac{-\mu_\oplus}{r_v^3} + \frac{3\mu_\oplus X_3^2}{r_v^5} \end{bmatrix}$$

$$F_2 = \left[\begin{array}{ccc|c} \frac{-Q_{31}}{R} & \frac{-Q_{32}}{R} & \frac{-Q_{33}}{R} & \\ \frac{-Q_{21}}{R} & \frac{-Q_{22}}{R} & \frac{-Q_{23}}{R} & \\ \hline & 0(3 \times 3) & & 0(6 \times 6) \\ \hline Q_{11} & Q_{12} & Q_{13} & \end{array}\right]$$

$$F_3 = \left[\begin{array}{ccccc} \frac{-2V_r}{R} & \omega_{T_X} & 0 & 0 & \frac{2V_r\omega_{LS_Y} + A_{r_Z}}{R^2} & \frac{-2\omega_{LS_Y}}{R} \\ -\omega_{T_X} & \frac{-2V_r}{R} & 0 & 0 & \frac{2V_r\omega_{LS_Z} - A_{r_Y}}{R^2} & \frac{-2\omega_{LS_Z}}{R} \\ 0 & 1 & 0 & -\omega_{T_X} & 0 & 0 \\ 1 & 0 & \omega_{T_X} & 0 & 0 & 0 \\ 0 & 0 & 0 & 0 & 0 & 1 \\ 2\omega_{LS_Y}R & 2\omega_{LS_Z}R & 0 & 0 & (\omega^2_{LS_Y} + \omega^2_{LS_Z}) & 0 \end{array}\right]$$

Filter I Measurement Matrix H

$$H(t_i) \triangleq \left.\frac{\partial h(X(t_i), t_i)}{\partial X}\right|_{\underline{X}_n(t_i)}$$

$$H = [0(5 \times 6) \quad I(5 \times 5) \quad 0(5 \times 1]$$

Appendix C

Linearization of the Filter II Model State and Measurement Equations

To develop the Filter II model, the first six states of the Filter I model were deleted and the inertial acceleration of the satellite with respect to the tracker in the tracker frame was defined as

$$(\underline{A}_r)^T = \frac{-\mu_\oplus[C_I^{LS}(\underline{R}_T)^I + (\underline{R}_{ST})^{LS}]}{|(\underline{R}_S)^I|^3} - (\ddot{\underline{R}}_T)^T \qquad \text{(C-1)}$$

Defining

$$(\underline{R}_T)^I = \begin{bmatrix} XALS(1) \\ XALS(2) \\ XALS(3) \end{bmatrix}, \quad (\underline{R}_{ST})^{LS} = \begin{bmatrix} R \\ 0 \\ 0 \end{bmatrix}, \quad (\ddot{\underline{R}}_T)^T = \begin{bmatrix} AT_X \\ AT_Y \\ AT_Z \end{bmatrix}$$

$$(\underline{R}_S)^I = (\underline{R}_T)^I + C_{LS}^I(\underline{R}_{ST})^{LS} = (\underline{R}_T)^I + (C_I^{LS})^T(\underline{R}_{ST})^{LS}$$

Therefore

$$(\underline{R}_S)^I = \begin{bmatrix} XALS(1) + C(1,1)R \\ XALS(2) + C(1,2)R \\ XALS(3) + C(1,3)R \end{bmatrix}$$

and

$$|(\underline{R}_S)^I|^3 = \{[XALS(1) + C(1,1)R]^2 + [XALS(2) + C(1,2)R]^2 + [XALS(3) + C(1,3)R]^2\}^{3/2}$$

and

$$A_{r_X} = \frac{-\mu_\oplus [XALS(1) + R]}{|(\underline{R}_S)^I|^3} - A_{T_X} \tag{C-2}$$

$$A_{r_Y} = \frac{-\mu_\oplus XALS(2)}{|(\underline{R}_S)^I|^3} - A_{T_Y} \tag{C-3}$$

$$A_{r_Z} = \frac{-\mu_\oplus XALS(3)}{|(\underline{R}_S)^I|^3} - A_{T_Z} \tag{C-4}$$

It follows that

$$\frac{\partial A_{r_X}}{\partial R} = \frac{\partial}{\partial R}\left\{\left(\frac{-\mu_\oplus}{|(\underline{R}_S)^I|^3}\right)[XALS(1) + R]\right\} = \frac{-\mu_\oplus}{|(\underline{R}_S)^I|^3}\frac{\partial}{\partial R}[XALS(1) + R]$$

$$+ [XALS(1) + R]\frac{\partial}{\partial R}\left(\frac{-\mu_\oplus}{|(R_S)^I|^3}\right) = \frac{-\mu_\oplus}{|(\underline{R}_S)^I|^3} - \mu_\oplus[XALS(1) + R]$$

$$\cdot \frac{\partial}{\partial R}\left(\frac{1}{|(R_S)^I|^3}\right) = \frac{-\mu_\oplus}{|(R_S)^I|^3} + \frac{1.5\mu_\oplus[XALS(1) + R]}{|(R_S)^I|^5}\ \frac{\partial|(\underline{R}_S)^I|}{\partial R}$$

$$\frac{\partial A_{r_X}}{\partial R} = \frac{-\mu_\oplus}{|(\underline{R}_S)^I|^3} + \frac{1.5\mu_\oplus[XALS(1) + R]P}{|(\underline{R}_S)^I|^5}$$

$$\frac{\partial A_{r_Y}}{\partial R} = \frac{1.5\mu_\oplus XALS(2)P}{|(\underline{R}_S)^I|^5}$$

$$\frac{\partial A_{r_Z}}{\partial R} = \frac{1.5\mu_{\oplus} XALS(3)P}{|(\underline{R}_S)^I|^5}$$

where

$$P = 2[C(1,1)(XALS(1) + C(1,1)R) + C(1,2)(XALS(2) + C(1,2)R)$$

$$+ C(1,3)(XALS(1) + C(1,3)R)]$$

Now, for Filter II

$$f_1 = \dot{\omega}_{LS_Y} = \frac{-A_{r_Z}}{R} - \frac{2V_r \omega_{LS_Y}}{R} + \omega_{LS_Z} \omega_{T_X} + W_1$$

$$f_2 = \dot{\omega}_{LS_Z} = \frac{A_{r_Y}}{R} - \frac{2V_r \omega_{LS_Z}}{R} - \omega_{LS_Y} \omega_{T_X} + W_2$$

$$f_6 = \dot{V}_r = A_{r_X} + R(\omega^2_{LS_Y} + \omega^2_{LS_Z}) + W_3$$

and therefore

$$P_1 \triangleq \frac{\partial f_1}{\partial R} = \frac{1}{R^2}\left[A_{r_Z}(R) - \frac{\partial A_{r_Z}}{\partial R} + 2V_r \omega_{LS_Y}\right]$$

$$P_2 \triangleq \frac{\partial f_2}{\partial R} = \left(\frac{-1}{R^2}\right)\left[A_{r_Y}(R) - \frac{\partial A_{r_Y}}{\partial R} - 2V_r \omega_{LS_Z}\right]$$

$$P_3 \triangleq \frac{\partial f_6}{\partial R} = \frac{\partial A_{r_X}}{\partial R} + \left(\omega^2_{LS_Y} + \omega^2_{LS_Z}\right)$$

then

$$F_{II} = \left.\frac{\partial f_{II}[\underline{X}(t),t]}{\partial \underline{X}}\right|_{\underline{X}_n(t)}$$

$$F_{II} = \begin{bmatrix} \frac{-2V_r}{R} & \omega_{T_X} & 0 & 0 & P_1 & \frac{-2\omega_{LS_Y}}{R} \\ -\omega_{T_X} & \frac{-2V_r}{R} & 0 & 0 & P_2 & \frac{-2\omega_{LS_Z}}{R} \\ 0 & 1 & 0 & -\omega_{T_X} & 0 & 0 \\ 1 & 0 & \omega_{T_X} & 0 & 0 & 0 \\ 0 & 0 & 0 & 0 & 0 & 1 \\ 2R\omega_{LS_Y} & 2R\omega_{LS_Z} & 0 & 0 & P_3 & 0 \end{bmatrix}$$

and

$$H = [\ I(5 \times 5) \ \vdots \ 0(5 \times 1)\ ]$$

Vita

Capt Robert E. Mann, Jr. enlisted in the United States Air Force in 1968. After attending technical school at Keesler AFB, Mississippi, he was stationed at Sewart AFB, Tennessee as a ground to air communications repairman until May 1970. Beginning in June 1970, he attended the University of Arizona under the Airmans Education and Commissioning Program and was awarded a Bachelor of Science in Physics in May 1971. After being commissioned in September 1971, he was assigned to the Special Space Projects Division of the 6595 Aerospace Test Wing, Vandenberg AFB, California. While stationed at Vandenberg, Capt Mann was a space systems engineer on the Space Test Program's Small Satellite Project and the Defense Meteorological Satellite Program (DMSP). In December 1973 he became the Field Program Manager - responsible for all Vandenberg activities - for DMSP. In addition, he served as an advisor on several other space programs and participated in several preliminary studies on the Space Shuttle. He entered the Air Force Institute of Technology in June 1975 to pursue a Master of Science degree in Electrical Engineering.

UNCLASSIFIED

SECURITY CLASSIFICATION OF THIS PAGE *(When Data Entered)*

(14) REPORT DOCUMENTATION PAGE		READ INSTRUCTIONS BEFORE COMPLETING FORM
1. REPORT NUMBER GE/EE/76-33	2. GOVT ACCESSION NO.	3. RECIPIENT'S CATALOG NUMBER
4. TITLE *(and Subtitle)* (6) High Accuracy Aircraft to Satellite Tracking: An Evaluation of Two Proposed Filter Models.		5. TYPE OF REPORT & PERIOD COVERED MS Thesis 6. PERFORMING ORG. REPORT NUMBER
7. AUTHOR(s) (10) Robert E. Mann, Jr Captain, USAF		8. CONTRACT OR GRANT NUMBER(s) (9) Master's thesis,
9. PERFORMING ORGANIZATION NAME AND ADDRESS Air Force Institute of Technology (AFIT/EN) Wright-Patterson AFB, Ohio 45433		10. PROGRAM ELEMENT, PROJECT, TASK AREA & WORK UNIT NUMBERS
11. CONTROLLING OFFICE NAME AND ADDRESS Air Force Avionics Laboratory/RWI Wright-Patterson AFB, Ohio 45433	(11)	12. REPORT DATE Dec 1976 13. NUMBER OF PAGES 141 (12) 144p.
14. MONITORING AGENCY NAME & ADDRESS *(if different from Controlling Office)*		15. SECURITY CLASS. *(of this report)* Unclassified 15a. DECLASSIFICATION/DOWNGRADING SCHEDULE

16. DISTRIBUTION STATEMENT *(of this Report)*

Approved for public release; distribution unlimited.

17. DISTRIBUTION STATEMENT *(of the abstract entered in Block 20, if different from Report)*

18. SUPPLEMENTARY NOTES

Approved for public release; IAW AFR 190-17

Jerral F. Guess, Captain, USAF
Director of Information

19. KEY WORDS *(Continue on reverse side if necessary and identify by block number)*

20. ABSTRACT *(Continue on reverse side if necessary and identify by block number)*

This study treats the high accuracy tracking of a satellite from an aircraft. The purpose is to evaluate the feasibility of several reduced order system models for implementation in an extended Kalman filter formulation whose estimates would be used to aid the tracker. The first filter model is a twelve state model in which filter estimates of the satellite inertial position and velocity are obtained and used in the estimation of the tracker states. A second, six state-model deletes these six satellite states, and tracker state estimation is accomplished by exploiting the information already available in

over

DD FORM 1 JAN 73 1473 EDITION OF 1 NOV 65 IS OBSOLETE

012225

UNCLASSIFIED

SECURITY CLASSIFICATION OF THIS PAGE *(When Data Entered)*

20. the tracking geometry, dominant modes of satellite dynamics, and the range measurement. Tracker state estimation is accomplished in the line of sight coordinate frame for both filter formulations. A covariance analysis was performed, evaluating each filter against a 42 state truth model. The tracking profile used in the study was specifically designed to evaluate each filter's state estimation capability when faced with a highly nonlinear tracker angular rate history. It was concluded that the six state filter is a viable alternative, and, with some proposed modifications, is preferable (because of its simplicity and lower computational burden) and warrants further study.